ABSTRACT

Title of Dissertation: CERAMIDE CHANNELS AND THE INDUCTION OF APOPTOSIS: STRUCTURAL INSIGHTS ON CHANNEL FORMATION AND REGULATION BY BCL-2 FAMILY PROTEINS.

Meenu Nadisha Perera, Doctor of Philosophy, 2012

Directed by: Professor Marco Colombini
Department of Biology

A critical event in apoptosis is the release of intermembrane space proteins from mitochondria following mitochondrial outer membrane (MOM) permeabilization (MOMP). The Bcl-2 family of proteins regulates MOM integrity and includes pro- and anti-apoptotic members, like Bax and Bcl-xL respectively. Preceding MOMP, the MOM becomes enriched with the sphingolipid, ceramide, which can self-assemble to form ceramide channels, contributing to MOMP.

Bax and ceramide channels were found to act synergistically in the generation of MOMP and a direct interaction between these was observed in phospholipid membranes. The apparent affinity of activated Bax for ceramide channels increases with ceramide channel size, consistent with an induced fit mechanism; Bax drives the enlargement of ceramide channels to an optimum fit for the Bax binding site. A ceramide channel specific inhibitor prevented the enhanced MOMP in the presence of Bax and ceramide indicating ceramide channels were the primary permeabilizing entity.

Analogs with changes to all the major structural features of ceramide were used to assess the molecular basis of stability of ceramide channels. Methylation of the C1-hydroxy group abrogated channel formation in mitochondria. Methylation of the amide nitrogen or a change in chirality at C2, which influences the C1-hydroxy group orientation, greatly reduced channel-forming ability whereas other changes were well tolerated. Competition experiments between ceramide and analogs resulted in synergism or antagonism, depending on compatibility of the analog structure with the ceramide channel model. The results provide evidence for ceramide channels being highly organized structures, stabilized by specific inter-molecular interactions.

Analogs that retained channel-forming ability were used to assess the structural features of ceramide channels required for regulation by Bcl-2 family proteins. The stereochemistry of the ceramide head group and access to the amide nitrogen is indispensible for regulation by Bax, implicating the polar portion of the channel as the Bax binding site. Bcl-xL's ability to disassemble ceramide channels depends on the length of the hydrophobic chains of ceramide. Specific Bcl-xL inhibitors reveal that Bcl-xL binds ceramide channels through its hydrophobic groove and this is supported by simulated docking. The opposite effects of pro-and anti-apoptotic proteins are achieved at different sites on the ceramide channel.

CERAMIDE CHANNELS AND THE INDUCTION OF APOPTOSIS: STRUCTURAL INSIGHTS ON CHANNEL FORMATION AND REGULATION BY BCL-2 FAMILY PROTEINS.

By

Meenu Nadisha Perera

Dissertation submitted to the Faculty of the Graduate School of the
University of Maryland, College Park in partial fulfillment
of the requirements for the degree of
Doctor of Philosophy
2012

Advisory Committee:

Professor Marco Colombini, Chair
Assistant Professor Ricardo C. Araneda
Professor Jeffrey Davis
Associate Professor Eric S. Haag
Professor Sergei Sukharev

PREFACE

This dissertation presents my research on ceramide channels and the important role they play in mitochondrial outer membrane permeabilization during apoptosis. Dr. Marco Colombini discovered ceramide channels just before the turn of the 21st century. When I joined his lab, I was presented with the opportunity to expand upon the foundational work conducted on ceramide channels by Dr. Leah Siskind and other former students. Thus, my quest for the past 5 years has been to understand the mechanisms behind the regulation of ceramide channels. What I discovered was that the molecular control of these novel lipid channels stems not only from the molecular identity of the molecules that comprise the channel, but from the interaction of the channel with specific protein modulators.

Chapter one is a general introduction, which begins by describing the process of apoptosis and its dependence on mitochondrial outer membrane permeabilization (MOMP). Also described are the Bcl-2 family of proteins, which regulate MOMP, and the research conducted on ceramide channels thus far.

Chapter two is a compilation of the major techniques and research tools used to accomplish this work. Provided for each method is a conceptual overview and detailed description of the specific conditions used with each technique.

The specific structural components of ceramide that contribute to channel formation and stability were explored in chapter 3. Ceramide analogs were provided by our collaborators: Dr. Leah Siskind, Dr. Alicja Bielawska, Dr. Zdzislaw Szulc from the Medical University of South Carolina and Dr. Robert Bittman from Queens College in

New York. This work was completed in collaboration with Vidyaramanan Ganesan and we discovered that some structural components of the ceramide channel are indispensible for channel formation while changes to other regions of the molecule were well tolerated. Combination experiments between natural ceramide and analogs reinforced previous data in support of ceramide channels being highly rigid and ordered structures; ceramide channels can be destabilized by the introduction of incompatible monomers, can tolerate compatible monomers and can be enhanced by the introduction of monomers that promote stability. This work was published in journal *Biochimica et Biophysica Acta* in 2012. This project demonstrates an additional layer of ceramide channel regulation: the cell has enzymes that generate the specific ceramide monomers that have the propensity for channel formation.

In chapter 4, the interaction of Bax and ceramide channels was explored. We discovered that Bax and ceramide together could induce a synergistic enhancement of MOMP. Further study revealed that the enhanced permeabilization was due to a direct interaction between ceramide and Bax that did not require other mitochondrial proteins or specialized lipids. The data is consistent with an induced fit mechanism: the binding of Bax to a ceramide channel induces the enlargement of the channel so that the binding site of Bax has an optimal fit. Vidyaramanan Ganesan and I worked together on this project, which was published in the journal *Apoptosis* in 2010.

Chapter 5 grew from my interest to understanding how two proteins of the same family, Bax and Bcl-xL, can have opposite regulatory effects on the same channel; Bax enhances ceramide channels and Bcl-xL disassembles them. Using the analogs that retain channel formation, I discovered that Bax binds the polar region of the channel while Bcl-

xL binding is dependent on the hydrophobic region of the channel embedded within the phospholipid membrane. Using known inhibitors of Bcl-xL that bind to the hydrophobic groove of Bcl-xL, I discovered that Bcl-xL binds the ceramide channel through its hydrophobic groove. Dr. Yuri K. Peterson ran molecular docking simulations that revealed possible binding modes of ceramide to the hydrophobic groove of Bcl-xL. This work culminated in a publication in the *Biochemical Journal* in 2012.

In the final chapter, a brief discussion including ideas on the direction of future studies is presented.

DEDICATION

I would like to dedicate this dissertation to my parents Anesta and Peter Perera and my sister, Manuri Perera, whom I love beyond words. I couldn't even begin to thank you for the sacrifices you have made for me, for the happiness you bring me, for being the most generous people I know and for always leading me in the right direction. You are the grace of my life and I thank God everyday for you.

ACKNOWLEDGEMENTS

I would like to express my deepest gratitude to my brilliant mentor, Dr. Marco Colombini, without whom this dissertation would not have been possible. Dr. Colombini is an ever calm, principled man who leads his lab with courage, kindness and by example. He taught me how to approach science with humility, creativity, an open mind and a critical eye. Thank you for your patience, for always being available, for being understanding, for offering encouragement and for having confidence in me. Our shared faith and interest in science made for some wonderful discussions, many of which have helped me develop intellectually as well as spiritually. Thank you Dr. Colombini, for being a great mentor, father-figure, and friend.

I would like to extend my appreciation to the members of my dissertation committee: Dr. Sergei Sukharev, Dr. Eric Haag, Dr. Ricardo Araneda and Dr. Jeff Davis. The insights and questions that stemmed from your diverse scientific backgrounds and expertise helped reveal aspects of this research I had yet to consider. Thank you for your advice and guidance throughout this journey.

I would like to thank my fellow graduate students past and present. We have shared the trials of research and joys of discovery and came out of it all with the bond of friendship that made over five years feel like just yesterday. First and foremost is Vidyaramanan Ganesan. When we joined the lab, we shared the unique experience of being the only two graduate students for quite a while. Since we didn't have a seasoned graduate student to show us the ropes not only did we work together but also learned from each other and challenged each other all the way to two publications. Your sense of

humor, imagination and easy-going but hardworking presence was very much appreciated. Thank you to Shang-Hsuan Lin, Kaiti Chang, Soumya Samanta, Bing Sun, Sarah O'Connell and Chenren Shao for all the wonderful discussions, ideas and fun times we shared during the past almost 6 years. To Wenzhi Tan and Johnny Stiban, although I had not had the pleasure of working with you all directly since your tenure here had ended when I started, thank you for being kind enough to share your experience and advice whenever I sought it out.

There were many undergraduate students that helped me with my research over the years: David Jones, Jinna Choi, Amy Hu, Toan Nguyen, Kevin Yang, Raksha Bangalore, Dipkumar Patel, Kirti Chadha, Stephanie Fischer, Chiemizie Onyewuchi, Pooja Nanavati, Ryan Haughey, Sasika Subramaniam, Viraj Raiker, Malcolm Stennett, Janani Karunaratne, Tim Walsh and Christy Cho. In teaching you and answering your questions, I was able to refine my own technical skills, as well as gain many new friends along the way.

I would like to thank the great administrative staff in the biology department, especially James Parker, Larry Shetler, Lindsey Johnson, KeCia Harper and Wan Chan. A very special thank you also to Lois Reid, who helped make the admissions process as painless as possible, even though I was half way around the world at the time.

To my best friends outside of lab, Shivon Patel, Mohammed Masum and Shagufta Faroqui, you all have truly and unconditionally supported me in so many ways for over 10 years now despite our lives moving in different directions, literally and figuratively. Thank you, for always providing me with laughter and perspective when I need it most. To Selasi Attipoe, meeting you during my first week of grad school was

truly a blessing in so many ways. We became best friends instantly and I'm so thankful to have such a genuinely good person in my life. Thank you for help proof reading parts of this document, your keen eye and the insights you provided was invaluable.

To my immediate family, brother-in-law, Godparents, aunts, uncles, cousins, and grandparents, I could never thank you enough. Your prayers, wisdom and encouragement were a constant presence in my life and your love continues to drive me in everything I pursue. Thank you also to my Godson Evan, I couldn't measure how just how much joy you bring me with every smile.

I would like to thank God, above all, for giving me the strength and peace to achieve this goal.

TABLE OF CONTENTS

LIST OF FIGURES

LIST OF TABLES

LIST OF ABBREVIATIONS

2-MeAA$_3$: 2-methoxyantimycin A$_3$

AIF: Apoptosis Inducing Factor

AK, AK2 : Adenylate kinase

AMP: ampicillin

Apaf-1: Apoptotic protease activating factor 1

Bak: Bcl-2 homologous agonist/killer

Bax: Bcl-2-associated X protein

Bcl-xL: Bcl-2 related protein x(Long)

Bcl: B-cell lymphoma

BH: Bcl-2 Homology

Bid: BH3 interacting domain death agonist

BSA: fatty acid depleted bovine serum albumin

C_{16}-Cer: N-palmitoyl-D-*erythro*-sphingosine , D-*e*-C_{16}-ceramide

$C_{18:1}$-Cer: *N*-oleoyl-D-*erythro*-sphingosine, D-*e*-$C_{18:1}$-ceramide

C_2-Cer: N-acetyl-D-*erythro*-sphingosine

C_{20}-Cer: N-arachidoyl-D-*erythro*-sphingosine

C_{24}-Cer: N-lignoceroyl-D-*erythro*-sphingosine

C_4-Cer: N-butyryl-D-*erythro*-sphingosine

C_8-Cer: N-octanoyl-D-*erythro*-sphingosine , D-*e*-C_8-ceramide

Cyt *c*: Cytochrome *c*

D-*e*-: D-*erythro*-

ddH_2O: double distilled water

DNP: 2,4-dinitrophenol

DPX: p-xylene-bis-pyridinium bromide

DTT: Dithiothreitol

EM: Electron micrograph

Endo-G: Endonuclease G

ER: Endoplasmic Reticulum

GST: Glutathione *S*-transferase

IMS: Intermembrane space

IPTG: Isopropyl β-D-1-thiogalactopyranoside

L-e-: L-*erythro*-

LB medium: Lysogeny Broth A.K.A. Luria-Bertani medium

MAC: Mitochondrial apoptosis inducing channel

MAM: Mitochondrial associated membranes

MIM: Mitochondrial inner membrane

MOM: Mitochondrial outer membrane

Omi/HtrA2: High temperature requirement protein

PBS: Phosphate buffered saline

PM: Plasma Membrane

PTP: Permeability transition pore

PUMA: p53 upregulated modulator of apoptosis

PVDC: polyvinylidene chloride; Saran

ROS: Reactive oxygen species

Smac/DIABLO: Second mitochondria-derived activator of apoptosis/Direct inhibitor of apoptosis binding protein with a low pI

tBid: truncated Bid

TBM: Terrific broth medium

TNF: Tumor necrosis factor

CHAPTER 1:

GENERAL INTRODUCTION

1.1 APOPTOSIS

Apoptosis is a form of programmed cell death that is vital to the survival of multicellular organisms. It is a beneficial process by which unwanted cells are eliminated for the greater good of the organism. Apoptosis is found to occur naturally in all stages of life, from embryonic development, where the digits of the hands and feet are sculpted to remove webbing, to adult tissue homeostasis, where cell death offsets mitosis to maintain a constant amount of cells. Importantly, this process of "cell suicide" is also initiated to prevent the perpetuation of a defective cell when that cell senses it is irreparably damaged. Such deleterious change can originate from within the cell, in the form of DNA damage resulting from mutations, aging, overproduction of reactive oxygen species (ROS), or exposure to cytotoxic agents and harmful conditions, e.g. toxins, viral pathogens, chemicals, UV light, heat-shock, ischemia and others. Thus, apoptosis is a process that is vital to the survival of an organism; however, it is potentially lethal if not scrupulously regulated. Indeed, alterations to the apoptotic machinery causing a shift in balance of when apoptosis is appropriate, leading to either too much or too little apoptosis, often result in pathogenesis. Autoimmune diseases, and cancers are examples of the kinds of diseases that result when a cell is rendered unable to initiate or execute apoptosis, leading to uncontrolled proliferation and accumulation of unwanted cells. However, when excessive apoptosis ensues, following only mild stimuli, it can lead to the elimination of cells that are necessary for the health and survival of an organism. Neurodegenerative diseases, like Alzheimer's disease and Parkinson's disease, and inflammatory diseases like multiple sclerosis and ischemic injury (i.e. stroke or heart attack), are a few examples of when cell death is undesirable and can have dire

consequences. Therefore, the study of apoptosis and how it is regulated is fundamental to understanding the development of a myriad of diseases and finding their cure.

1.1.1 Morphological and Biochemical Characteristics of Apoptotic Cells.

When a cell chooses to undergo apoptosis, a series of events are "programmed" to be executed in an active (energy requiring) and controlled manner: the cell expends energy to ensure cellular contents are systematically degraded and carefully packaged so they may phagocytosed and eliminated without contaminating the extracellular space. Apoptosis is distinguished from other forms of cell death by specific morphological and biochemical changes. Kerr and associates described the distinct morphological changes that take place in apoptotic cells using electron microscopy (EM) (Kerr et al., 1972). These morphological changes (DNA fragmentation, chromatin condensation, plasma membrane (PM) blebbing, phosphatidylserine externalization to the outer leaflet of the PM, cytoplasmic condensation, and the packaging of cellular contents into apoptotic bodies) are now considered to be indicative of the late stages of apoptosis. Interestingly, organelles of apoptotic cells such as mitochondria and lysosomes retain their normal ultrastructure with minimal to no swelling (Kerr et al., 1972) and the integrity of the plasma membrane is maintained. The resulting apoptotic bodies are neatly engulfed by macrophages or proximal cells, which then degrade and recycle the ingested contents. As an active process, functional mitochondria are required to maintain ATP levels, and consequently mitochondrial transmembrane potential, until late apoptosis. Depending on the apoptotic stimulus, the mitochondrial outer membrane may be permeabilized, leading to caspase activation that will facilitate the progress of the apoptotic program (Saraste, 1999).

When traumatic injury to a cell results in the loss of ATP synthesis and the method of cell death is “passive” or energy-independent, termed oncosis (Majno & Joris, 1995), this will result in a necrotic morphology, termed primary necrosis. It is important to note that apoptosis typically confers an advantage to an organism and affects only a single cell or small group of cells. On the contrary, necrosis does not confer an advantage and is characteristic of large-scale damage to cells and tissues in a particular area as in the case of gangrene. Morphologically, necrosis is characterized by swelling of the cell and its organelles and the loss of membrane integrity (Searle et al., 1982). Permeabilization of the mitochondrial inner membrane (MIM) leads to the loss of the transmembrane potential required for the generation of ATP; and mitochondrial swelling can lead to the rupture of the mitochondrial outer membrane (MOM), leading to caspase activation. Loss of lysosomal membrane integrity results in the release of harmful enzymes into the cytoplasm and nuclear membrane disintegration can lead to the breakdown of DNA and RNA. Ultimately the cell contents are spilled into its surroundings initiating an inflammatory response.

There is evidence in some cases of a shift between an apoptotic cell fate and one that results in necrosis, which occurs when the apoptotic program cannot be completed as designed. This case is termed secondary necrosis. For instance, if a cell receives an apoptotic stimulus that causes the MIM to be compromised, the apoptotic program can be completed so long as a sufficient number of mitochondria can generate the ATP needed (Krysko et al., 2001). However, if the MIM becomes permeabilized at some point in this process, upstream or downstream of MOM permeabilization, and ATP synthesis is lost, the cell will switch to a passive means of cell death and progress to a necrotic

morphology (Searle et al., 1982; Leist et al., 1997). Another instance where secondary necrosis may result is if the phagocytes do not reach the apoptotic bodies in sufficient time to clear them, leading to an inflammatory response. Evidently, apoptotic bodies cannot remain intact indefinitely as clearance must occur within a given time frame (Silva et al., 2008). Nevertheless, M.T. Silva has suggested that secondary necrosis should be understood as a possible outcome of a completed apoptotic regimen, rather than the result of a failed immune response or a "fall-back" plan (Silva, 2010).

1.1.2 Extrinsic vs. Intrinsic Apoptosis

A cell can undergo apoptosis by two primary mechanisms: extrinsic or intrinsic apoptosis. These pathways are defined by the origin of the signals leading to apoptotic initiation. In extrinsic apoptosis, the signal originates outside of the cell and leads to the ligation of death receptors of the Tumor Necrosis Factor (TNF) family, like TNF-α and CD95, on the PM (Lavrik & Krammer, 2009). The ligation of these death receptors leads to the recruitment of intracellular components to form the Death-Inducing Signaling Complex (DISC), which results in the activation of caspase-8. Cells are classified as type 1 if caspase-8 then directly initiates the effector caspases- 3, -6, and -7 leading to the execution phase of apoptosis. If caspase-8 leads to apoptosis through the engagement of mitochondria, the cells are classified as type II. In this instance, caspase-8 cleaves a pro-apoptotic activator protein Bid to its active form, which will lead to the accumulation of pro-apoptotic lipids and proteins on the MOM to cause MOMP and intermembrane space (IMS) protein release and subsequent effector caspase activation (Krammer et al., 2007; Kroemer et al., 2007). In the intrinsic pathway of apoptosis, the signal to initiate the apoptotic process comes from within the cell. Typically, when cellular or DNA damage is

detected, the levels of p53, a tumor suppressor protein and a transcription factor, become elevated within the cell (Kroemer et al., 2007). p53 induces cell cycle arrest until DNA can be repaired. If the DNA damage is too severe to be repaired, activated p53 will lead to the upregulation of a number of pro-apoptotic proteins, namely of the Bcl-2 family of proteins (Hemann & Lowe, 2006) and can in some cases cause an increase in the bio-active sphingolipid ceramide (Heffernan-Stroud & Obeid, 2011). The activation of the pro-apoptotic members of the Bcl-2 family and neutralization of anti-apoptotic Bcl-2 family of proteins will prime the MOM for the release of key intermembrane proteins like cytochrome *c* (Liu et al., 1996). Once in the cytosol, cytochrome *c* along with apoptotic protease activating factor 1 (APAF-1) and procaspase-9 form what is collectively called the apoptosome, resulting in cleavage and activation of caspase 9 which activates the downstream effector caspases-3, -6, and -7 (Li et al., 1997b). Effector caspase activation will lead to the execution of apoptosis and the hallmark morphological changes associated with it. In apoptosis, MIM permeability transition typically occurs downstream of caspase activation, and leads to mitochondrial inner membrane swelling and the eventual rupture of the MOM.

1.2 MITOCHONDRIA-MEDIATED APOPTOSIS

Mitochondria, while most famous for being the powerhouse of the cell, are also a key mediator of apoptosis, and several modes of apoptotic regulation converge at the mitochondrial interface. This is because mitochondrial outer membrane permeabilization to IMS proteins, especially cytochrome *c*, can commit a cell to undergo apoptosis and is

essentially the point of no return (Liu et al., 1996). For example, if cells are deprived of growth factor, cytochrome *c* and other proteins will be released from the IMS of mitochondria to the cytosol and the cell will be irreversibly committed to the execution phase of apoptosis. However, if growth factor is restored before MOMP occurs, cytochrome *c* will not be released and the cell will survive (Vander Heiden et al., 1999). Although a number of apoptosis-relevant proteins are released from mitochondria, only release of cytochrome *c* is required to initiate downstream caspase activation and microinjection of even small amounts of cytochrome *c* into normal cells can induce apoptosis (Zhivotovsky et al., 1998). The other apoptosis-relevant IMS proteins released includes: apoptosis inducing factor (AIF), endonuclease-G (Endo-G), second mitochondria-derived activator of caspase/direct inhibitor of apoptosis binding protein with a low pI (Smac/DIABLO), and Omi/high temperature requirement protein A2 (Omi/HtrA2) (Kroemer et al., 2007). AIF and Endo-G can directly promote DNA fragmentation and chromatin condensation. Smac/DIABLO and Omi/HtrA2 promote cell death indirectly by countering the survival efforts of the family of inhibitor of apoptosis proteins (IAP), which prevent effector caspase activation (Kroemer et al., 2007).

1.2.1 Characteristics of Mitochondrial Outer Membrane Permeability

From the time a cell is exposed to a cytotoxic agent or stress, the cell begins preparations to decide its own fate. When the cell is not salvageable, the decision to proceed with the organized breakdown of the cell is characterized by the increase in permeability of the mitochondrial outer membrane to IMS proteins. The increase in permeability of the MOM has been demonstrated to be a highly coordinated and fast event with most of the mitochondria in a cell releasing their cytochrome *c* within 5-10

minutes (Martinou et al., 2000). However, there is evidence that suggests that there is some heterogeneity of mitochondria within cells (D'Herde et al., 2000); while most mitochondria do become permeabilized, a small population of normal mitochondria can retain their cytochrome *c*. Taken together, this suggests that for apoptosis to progress to the execution phase, sufficient cytochrome *c* release must occur in order to have enough effector caspase activation. Some factors that might affect this threshold are cell type, the nature of the mutations the cell has incurred, and how primed the mitochondria are in these cells to allow for IMS protein release. The MOMP inducing entity must be non-selective because a variety of proteins are released concomitantly with cytochrome *c* (Munoz-Pinedo et al., 2006). In fact, cytochrome *c* represents the lowest molecular weight cutoff for a pro-apoptotic mitochondria pore as other IMS proteins known to exit mitochondria are much larger i.e. Adenylate Kinase 2 (AK2, 140kDa) (Kohler et al., 1999) and other complexes, like EndoG (66 kDa dimer) (Cote & Ruizcarrillo, 1993). Moreover, evidence suggests that the pore must be stable enough to remain open for long periods of time post cytochrome *c* release as proteins like AIF, a mitochondrial inner membrane protein, require processing before it can be released (Munoz-Pinedo et al., 2006).

1.3 REGULATION OF MITOCHONDRIAL OUTER MEMBRANE PERMEABILIZATION: THE BCL-2 FAMILY OF PROTEINS

A highly studied family of proteins called the Bcl-2 family proteins regulates MOMP. Bcl-2 family proteins are all nuclear encoded and can be categorized into two

functional categories: pro-apoptotic and anti-apoptotic. Based on sequence homology, anti-apoptotic members contain up to four Bcl-2 homology domains (BH1234) and pro-apoptotic members contain up to three Bcl-2 homology domains (BH123). A sub class of pro-apoptotic members contains only the BH3 domain (BH3) and typically function to activate the pro-apoptotic Bcl-2 family members or neutralize anti-apoptotic Bcl-2 members. Some prototypical members of the anti-apoptotic side of the family tree include of Bcl-2, Bcl-xL, BFL/A1, Bcl-w, and Mcl-1. Pro-apoptotic multi-domain proteins include Bax, Bak and Bok and some of the BH3 only members include Bid, Bim, Bad, Puma, Noxa and Bik. A major way by which Bcl-2 family proteins are thought to regulate apoptosis is by antagonizing the actions of members with opposing functions at the mitochondrial interface (Leber et al., 2010). The BH3 domain, which is shared by all Bcl-2 family proteins, facilitates the direct antagonism between the pro- and anti-apoptotic proteins.

In normal cells both pro- and anti-apoptotic Bcl-2 family proteins have been found to occupy a variety of sub-cellular locations. Mitochondria of normal cells contain Bak, which is held in its inactive conformation by interactions with the Voltage Gated Anion Channel isoform 2 (VDAC2) (Cheng et al., 2003; Lazarou et al., 2010), along with anti-apoptotic proteins Bcl-2, Bcl-xL and Mcl-1 (Boise et al., 1993; Mikhailov et al., 2001; Andersen & Kornbluth, 2012). While Bak and Bcl-2 are constitutively localized to mitochondria, Bcl-xL and Mcl-1 reserves reside in the cytosol, and are held inactive with neutralizing BH3 only proteins (Yao et al., 2009). Bax and Bid are cytosolic proteins and some Bax can be found loosely attached to the MOM (Antonsson et al., 2001; Er et al., 2006).

Upon applying an apoptotic stimulus, a number of changes in sub-cellular location, conformation, and expression of Bcl-2 proteins take place. Bid is cleaved by caspase 8 to yield the active 15kDa fragment, tBid, which disassociates from its inactive fragment upon binding to the mitochondrial membrane (Billen et al., 2008; Lovell et al., 2008). tBid and Bim can activate Bax in the cytosol, causing a conformational change that exposes the hydrophobic interior of Bax, which allows its translocation to the MOM (Zhou et al., 2006; Renault & Manon, 2011). At the MOM, tBid facilitates the insertion of Bax into the MOM and promotes the oligomerization of activated Bax with other Bax and/or Bak molecules (Annis et al., 2005; Zhang et al., 2010). Activated Bax itself can also activate and oligomerize with other Bax molecules without tBid (Tan et al., 2006). tBid also activates Bak to dissociate from VDAC2. The increase of active pro-apoptotic Bcl-2 family proteins in the MOM are prevented from causing MOMP by a concomitant translocation of their anti-apoptotic counterparts, Bcl-xL and Mcl-1. The pro- and anti-apoptotic proteins heterodimerize in the MOM, antagonizing and effectively neutralizing each other until the cell has decided whether the damage inflicted can be reversed. If the damage can be fixed, an increase in expression of the anti-apoptotic proteins will overcome the increased concentration of pro-apoptotic proteins in the MOM and MOMP is prevented. If the extent of damage is too severe, the cell will signal the increase in expression and activation of pro-apoptotic Bcl-2 members. The BH3 only protein Bad will neutralize Bcl-xL, Bcl-2 and Mcl-1 by binding to hydrophobic groove of these proteins. Once the anti-apoptotic proteins are neutralized and outnumbered by the pro-apoptotic proteins, the mitochondrial outer membrane will become permeabilized to IMS

proteins, and the execution phase of apoptosis will commence. Thus, it is the sensitive balance of anti-and pro-apoptotic proteins that hold the key to life and death of the cell.

1.3.1 Bax Channels

The true nature of the entity responsible for MOMP remains unknown and is the topic of much debate. However, the major paradigm implicates channels composed of Bax homooligomers or heterooligomers of Bax and Bak as responsible for IMS protein release during apoptosis. The finding that Bax can form channels grew from studies that described structural similarities of Bcl-xL to the pore forming domains of diphtheria toxin and bacterial toxins called colicins A1 and E1 (Muchmore et al., 1996) and the discovery that Bcl-xL could form ion channels in synthetic membranes (Minn et al., 1997). The membrane active structure of Bax is currently unknown and a number of conformational changes are known to precede membrane association, oligomerization and channel formation. The N-terminus of the protein, containing α-helix 1, contains the mitochondrial targeting sequence termed the Apoptotic Regulation of Targeting domain (Goping et al., 1998). The C-terminal α-helix 9 has also been shown to play a role in mitochondrial targeting (Nechushtan et al., 1999). α-helixes 5 and 6 form the hydrophobic groove of the protein and are flanked by the other 7 helices (Suzuki et al., 2000). The C-terminal α- helix 9 sits within the hydrophobic groove, stabilizing the protein in its inactive form. The N-terminal face of Bax contains a binding site for activating BH3 only proteins and this site is opposite to the BH3-groove. When an activating BH3- only protein binds Bax, the Apototic Regulation of Targeting Domain undergoes a shift and this is sufficient to target the protein to the MOM (Goping et al.,

1998) as well as expose the Bax BH3 domain found on α-helix 2 (Gavathiotis et al., 2010). Binding of tBid also causes a conformational change at α-helix 9 which now moves to expose the hydrophobic groove of Bax. Exposure of this hydrophobic groove activates Bax and leads to membrane insertion. Active membrane bound Bax can activate other Bax molecules as well (Tan et al., 2006). Further conformational changes in the membrane occur leading to oligomerization and/or channel formation. It is known that α-helices 5, 6 and 9 are transmembrane domains and α-helix 5 and 6 form the lumen of the channel (Heimlich et al., 2004).

Bax mediated membrane permeabilization has been shown to display a number of different properties and it is quite possible that Bax channels are not entirely proteinaceous in nature. For example, Bax can form small ion channels that are impermeable to cytochrome *c* when activated by tBid (Schlesinger et al., 1997; Roucou et al., 2002); oligomeric Bax can also form large supra-molecular openings in liposomes (Kuwana et al., 2002) capable of releasing dextrans of up to 2 MDa in size; Bax and/or Bak oligomers can form Mitochondrial Apoptosis Inducing (MAC) channels which are voltage independent and just large enough to release cytochrome *c* (Martinez-Caballero et al., 2009); and Bax peptides corresponding to α-helices 5 and 6 can induce proteo-lipidic toriodal pores with similar properties to full-length Bax (Garcia-Saez et al., 2005; Garcia-Saez et al., 2006). Recent findings have indicated that Bax can form two types of channels: one that is small and one that is large. The small channels are of a uniform size, cytochrome *c* impermeable, and voltage dependent; while the large channels are protein permeable and voltage independent with a variable size (Lin et al., 2011).

With such a wide range of properties described for Bax channels, the lack of uniformity of these studies suggest that Bax channel properties are affected by cell-type, apoptotic stimuli, intrinsic membrane curvature, and the method by which Bax is activated. Although there is even some controversy of whether activated Bax is even an oligomer (Ivashyna et al., 2009), the current opinion in the field of apoptosis suggests that oligomeric Bax channels are responsible for cytochrome *c* release and the induction of apoptosis. The study by Lin and associates would suggest that both small and large Bax channels could exist, with an as yet unknown molecular component being responsible for switching between the two when IMS protein release is signaled (Lin et al., 2011).

1.4 THE ROLE OF CERAMIDE IN APOPTOSIS

Ceramide is a bioactive sphingolipid that has been implicated in many different biological processes such as cell signaling, cell senescence, and cell differentiation. Importantly, many studies have implicated ceramide as a pro-apoptotic and anti-proliferative lipid, earning it the nickname "the tumor suppressor lipid" (Fig 1.1).

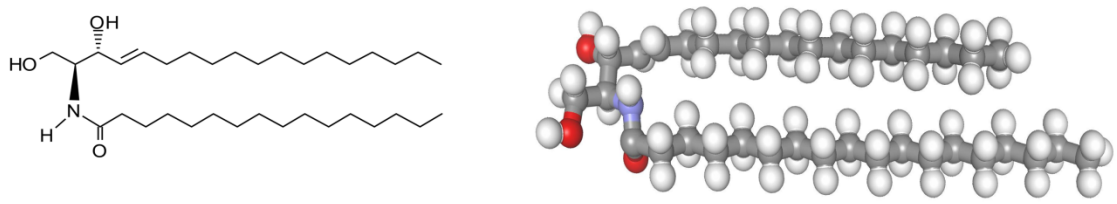

C16-Cer (2*S*,3*R*,4*E*) C16-ceramide

Figure 1.1 The Structure of Ceramide.
Natural long-chain ceramide is shown here with a fatty acyl chain length of 16 carbons. Other naturally occurring ceramide species vary in fatty acyl chain length from 12 to 24 carbons whereas synthetic ceramides can range between two ten carbons.

A variety of apoptotic stimuli can lead to an increase in intracellular ceramide levels, including TNF-α, etoposide, endotoxin, staurosporine, ionizing irradiation, and UV irradiation. Ceramide generation can occur either upstream or downstream p53 activation or independently of p53 activation (Heffernan-Stroud & Obeid, 2011). Stimulating ceramide generation can promote cell death whereas inhibiting ceramide generation or metabolizing ceramide to other non-threatening species can delay or prevent cell death (Mullen & Obeid, 2012). Thus, it has been demonstrated that cell death can be mediated by controlling ceramide levels (Lucci et al., 1999a; Itoh et al., 2003; Liu et al., 2004; Reynolds et al., 2004). It has been found in a number of different cells lines that a cellular sensitivity to number of chemotherapeutic agents is mediated by the ability to elevate ceramide, including gemcitabine, circumin and doxorubicin (Lavie et al., 1997; Lucci et al., 1999b; Reynolds et al., 2004; Dumitru et al., 2009). Thus, importance of ceramide in apoptosis is widely acknowledged and understanding its role in apoptosis is vital to understanding and preventing disease (Siskind, 2005; Carpinteiro et al., 2008; Mullen & Obeid, 2012).

1.4.1 Ceramide Metabolism

Sphingolipid metabolism involves a multitude of enzymes with unique functions and several metabolites found in a number of sub cellular compartments. New enzymes continue to be discovered as more studies are undertaken to better understand this intricate metabolic scheme (Mullen & Obeid, 2012). With such a complex system, there is much overlap between ceramide generating pathways, which allows both functional redundancy as well as many opportunities for the system to go awry, making the precise control of ceramide levels in *in vivo* quite difficult to study. The effectiveness of specific

pharmacological inhibitors of ceramide synthesis, or other sphingolipids, is often curtailed as the product of interest can often be generated by other means. Despite this level of complexity, upon an apoptotic stimulus, the cell manages to elevate ceramide levels, specifically in mitochondria, with the exact stereochemistry, extent of unsaturation and hydrocarbon chain length required for apoptotic control. Clearly this is a highly controlled and deliberate mechanism of apoptotic control in cells.

Two main pathways could generate the ceramide accumulated in mitochondria under apoptotic stress: the *de novo* pathway and the salvage pathway (Fig 1.2). *De novo* synthesis occurs in the endoplasmic reticulum (ER) (Hanada et al., 2003; Lahiri & Futerman, 2005). The salvage pathway leads to the generation of ceramide from other lipid species including the conversion of sphingomyelin, by sphingomyelinases, sphingosine, by ceramide synthase, and glycosphingolipids, like glucosylceramide, by glycosidases, like glucocerebrosidase (Mullen & Obeid, 2012).

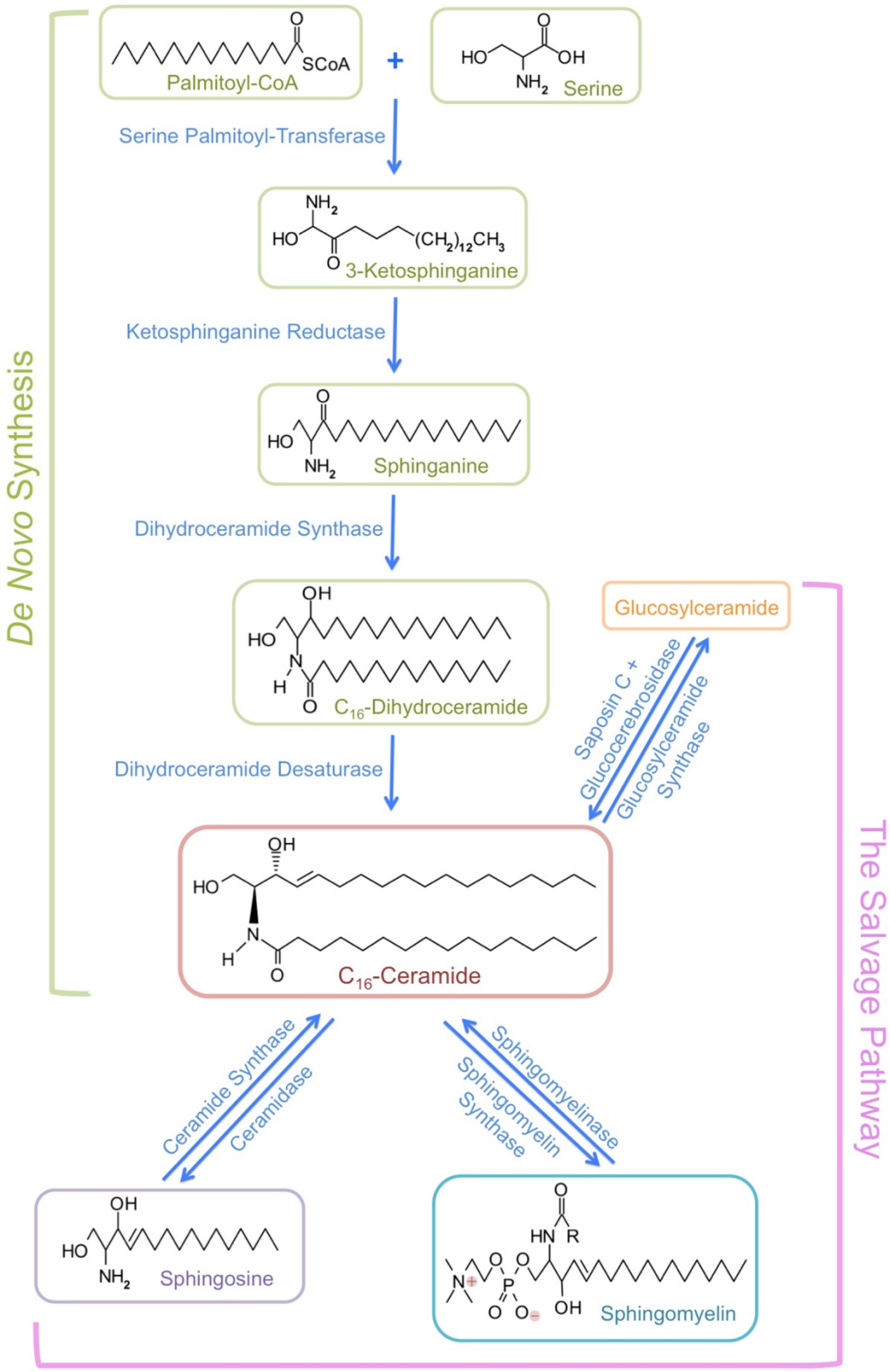

Figure 1.2 Major Pathways Involved in the Metabolism of the Sphingolipid Ceramide

1.4.2 Modulation of Ceramide Metabolism: Balancing Cell Death and Immortality

Modulating ceramide generation reveals the importance of ceramide in cell death and how lack of ceramide can contribute to the immortality of cancer cells. The majority of sphingolipid metabolism occurs outside of the mitochondria, in the ER, Golgi apparatus, and lysosomal, nuclear and plasma membranes. However, Birbes and associates found that only targeting sphingomyelinase to mitochondria resulted in apoptosis (Birbes et al., 2001; Birbes et al., 2005). Thus, while the mechanism of ceramide formation in mitochondria during apoptosis is incomplete, mitochondrial ceramide must play a key role in mitochondria-mediated apoptosis. There is now evidence that mitochondria possess the enzymes necessary to generate ceramide (Shimeno et al., 1998; Wu et al., 2010) and ceramide can be rapidly transferred to mitochondria from mitochondrial associated membranes (MAMs) (Stiban et al., 2008) and from the plasma membrane (Babiychuk et al., 2011). Exogenously added ceramide can also induce cell death in cells (Obeid et al., 1993; Cifone et al., 1994; Jarvis et al., 1994; Quintans et al., 1994; Flowers et al., 2012). A study by Yang and associates demonstrated that if sphingomyelin synthase 1, which generates sphingomyelin and diacylglycerol from ceramide and phosphatidylcholine, were expressed in yeast, these cells showed an increased resistance to cell death induced by ceramide treatment (Yang et al., 2006). Multiple studies by M.C. Cabot and others have demonstrated that glucosylceramide synthase overexpression, and subsequent increase in the level of glucosylceramide is a main contributor to the development of multidrug resistance in cancer cells and inhibition of the glycosylation can re-sensitize cells to chemotherapeutic drugs (Komori et al., 1999; Liu et al., 1999; Lucci et al., 1999a; Liu et al., 2001;

Kohyama-Koganeya et al., 2004; Patwardhan et al., 2009). Another study found that inhibition of ceramide glycosylation can also re-instate p53 dependant apoptosis in p53 mutant cells (Liu et al., 2011). Thus, if the ceramide generating enzymes are increased in a cell, then cell death can be promoted; if ceramide consuming enzymes are increased, then cell death is prevented (Fig 1.3).

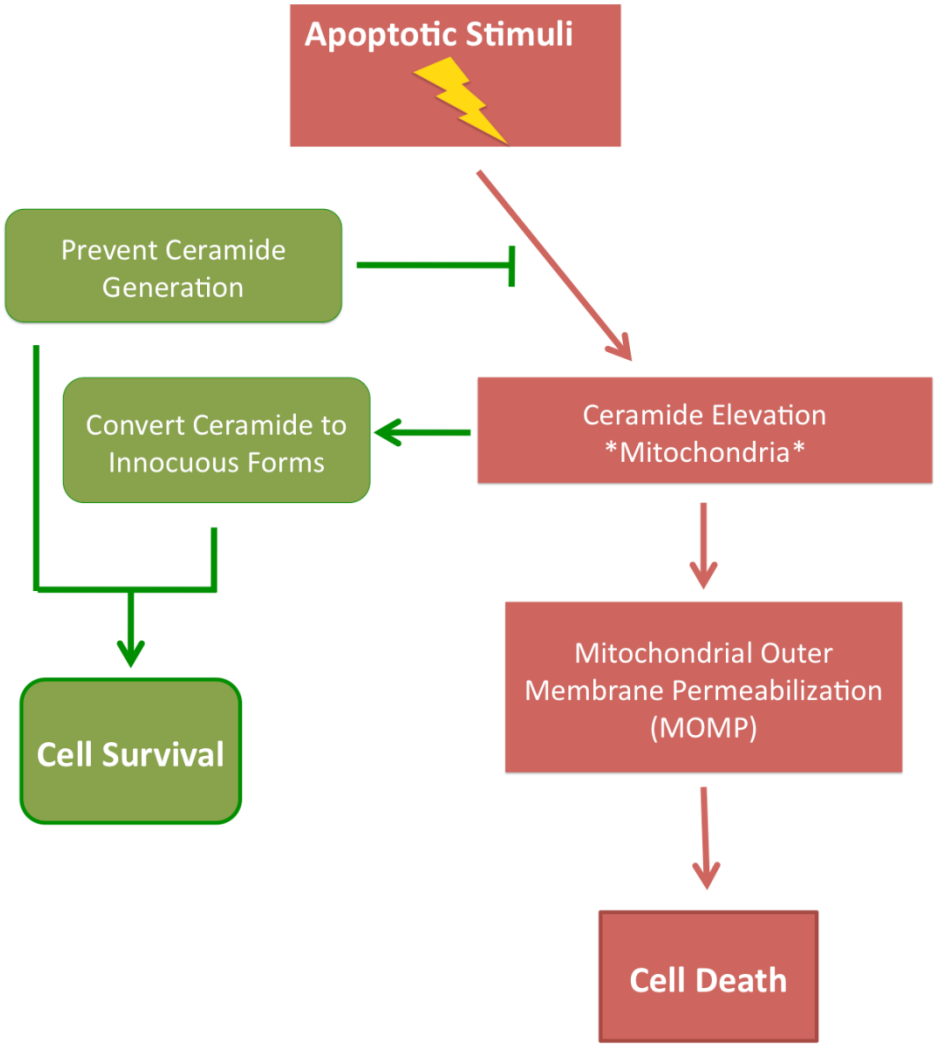

Figure 1.3 Control of Cell Death and Survival Through Modulation of Ceramide Metabolism.

Upon an apoptotic stimulus, ceramides become elevated in the outer membrane of mitochondria. If this elevation can be prevented or if the ceramide generated is converted to less lethal species,

the cell may survive. If the mitochondrial outer membranes become permeabilized, cell death is imminent.

1.5 CERAMIDE CHANNELS

The exact mechanism by which ceramide mediates cell death is still a matter of debate. Is ceramide elevation simply priming the mitochondrial outer membrane for permeabilization by other pro-apoptotic factors or could ceramide play a more direct role? It was found by multiple laboratories that natural ceramide could increase the permeability of the MOM to IMS proteins (Ghafourifar et al., 1999; Siskind & Colombini, 2000; Di Paola et al., 2004). Dr. Siskind and Dr. Colombini discovered that ceramide can form stable transmembrane channels in membranes that are large enough for the release of IMS proteins, which is the irreversible step committing the cell to apoptosis (Siskind & Colombini, 2000). Two key pieces of evidence further implicated the role of ceramide channels as an important piece of the MOMP generating and regulating machinery: first, that, unlike the parental strain, Bax/Bak double knockout cells, which are highly resistant to apoptosis, are also unable to elevate mitochondrial ceramide levels (Siskind et al., 2010) and second, anti-apoptotic Bcl-2 family proteins can disassemble ceramide channels directly and prevent MOMP (Siskind et al., 2008). This section will focus on novel studies that have been conducted to characterize this unique channel as this may be the pathway by which key proteins escape the MOM to initiate apoptosis.

1.5.1 Structure of Ceramide Channels

Like protein assemblies or complexes, ceramide channels take a form dictated by its monomers. There are five important features of the ceramide molecule that allow for the formation of ceramide channels. These features are highlighted in (Fig 1.4, top).

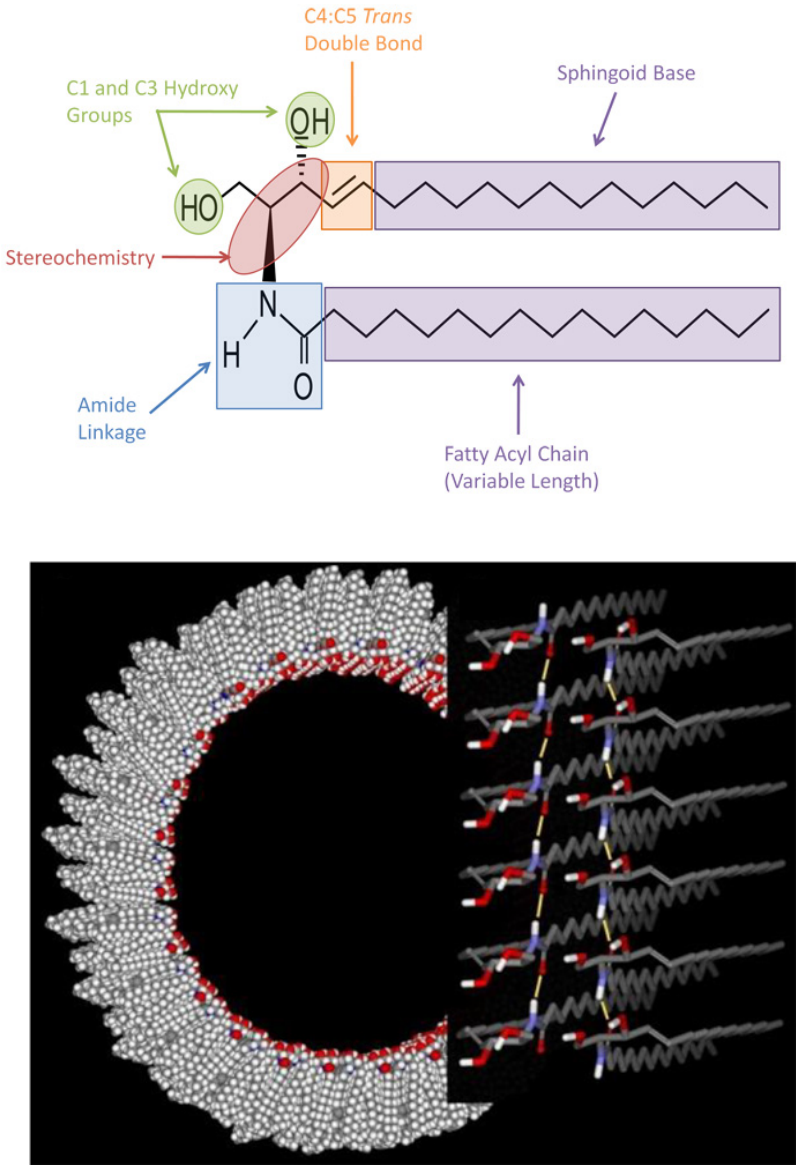

Figure 1.4 Model of a Ceramide Channel

Top: Five important areas of the ceramide molecule contribute to channel formation. Bottom: Ceramide molecules arrange themselves into columns with a free amide nitrogen on one end and

a free carbonyl group at the other. Adjacent ceramide columns have an antiparallel orientation to satisfying the dipole moment of each column. Ceramide columns are held together by hydrogen bonding between C1 and C3 hydroxy groups to form a cylindrical channel. An expanded view of two ceramide columns in antiparallel orientation is shown on the bottom right. Each column consists of a stack of 6 ceramide molecules. The figure shows the hydroxyl groups that would face the channel lumen and the hydrocarbon chains extending into the background, toward the lipid bilayer. The yellow bars indicate the hydrogen-bonding between the amide group of one ceramide and the carbonyl group of the adjacent ceramide. Bottom image is reproduced from (Perera et al., 2012)

The C4:C5 trans double bond is thought to confer the pro-apoptotic function of ceramide as the precursor dihydroceramide, which lacks the double bond at this position, is widely considered the inactive form (Bielawska et al., 1993; Obeid et al., 1993; Ahn & Schroeder, 2010; Grösch et al., 2011). In fact, the presence of dihydroceramide can inhibit ceramide channel formation, suggesting the molecular incompatibility of these molecules when it comes to channel formation (Stiban et al., 2006). The amide linkage is responsible for stabilizing the secondary structure of proteins, like in an α–helix, and allows for the arrangement of ceramide monomers into ceramide columns (Fig 1.4, bottom left). These ceramide columns have one free amide nitrogen at one end and a carbonyl oxygen at the other and this results in a dipole moment. Ceramide columns arrange themselves in an anti-parallel fashion in order to offset their respective dipoles. The C1 and C3 hydroxy groups hold these columns together to form a channel in the membrane (Fig 1.4, bottom right). The length of the fatty acyl chain and the sphingoid chain have little influence on the ability of ceramide to form channels as even a fatty acyl chain of only 2 carbons can easily form channels. It is important to note however that only long chain natural ceramides, C16, C18 and C20 ceramides are commonly elevated

upon an apoptotic stimulus and this must be of some physiological relevance (Mizutani et al., 2005; Pewzner-Jung et al., 2006; Grösch et al., 2011). Molecular dynamics studies (Anishkin et al., 2006) highlighted another important structural characteristic of ceramide important for channel formation: ceramide probably has a dual curvature (Fig 1.5). The intrinsic curvature of a lipid is the ratio of the relative bulk of the head group compared to the hydrophobic region. If the head group and the hydrophobic region of a given lipid have approximately the same size, then it will form a membrane with zero curvature. If the head group is smaller, than the lipid will favor a negative curvature; if the opposite were true, the lipid would favor a positive curvature. The dual curvature of the ceramide

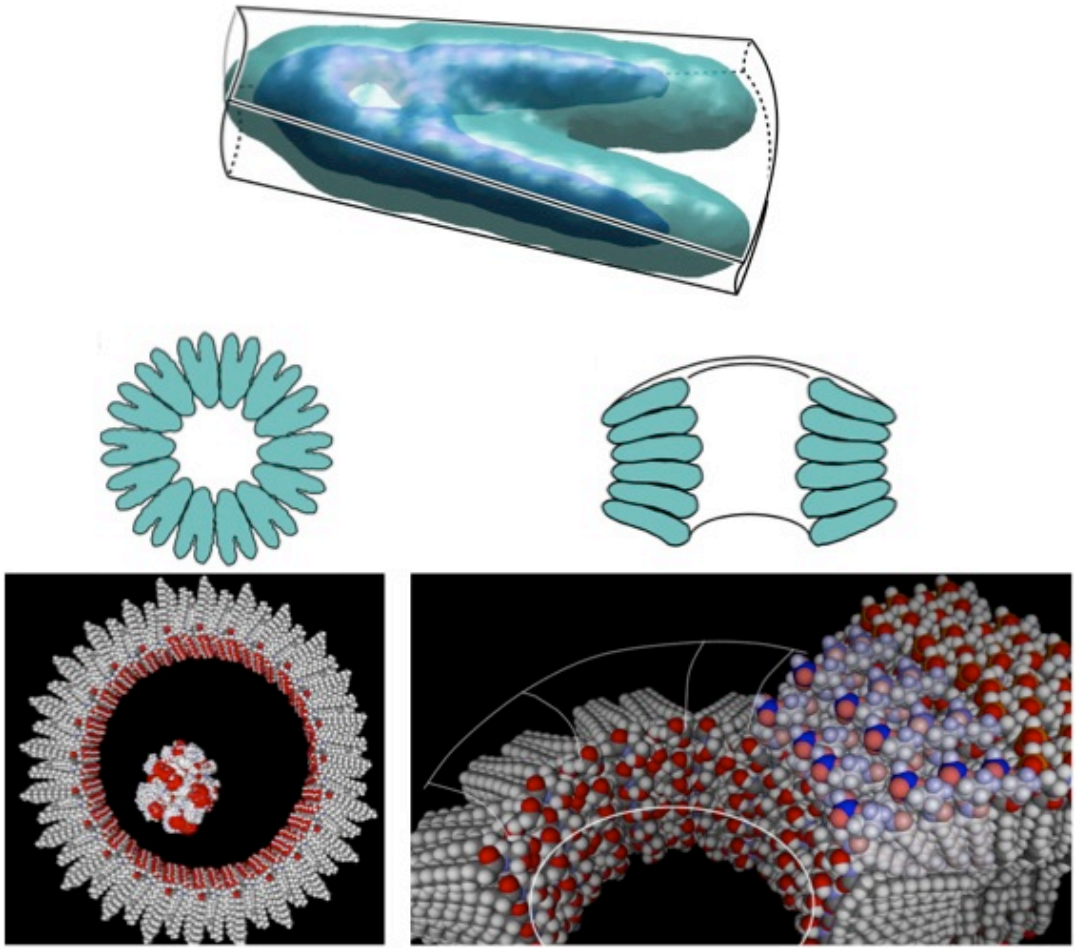

Figure 1.5 Ceramide Channels Have a Dual Curvature

Top: Molecular dynamics simulations revealed that ceramide probably has a dual curvature (Anishkin et al., 2006). This allows ceramide to form cylindrical channels with a negative curvature in the plane of the membrane (bottom right). Cytochrome *c* is pictured in the lumen of the channel. Bottom left: ceramide channels have a positive curvature perpendicular to the plane of the membrane. The positive curvature as shown here allows for a low energy compromise by both the ceramide channel and phospholipid membrane to mutually curve to stabilize the channel-membrane border, and thus the stability of the channel, and prevent high energy exposure of the a-polar regions to the aqueous phase. The phospholipids (shown with the light blue head group) curve in to form a continuous polar surface with the ceramide channel. The bottom images are reproduced from (Samanta et al., 2011) and all others are from (Anishkin et al., 2006).

molecule allows ceramide channels to form a negative curvature in the plane of the membrane and a positive curvature perpendicular to the plane of the membrane (Fig 1.5). This allows for the stabilization of the channel-membrane interface, and essentially allowing for the lowest energy interaction.

Evidence from studies conducted by Siskind and associates demonstrated that ceramide does not simply induce membrane defects or have detergent like effects but indeed forms channels. For example, ceramide channels formed in the MOM are easily disassembled when fatty acid free bovine serum albumin (BSA) is added, in a mechanism consistent with shifting the dynamic equilibrium of ceramide molecules away from channel formation and to ceramide monomers and ceramide bound to BSA (Siskind et al., 2002). In planar phospholipid bilayers containing a ceramide channel, lanthanum ions induce channel disassembly after a variable delay and the channel disassembles preferentially in multiples of 4 nS, or multiples of two ceramide columns (Siskind et al., 2003). The variable delay indicates that channel disassembly is a stochastic event, inconsistent with that of a membrane defect. Moreover, while detergents can easily lyse erythrocyte membranes and disrupt solvent free planar phospholipid membranes, ceramide does not do either (Siskind et al., 2006). In fact, mitochondria can be permeabilized a level greater than 75% of maximum by treatment with ceramide and this is still reversible by the addition of BSA while mitochondria treated with detergent or hypotonic shock do not re-anneal (Siskind et al., 2002).

1.5.2 Properties of Ceramide Channels.

For ceramide to be a good candidate pathway for the release of IMS proteins from mitochondria, the properties of ceramide channels should be in line with the known properties of the enigmatic pathway responsible for the permeabilization of mitochondria, and most importantly ceramide channels must be tightly regulated.

1.5.2.1 Size of ceramide channels

Ceramide channels can form in a variety of sizes as observed in planar bilayer membranes, liposomes and mammalian mitochondria. Ceramide channels were recently visualized using transmission electron microscopy of negatively stained liposomes (Samanta et al., 2011). This method allows one to visualize a topographical view of the liposome. Ceramide channels are detected as a stain filled cylindrical pores (Fig 1.6, arrow). The average size of the pore detected through this method was about 10 nm in diameter, which could allow the passage of proteins <500kDa. As discussed in section 1.2, a variety of proteins exit the mitochondria upon apoptosis and the apoptotic pore is both unselective and large enough to accommodate up to 150kDa MW proteins (Munoz-Pinedo et al., 2006). A ceramide channel would easily accommodate cytochrome *c* (12 kDa, 3.4 nm in diameter) and also the largest proteins known to exit the mitochondria during apoptosis: e.g. Htra2/omi (108 kDa trimer) and APAF-1 (137 kDa).

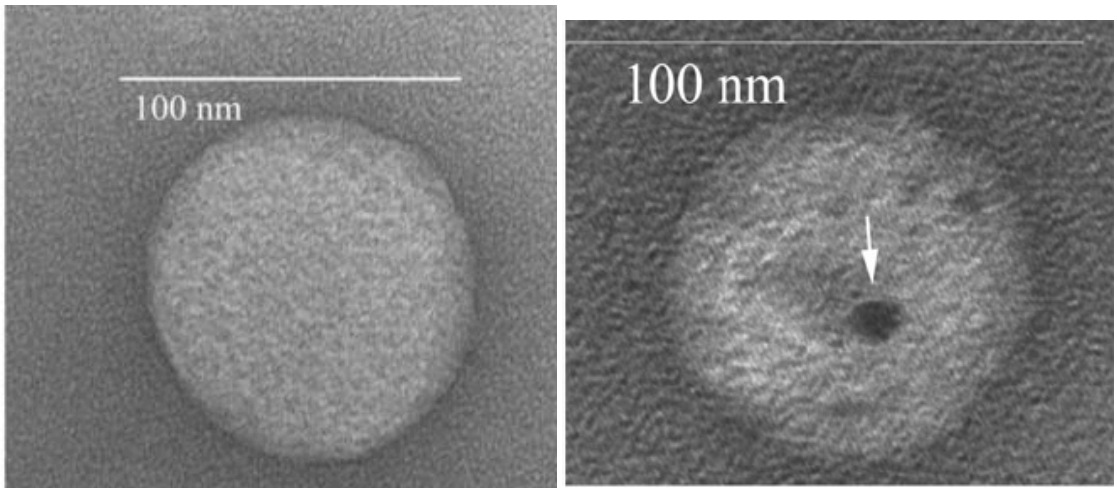

Figure 1.6 Electron Micrograph of a Ceramide Channel in a Liposome

Left: Negative stained liposome that was not treated with ceramide. Right: C_{16}-Ceramide treatment of a liposome resulted in the formation of a ceramide channel, which is seen here filled with negative stain. These images are reproduced from (Samanta et al., 2011).

1.5.2.2 Ceramide channel lifetime.

Ceramide channels are highly stable long lasting structures as detected in mammalian mitochondria and in electrophysiological recordings of channels formed in planar membranes. During apoptosis, it was found that the release of cytochrome *c* occurred in a synchronized fashion from all or most of the mitochondria in a cell (Heiskanen et al., 1999; Goldstein et al., 2005). However, while the release of cytochrome *c* alone is sufficient to induce apoptosis, another protein known to exit the mitochondria upon MOMP, AIF is a MIM protein and requires processing before it can exit the MOM (Otera et al., 2005). Published evidence by Munoz-Pineda et al. suggests that, due to the sustained release of AIF over a long period of time following MOMP, the pro-apoptotic pore must be long lived and stable (Munoz-Pinedo et al., 2006). Ceramide

channels as observed in mammalian and yeast mitochondria, using the cytochrome *c* accessibility assay that detects real-time permeabilization, can persist for at least 40 min (this is a minimum as tests of longer times have not been conducted, unpublished data). In planar bilayer membranes, ceramide channels can remain stable for hours.

1.5.2.3 Membrane specificity of ceramide channels

Another interesting property of ceramide channels is that they are specific to the mitochondrial outer membrane. Birbes and associates demonstrated that while ceramide levels could be elevated in cellular and sub-cellular membranes, only a mitochondrial ceramide increase resulted in the release of cytochrome *c* and cell death (Birbes et al., 2001; Birbes et al., 2005). To test whether ceramide channel formation could occur in plasma membranes, erythrocytes were employed as a model plasma membrane. The results indicated that a 60-fold increase in the ceramide needed to permeabilize MOMs did not elicit detectible permeabilization in erythrocytes (Siskind et al., 2006).

In addition, ceramide channels do not form in the MIM. Whole mitochondria were treated with ceramide and assayed for the release of fumarase, a mitochondrial matrix protein; and while the mitochondrial outer membrane was permeabilized to cytochrome *c*, no fumerase release could be detected (Siskind et al., 2002). Moreover, natural long-chain ceramides are a potent inhibitor of MIM permeabilization and the permeability transition pore (PTP) formation in response to calcium overload (Novgorodov et al., 2008b). As PTP and mitochondrial depolarization is typical of late apoptosis downstream of effector caspase activation and more often seen in necrosis, it is possible that the elevation of mitochondrial ceramides, concurrently promotes MOMP,

and inhibits MIM permeabilization in order to allow for the completion of the apoptotic program (Novgorodov et al., 2008a).

The difference must lie in the composition of these membranes and warrants further study. However, what is clear is that through the process of evolution, traits that confer an advantage to survival persevere and thus, the sensitivity of MOM's to permeabilization by ceramide and the resistance to permeabilization of the plasma membrane and the MIM, must be beneficial to survival.

1.5.2.4 Regulation of Ceramide Channels

Any factor that promotes or prevents apoptosis must be tightly regulated as the fate of the cell, and in some cases the whole organism, hangs in the balance. There are a number of ways that ceramide is regulated by the cell (Mullen & Obeid, 2012). First, the cell controls the levels of ceramide in mitochondria. Mitochondrial ceramide levels are kept low, and increase in the MOM, only when a pro-apoptotic signal is delivered. Second, while total cellular levels of ceramide are elevated in multiple compartments of the cell, ceramide channel formation is restricted to the MOM (Siskind et al., 2002; Siskind et al., 2006; Mullen & Obeid, 2012). The specific composition of the MOM is such that it is conducive to channel formation while the compositions of other membranes are not. Third, the anti- apoptotic Bcl-2 proteins, CED-9 (the Bcl-2 homolog of *C. elegans*) and Bcl-xL, can regulate ceramide channels (Siskind et al., 2008). These anti-apoptotic proteins can directly disassemble ceramide channels formed in isolated mammalian mitochondria, isolated yeast mitochondria (which lack other Bcl-2 proteins), and solvent free planar bilayer membranes (which are devoid of proteins and other

mitochondrial factors). This suggests that while other proteins and mitochondrial factors may be involved, the regulation of ceramide channels by anti-apoptotic Bcl-2 family proteins is direct and does not require other such factors for this interaction.

1.6 THE SCOPE OF THE PRESENT STUDIES

The work presented in this dissertation was designed with the aim of identifying the key features of ceramide that allow ceramide channel formation and regulation in the context of mitochondrial outer membrane permeabilization. To elucidate the specific structural features of the ceramide molecule that contribute to ceramide channel formation and stability, a collection of ceramide analogues, or mutants if you will, were studied in Chapter 3. These results lead to the publication "Ceramide Channels: Influence of Molecular Structure on Channel Formation in Membranes," in the journal *Biochimica et Biophysica Acta* in 2012. In Chapter 4, "Ceramide and Activated Bax Act Synergistically to Permeabilize the Mitochondrial Outer Membrane," the interaction of ceramide channels and the pro-apoptotic Bcl-2 family protein, Bax, is explored. This work was published in the journal *Apoptosis* in 2010. The work described in chapter 3 and 4 is the result of a fruitful collaboration with a fellow grad student, Vidyaramanan Ganesan, who made an equal contribution to those publications. The fifth chapter of this thesis explores the location of a molecular site of interaction of both anti- and pro-apoptotic Bcl-2 family proteins on ceramide channels by use of ceramide analogues that retained channel formation. This work culminated in the publication of "Bax and Bcl-xL

Exert Their Regulation on Different Sites of the Ceramide Channel" in the *Biochemical Journal* in 2012. In the final chapter, ideas for future studies are discussed.

CHAPTER 2:

GENERAL METHODS

RATIONALE OF MAJOR METHODS AND TECHNICAL DETAILS

2.1 PURIFICATION OF FULL LENGTH RECOMBINANT HUMAN BAX

2.1.1 Overview of Bax purification

The purification of Bax is facilitated by the use of a pTYB1 vector (IMPACT-CN system, New England Biolabs) which adds a C-terminal Intein tag to the protein. The protein, once expressed in *E. coli*, can be purified by affinity chromatography using chitin beads which bind the Intein tag. The advantage of this system is Bax can be eluted from the chitin column in one step by the addition of a thiol such as DTT, which induces a specific self-cleavage of the intein tag from the Bax protein; the Intein remains bound to the column and Bax is eluted without the addition of any extra residues to the protein or the use of proteases as with other purification techniques. No detergents should be used during the isolation process as the goal of the purification is to isolate pure, monomeric and inactive protein. Detergents can not only activate the protein leading to changes in conformation but may cause the protein to oligomerize with a wide range of high MW structures being formed. SDS-PAGE analysis with reducing conditions would disrupt many of these oligomers, and unfortunately many studies site such analysis as proof of the homogeneity of their monomeric Bax preparations. Moreover, purified monomeric Bax can oligomerize over time when stored at 4 °C (the protein can be stored with a low concentration of DTT to prevent oligomerization, although long term storage in these conditions is not recommended). In our hands, without the use of detergent, we are able to purify inactive monomeric protein (confirmed by SDS-PAGE with and without reducing conditions, planar membrane experiments, and mitochondrial experiments) and we employ a technique of rapidly freezing our protein that preserves the function and native monomeric state of Bax which ensures the homogeneity of our protein sample

over time and across experiments. I would like to thank Dr. Richard Youle for the gift of the Bax plasmid and Dr. Antonella Antigani for assistance with the purification procedure.

2.1.2 Detailed Bax purification procedure

Recombinant human Bax was purified as described previously by (Suzuki et al., 2000) and the modifications to the original procedure are described as follows. DH5α *E. coli* cells were transformed with the plasmid pTYB1-Bax according to the manual (Z-Competent Cells, Zymo Research). These transformed cells were used to generate stock plasmid preps according to standard mini-prep kit instructions (Qiagen) and plasmid DNA was stored -80 °C (samples for sequencing are stored in double distilled H_2O (ddH_2O), all others are stored in TE buffer (10mM Tris-HCl, 1mM EDTA pH 8.0)). Before every protein purification, BL21(DE3) *E. coli* competent cells are freshly transformed and plated on LB plates containing ampicillin (AMP), as the plasmid confers resistance to this antibiotic, and incubated in a 37 °C oven overnight. In the morning, the day before the purification, all the colonies are inoculated into 40 mL of Terrific Broth Medium (TBM) containing AMP (100 mg/L) and incubated with shaking for two hours at 37 °C. Aliquots of pure TBM are saved in sterile microfuge tubes for later use when monitoring the O.D. of the bacterial cultures. Equal parts of the 40 mL culture are added to two large flasks containing 980 mL TBM containing AMP and incubated at 37 °C with shaking for approximately 1.5-2 h until the $O.D._{600nm}$ =0.6-0.8 at which point the culture is induced with a 1 M stock of IPTG (final concentration 0.1 mM) for an additional three hours. The cells are harvested by pouring the cultures into two 1 L centrifuge bottles, and centrifuging at 3000 g for 15 min (Beckman J-6B centrifuge). The supernatants are

discarded and the bottles are placed upside down to drain any excess fluid for 5 min. The bottles containing the pellets can stored at -80 °C until the following morning but it was found that resuspending cells stored in this manner is quite difficult. Thus, it was preferable to resuspend each pellet of cells in about 30 mL of TEN* buffer (20 mM Tris-HCl, 5 mM EDTA, 500 mM NaCl, pH 8.0) and transferring the suspension to 50 mL conical tubes before freezing overnight at -80 °C. The French press cell and all tubes and vessels to be used for the purification the following day should be washed with double distilled water and air dried. The French press cell and all of its parts should be placed in the refrigerator at 4 °C to cool overnight.

The day of the purification, the frozen cell suspensions are removed from the freezer and placed in a beaker with several changes of room temperature water until they are just thawed and then placed immediately on ice. This way of thawing the cells is not only faster, but the cells are kept cool during the process. All other tubes should be placed on ice, tubes used to hold the lysate should be rinsed with TEN buffer (20 mM Tris-HCL, 1 mM EDTA, 500 mM NaCl, pH 8.0). Once the cells are thawed and cooled on ice, the French press cell should be removed from the refrigerator and a generous coating of silicone grease should be applied to the o-rings. The cells are then French pressed at 1000 psi for two passes (or just until the lysate appears translucent and is no longer opaque; no more than three passes as this process is not innocuous). Samples are kept on ice between passes through the French press as this process can generate heat. The lysate is then transferred to 10 mL ultracentrifuge tubes, carefully balanced, and spun at 40k rpm (Beckman L8-70M ultracetrifuge, 50Ti rotor) for 30 min at 4 °C to spin down cell fragments. After the centrifugation is complete, the supernatants are carefully removed so

as not to disturb the pellets and filtered through a 0.2 μm filter to ensure the lysate is free of bacteria and any debris that could potentially clog or contaminate the chitin column. The lysate is then loaded on to the chitin column (~10 mL of chitin beads are packed into the column, beads are regenerated and reused up to 5x according to manufacturer protocol, New England Biolabs), prewashed with 50 mL TEN, in a cold room at 4 °C. The flow rate should be slow at a rate of about 0.5-1 mL/min. The column is then washed with about 50 mL of TEN, taking care that all the walls of the column have also been washed of lysate. About 7-10 mL of TEN + 30 mM DTT is quickly flushed through the column and more of the same solution is added to induce on-column specific self cleavage of the Intein tag from the Bax protein. The column is stopped with about a 6- 8 mL reservoir above the beads and a clean conical tube is placed underneath the column in case of any leakage. After three days, about 15-17 mL of protein is eluted (the Intein tag remains bound to the column) with TEN buffer and transferred into two separate dialysis bags (12,000 M.W.C.O.) and dialyzed against 3 L of 10 mM Tris-HCl, 1 mM EDTA, pH 8.0 overnight to remove the DTT. The bags are then dialyzed against 5 L of 10 mM Tris-HCl pH 8.0 for another 24 hours with constant stirring. I recommend refrigerating the dialysis solutions before adjusting the pH as the pH is more basic at colder temperatures. The protein is then filter sterilized and the protein concentration is determined by the micro BCA assay (PIERCE). The typical yield of protein is between 15-30μg/mL. The protein is 95% pure as assayed by SDS-Page and silver stain.

It is typical for others who purify Bax to store the protein at 4 °C for a month or more with or without a low concentration of DTT. In our experience as well as others in field (Brustovetsky et al., 2010), the monomeric Bax that is isolated has a tendency to

oligomerize over time and this has also been noted by others in the field as well (Brustovetsky et al., 2010). To avoid this complication and to ensure the uniformity of the protein we use for our assays, we add sterile glycerol to our protein to 10% (v/v) as a cryoprotective agent and rapidly shell-freeze our protein using ethanol/dry ice in small one-time use aliquots (50-300µL in sterile thin-walled glass tubes) and stored these at -80 °C. A fresh protein sample is thawed on ice before use and a sample is never refrozen.

2.1.3 Activation of monomeric Bax

The monomeric Bax purified by this method is activated by incubating the sample with 10% *β*-octyl glucoside to a final concentration of 1% on ice for at least 30 min. At these conditions, it was published that over 95% of the protein is activated (Hsu & Youle, 1997; Antonsson et al., 2000) and we confirmed the activation on our protein by taking advantage of previously published methods showing that activated Bax is partially resistant to trypsin digestion (Lucken-Ardjomande et al., 2008) (Fig 2.1).

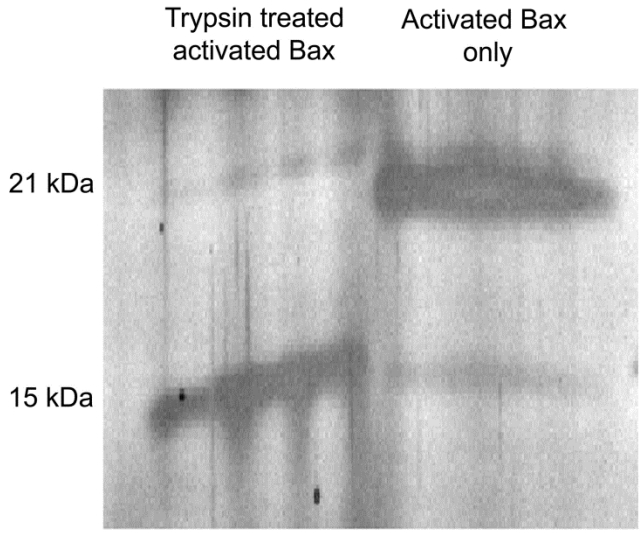

Figure 2.1 SDS-PAGE analysis of activated Bax treated with trypsin.

Activated Bax is partially resistant to Trypsin digestion yielding a15 kDa digestion fragment as seen on the left. Untreated, detergent activated Bax is shown on the right.

2.2 PURIFICATION OF FULL LENGTH HUMAN BCL-XL

2.2.1 Overview of Bcl-xL purification

A pGEX2T vector (Amersham Pharmacia Biotech) was used to clone glutathione *S*-transferase (GST) tagged full length human Bcl-xL with a thrombin cleavage site between the tag and the protein. Using a bacterial expression system to produce the protein, the protein can be purified from the lysate using glutathione-agarose beads which bind GST. Adding biotinylated thrombin to the column results in cleavage of the protein from the GST tag while the GST remains bound to the column. Once the protein is eluted, biotinylated thrombin can be removed by incubating the elute with streptavidin beads which can be sedimented and discarded. Finally, the buffer can be changed to the by dialyzing against the desired solution. Unlike Bax, which is a cytosolic protein in the inactive form, Bcl-xL is a membrane protein thus Triton X-100 is used increase the recovery of the protein and to help disrupt inclusion bodies. To determine the effect of using detergent during the isolation on protein function, I isolated Bcl-xL with and without Triton X-100 and found that the function of the protein remained unchanged with either method while the yield was obviously much greater with Triton X-100. I would like to thank Dr. Marie Hardwick for providing us with the Bcl-xL plasmid and Heather Lamb for providing the purification procedure.

2.2.2 Detailed Bcl-xL purification procedure

The purification of GST-Bcl-xL was originally described by (Basañez et al., 2001) and the modifications are described in detail as follows. The plasmid stock is generated using DH5α *E. coli* cells. Prior to each protein purification, BL21 competent *E. coli* cells are freshly transformed with the Bcl-xL plasmid. The transformed bacteria are plated on

LB plates with AMP, the selection marker encoded by the plasmid, and incubated in a 37 °C oven overnight. The following evening, 10 mL of LB + AMP is inoculated with four of the resulting colonies and grown at 37 °C with shaking overnight. The French press cell and other vessels to be used during the isolation should be rinsed with ddH_2O and air dried and French press cell should be placed in the refrigerator overnight. The next morning, the dense culture is transferred to 1 L of LB + AMP and grown with the same conditions until the $O.D._{600nm}$=0.600 (approximately 2.5-3 hours). The culture is then induced with a 1M IPTG stock to 0.1 mM final concentration for 2 h. Cells are harvested by centrifugation at 4000 g in a 1 L bottle for 15 minutes (Beckman J-6B centrifuge). The supernatant is discarded and the pellet is resuspended in 40 mL of phosphate buffered saline (PBS) and the following is added and mixed well after each addition: 1% Triton X-100, 140 U lysozyme, and 36 μM phenylmethylsulfonyl fluoride (PMSF) (PMSF is dissolved in isopropanol, to avoid a high concentration of solvent locally one should vortex while adding). Incubate this mixture with the cells on ice for 15- 20 min. Only after this step should the French press cell be removed from the refrigerator and silicone grease should be applied to the o-rings. The cells are lysed by two passes through the French press (but no more than thrice) at 1000 psi. Between passes, the cells are kept on ice to prevent them from warming up. The lysate is transferred to 10 mL ultracentrifuge tubes, balanced and spun at 40k rpm (Beckman L8-70M Ultracentrifuge, 50Ti rotor) for 30 min at 4 °C to remove cell fragments. The supernatant is carefully removed as to not disturb the pellets and is filtered through a 0.2 μm syringe filter to remove any additional debris or cells that could potentially clog the column. The lysate is then incubated with 5 mL (packed volume) of pre-washed glutathione agarose beads for 2

hours at 4 °C with gentle rotation. The beads are then packed into a column and the flow through is discarded. The beads are washed with at least 10 column volumes of cold PBS + 36 mM PMSF followed by 10 column volumes of 20mM Tris-HCl, pH 8.0 without any protease inhibitors. 10 mL of 20 mM Tris-HCl pH 8.0 with 5 U of biotinylated thrombin is then added to the beads and incubated overnight at 4 °C with gentle rotation (this incubation could also be conducted at room temperature with or without rotation as no detriment to the activity of the protein was detected in our assays). The next day, the protein is eluted from the column and an additional 2-3 mL of 20mM Tris-HCl pH 8 buffer is added to recover any additional protein. The GST tag remains bound to the column however the biotinylated thrombin must be removed by incubating the elute with a sufficient volume of streptavidin beads to bind the added biotinylated thrombin (streptavdin beads should be pre-washed with the 20mM Tris-HCL pH 8.0 buffer). This incubation should be done for at least 30 min with rotation at room temperature. The streptavidin beads are pelleted and discarded. The pure protein is filter sterilized through a 0.2 micron filter and frozen as described earlier for the Bax protein (section 2.1.2). The concentration is determined by the micro BCA assay and is typically measured to be around 160 µg/mL for batches isolated without detergent and around 1.3 mg/mL for batches isolated with the use of detergent.

2.3 PURIFICATION OF RECOMBINANT N/C BID (CLEAVED HUMAN BID, tBID)

2.3.1 Overview of N/C Bid Purification

Full length human Bid with 6-histidine tag attached to the COOH-end was cloned into a pGEX4T1 vector which, like the pGEX2T vector used to purify Bcl-xL described above, adds a GST tag and allows for the purification of the protein using GST affinity chromatography. In addition, a thrombin cleavage site was inserted in place of residues 57-62. In a cell, Bid is cleaved at this position by caspase 8 to yield the COOH-terminal active fragment called truncated Bid (tBid). Thus, when the full length GST-Bid is bound to the GST column, incubation with thrombin will yield the COOH-active fragment tBid-His_6. The major advantage of this method allows one to purify and separate both inactive and active fragments of Bid (N/C Bid: N-terminal inactive fragment, C-terminal active fragment) resulting from caspase 8 cleavage by making modifications to the final steps of the same purification and avoiding the need to make multiple constructs and multiple purifications. We thank Dr. Donald D. Newmeyer for the gift of the N/C Bid plasmid and Ryan Hastie for assistance with the purification procedure.

2.3.2 Detailed N/C Bid Purification Procedure

Recombinant full length Bid was purified as previously described (von Ahsen et al., 2000) (Kuwana et al., 2002) and the modifications are described in detail as follows. DH5α *E. coli* cells are used to produce plasmid stocks and BL21 *E. coli* cells are freshly transformed with the N/C Bid plasmid and plated on LB plates with AMP (the selection marker) overnight at 37 °C. The next morning, all plated colonies are inoculated into 40

mL of pre-warmed LB+ AMP (100 mg AMP/L LB) medium and are incubated with shaking for 3 hours at 37 °C. This culture is transferred to a flask containing 400 mL pre-warmed LB medium with AMP and grown with the same conditions for about another 1.5 h until the $O.D._{600nm}$= 0.6. At this point the culture is induced with IPTG to a final concentration of 0.4 mM. The culture is incubated for another 3.5 hours with shaking at a reduced temperature of 30 °C. The cells are then harvested by centrifugation at 4000 rpm in 1L centrifuge bottles for 15 min. The cells are then resuspended in about 30 mL of "PBS-EN buffer" (PBS with 1mM EDTA, 500mM NaCl pH 7.4) and frozen in a 50 mL tube at -80 °C overnight. The French press cell and all vessels to be used the next day should be rinsed with ddH_2O and air dried. The French press cell should be placed in the refrigerator overnight.

In the morning, the cell resuspension is thawed in a beaker of room temperature water until just thawed and then placed on ice. The French press cell is removed from the refrigerator and the o-rings are lubricated with silicone grease. Tubes to hold the lysate are pre-rinsed with PBS-EN buffer. The cells are lysed using 2 passes through the French press at 1000 psi and placed on ice. Triton-X100 is added while vortexing to a final concentration of 0.1%. The lysate is transferred into cooled ultracentrifuge tubes, carefully balanced and centrifuged at 40,000 rpm using the 50-Ti rotor for 30 min at 4 °C in the Beckman J-6B ultracentrifuge. The lysate is carefully removed so as not to disturb the pellets and the pellets are discarded. The lysate is filter sterilized through a 0.2 μm filter to remove any particulates or cells that could potentially clog the column. In a 50 mL conical tube, incubate the lysate with 1 mL glutathione-sepharose beads (prewashed with at least 20 mL PBS-EN buffer) and gently rotate at 4 °C overnight. The next

morning, the beads are spun down at 3000 RPM for 2 min (Fisher Scientific Marathon 21K/BR centrifuge). The supernatant should be carefully removed and discarded. The protein-bound beads are washed with 20 mL PBS (without the additional EDTA and NaCl) and spun down. The supernatant is discarded and the beads are suspended in a small volume of PBS and transferred into a column. The column is washed with an additional 10 column volumes of PBS. To isolate tBid, 10U of biotinylated thrombin is added to the column in a volume of 500 μL PBS and incubated overnight at room temperature. In the morning, 4 mL of tBid was eluted from the column with PBS. Streptavidin beads are added to the elute to remove thrombin and incubated at room temperature for 30 min. The streptavidin beads are spun down and the supernatant is transferred into 8 kDa M.W.C.O. dialysis bags and dialyzed with constant stirring against 5 L of 50 mM Tris-HCl pH 8.0 (the dialysis solution was cooled before the pH was adjusted to 8.0) at 4 °C overnight. The protein is then filter sterilized through a 0.2 μm filter, the concentration is determined, and frozen in 100 μL aliquots (see section 2.1.2 for details on the freezing method. The typical yield of tBid is about 4 mg/mL and this can be diluted to an appropriate or useful concentration with 50 mM Tris-HCl pH 8.0 before freezing (typically we dilute the protein to 0.4mg/mL before freezing).

2.4 ISOLATION OF MITOCHONDRIA

2.4.1 Isolation of Rat Liver Mitochondria

Rat liver mitochondria were isolated from male Sprague Dawley rats by differential centrifugation of tissue homogenates as described previously (Parsons et al.,

1966) and modified (Siskind et al., 2002). The evening before the isolation, one rat is transferred into a new cage with new bedding and water (rats are only fed distilled or filtered water) and fasted overnight. In the morning, all solutions to be used are removed from the freezer and thawed in warm water until just thawed and promptly placed on ice to cool down. It is important that all steps of this isolation, and all vessels and solutions used are kept at ice cold temperatures to ensure the quality and integrity of the organelles we purify. 300 mL of H-buffer (70 mM sucrose, 210 mM mannitol, 5 mM HEPES, 0.1 mM EGTA, pH 7.4) is poured into a beaker (pre-rinsed with the same solution) and 0.5% (w/v) of fatty-acid depleted bovine serum albumin (BSA) is added to the beaker and allowed to float until dissolved (do not stir) to make HB-buffer. Once the BSA has dissolved, the beaker is gently swirled to mix. A glass petri dish, a 100 mL beaker, and homogenizing tube with pestle are pre-rinsed with HB and placed on ice. Several 50 mL tubes are also placed on ice but are pre-rinsed with the appropriate buffer (HB-, H- or FH- buffer) and placed on ice.

The rat is anesthetized with carbon dioxide and sacrificed by decapitation using a guillotine. Quickly, while the heart is still beating, the abdomen is dissected with scissors and the liver is excised, with care to avoid hair and other organs, and placed in a cold 100 mL beaker with two changes of HB to wash the liver of blood. The liver is then placed in the petri dish with some more HB and chopped with scissors into small pieces. One fourth of liver is homogenized at a time, with HB added to ¾ of the capacity of the homogenizing tube. Two passes using a motorized Potter-Thomas Teflon-glass homogenizer was sufficient to break the cells and care was taken not to infuse air into the homogenate during the process. The mitochondria are then purified using differential

centrifugation and all the following steps are conducted at 4 °C. The homogenate is transferred into 50 mL tubes and spun using the pre-cooled Sorvall RC-5B centrifuge with the SS-34 rotor at a low speed (about 620 RCF (average)) for 10 min. The supernatant is transferred into new tubes and the pellet is discarded. The supernatant is spun at high speed (8700 RCF (average)) for 10 min. Following this spin, the supernatant is now discarded and the walls of the tubes are wiped free of fat and other contaminants using a Kimwipe. The pellets are gently rinsed with HB buffer twice and then resuspended with a small amount of HB using a blunted glass pipet and bulb to gently blow solution at the pellet. Care is taken to avoid resuspending any blood cells that may be left over at the center of the pellet or blowing air at the pellet. The organelle suspensions in four tubes are combined into two new tubes and filled with HB. These tubes are spun at low speed for 10 min and the supernatants are poured into new tubes, taking care to avoid the pellet. These are then spun at high speed for an additional 10 min and the supernatants are discarded. The pellets are rinsed twice and resuspended with H-buffer (without BSA), taking care to avoid resuspending any lysosomes or peroxisomes that may be left over at the very bottom and center of the pellet, and spun again at high speed for 10 min. The previous step is repeated to ensure the BSA has been removed. The supernatant is discarded and the pure mitochondria are resuspended with about 5 mL of FH buffer (280 mM mannitol, 0.1 mM EGTA, 2 mM HEPES, pH 7.4) and stored on ice. The animal use protocols were approved by the Institutional Animal Care and Use Committee. The animals were euthanized by a procedure consistent with the Panel on Euthanasia of the AVMA. The animal facility used to house the animals is accredited by AAALAC.

2.4.2 Isolation of Yeast Mitochondria

The procedure used for isolating *S. cerevisiae* mitochondria was published by (Daum et al., 1982) and modified by (Lee et al., 1998). The following procedure elaborates on further modifications to the procedure but it remains largely the same as published by (Lee et al., 1998). Yeast stocks (9 mL) were recultured every 3 months. Stock yeast cells were made by inoculating a colony of yeast cells into 100 mL of yeast medium (0.3 g yeast extract, 0.1 g potassium phosphate, 0.1 g of NH_4Cl, 0.05 g $CaCl_2$, 0.05g NaCl, 0.06 g $MgSO_4$, 30 µL of 1% $FeCl_3$, 2.4 mL of 85% lactic acid, pH 5 was reached by slowly adding about 2 g solid KOH and this medium is autoclaved under a fluid cycle for 15 min at 230°C) and grown with shaking at 30 °C until the $O.D._{600nm}$ is between 0.6 and 0.8 (blanked with lactic acid). At this point, 9 mL aliquots were dispensed into autoclaved glass culture tubes, capped and stored at 4°C.

The day before the yeast mitochondria isolation, two liters of yeast medium are inoculated with one 9 mL stock each and are grown for a minimum of 24 hours (can be up to 27 hours depending on the O.D. measurement) at 30°C with shaking until the O.D. at 600 nm is 0.6. Cells were harvested in 1 L bottles by spinning at 4000 RPM for 15 min. The supernatant is discarded and the pellet is rinsed and resuspended with ddH2O (about 40 mL per bottle) and transferred into two pre-weighed 50 mL tubes. The cells are then centrifuged in the Sorvall RC-5B centrifuge using the SS-34 rotor for 5 min at 10k RPM. Then, the supernatant is discarded and the tubes are weighed again to calculate the wet weight of the pellet (typically 4-5 grams of cells are collected). 1 mL of Tris-buffer is required per 0.5 g of cells, so once the volume of Tris-buffer (100mM Tris-SO_4, pH 9.4) needed is determined, then the required amount of DTT is measured and added to

this volume so that the final concentration of DTT is 10 mM. This volume of Tris-buffer with DTT is added to the cells which are resuspended using a blunted glass pipette and combined into one tube and incubated with shaking for 10 min at 30 °C. After this incubation, the cells are once again centrifuged at 10k RPM for 5 min. The supernatant is discarded and the cells are resuspended in1.2M sorbitol and spun again with the same conditions. The supernatant is discarded and the cells are resuspended in 20 mL of sorbitol-phosphate buffer (1.2 M sorbitol, 20 mM K_2HPO_4, pH 7.2) and 10 mg of Zymolyase (20 kU/g) was added per gram of cells and incubated at 30 °C with very gentle shaking for 25 min to digest the cell wall. To monitor spheroplast formation, a glass slide was prepared with a sample of the cells subject to enzymatic digestion of the cell wall, and extent of lysis after adding a drop of 10% N-lauroylsarcosine to the corner of the coverslip was visualized with a phase contrast microscope.

The rest of the isolation should be conducted with all vessels, centrifuges, rotors and solutions being pre-cooled to 4 °C. The cells are transferred into a 250 mL centrifuge bottle and using the adaptors, the cells and the balance bottle should be spun at 6 k RPM for 5 min using the SLA-1500 rotor. The pellet will form in the bottle adjacent to the outer wall of the rotor. The supernatant is discarded and the pellet is gently rinsed twice with sorbitol-phosphate buffer by pouring a small amount into the bottle, swirling and discarding the waste. More sorbitol-phosphate buffer is added (enough so that when the bottle is held at a tilt and the pellet is adjacent to the outer wall of the rotor, the entire pellet is covered with solution). To thoroughly but gently wash,, the bottle is rotated 180 degrees (about the long axis of the bottle, so that the pellet is now near the center of the rotor and not the outer wall), and spun at 6 k RPM for 5 min. The supernatant is

discarded, and the pellet is again rinsed, turned 180 degrees and spun as before with more Sorbitol-Phosphate-Buffer. The supernatant is discarded and 40 mL of HY-buffer (0.6 M mannitol, 0.1 mM EGTA, 10 mM Tris, and 6 g polyvinylpyrrolidone, pH 7.2) is added to the washed spheroplasts. A blunted glass pipette is used to gently suspend the spheroplasts in this hypotonic solution and lyse the spheroplasts effectively without employing harsh methods such as homogenizing or blending the cells and minimizing damage to the mitohcondria. The resuspension is transferred to a 50 mL tube and centrifuged for 5 min at 3 k RPM. The supernatant is saved and placed on ice while the pellet is resuspended as before with HY-buffer and the centrifugation is repeated. The supernatant is transferred into a new tube and both supernatants are centrifuged at 8500 RPM for 10 min. The resulting pellets are resuspended with 20 mL HY-Buffer each, combined into one tube and spun at 3000 rpm for 5 min. The supernatant is transferred into a new tube and the purified mitochondria are sedimented at 8500 RPM for 10 min. The mitochondria are resuspended in about 3 mL of HY-Buffer and placed on ice.

2.4.3 Measurement of Mitochondrial Protein Concentration and Determination of the Number of Mitochondria

The concentration of mitochondria is measured following the method described by (Clarke, 1976) by taking 1/20 dilution of the mitochondria in H-Buffer (25 µL mitochondria, 475 µL H-buffer) and mixing with an equal part of P-buffer (100 mM Tris-H_2SO_4, 0.4 % SDS pH 8.0) and reading the absorbance at 280 nm and 310 nm (blanked with equal parts H-buffer and P-buffer). The concentration of mitochondrial protein (mg/mL) is given by $40 * \left(\frac{\mathbf{A_{280}-A_{310}}}{\mathbf{1.05}}\right)$.

It has been published that there are $7.2x10^9$ mitochondria per mg of mitochondrial protein (Estabrook & Holowins.A, 1961), thus the number of mitochondria in a given sample can be calculated for known concentration of mitochondrial protein.

2.4.4 Measurement of the Intactness of Mitochondria

The method of subjecting mitochondria to mild hypotonic shock was described by (Douce et al., 1987) and modifications were made to the original procedure. Rat liver mitochondria are osmotically shocked by adding twice the amount of mitochondria used for the mitochondrial dilution one is using for a respective experiment (ex. if the dilution being used is 0.5 mg/mL H-buffer, then make 1 mg/mL ddH_2O) and adding ddH_2O to 1 mL. This dilution is incubated on ice for 10 min and the osmotic pressure is restored by adding an equal volume of shocked mitochondria to 2H-buffer (H-buffer with twice the contents). The percent intactness of the mitochondria is determined by comparing the rate of oxidation of exogenously added cytochrome *c* (described in section 2.5.1) by an equal amount control mitochondria vs. mitochondria subject to mind hypotonic shock: $\left(\frac{\mathbf{Rate_{lysed}} - \mathbf{Rate_{intact}}}{\mathbf{Rate_{lysed}}}\right) * 100$. For rat liver mitochondria, the intactness is typically about 85%. For yeast mitochondria, the procedure is the same except the appropriate yeast buffers are used instead (HY- instead of H-buffer etc.) and above 95% intactness in typically achieved.

2.5 DETECTION OF CHANNEL FORMATION IN MEMBRANES

2.5.1 Cytochrome *C* Oxidase Accessibility Assay

This assay detects real-time permeabilization of the mitochondrial outer membrane (MOM) by monitoring the oxidation of exogenously added cytochrome *c* by cytochrome *c* oxidase (complex IV of the electron transport chain), found on the mitochondrial inner membrane (MIM). The MOM is impermeable to exogenously added reduced cytochrome *c* (~12 kDa), and thus cannot access cytochrome *c* oxidase which is found on the inner mitochondrial membrane, unless the integrity of the MOM is compromised by the formation of a channel, a pore or damage like osmotic shock. Thus, channel formation can be detected by monitoring the oxidation of exogenously added reduced cytochrome *c* either by monitoring oxygen consumption or directly by monitoring the absorbance of reduced cytochrome *c* ($\varepsilon_{550(red\text{-}ox)}$ = 18.5 mM^{-1} cm^{-1} (Margoliash & Frohwirt, 1959)) which will decrease as the protein becomes oxidized. This assay is useful to detect the real-time permeability of the MOM as well as detect changes in permeability over time whereas release assays can only tell you that the mitochondria were permeabilized at some point, perhaps transiently.

This assay is conducted as described by (Wojtczak et al., 1972) and modified by (Siskind et al., 2002). Further modifications have been introduced to optimize reproducibility of results and the integrity of the mitochondria over time. Freshly isolated mitochondria are suspended as a concentrated stock in FH-buffer (or HY-buffer for yeast) as mitochondria have been found to be more stable at high concentrations. Once the concentration of mitochondrial protein has been determined (section 2.4.3) a working

dilution is made in the same buffer, typically between 0.2-0.5 mg/mL and stored on ice, and a new working dilution is made for every set of samples tested in parallel. 50 µL of this dilution is added to microfuge tube containing 650 µL of room temperature reaction buffer H* (for rat liver mitochondria, this is the same as FH buffer supplemented with 5 mM DNP and 1.4 µM antimycin A pH 7.25, if a reaction buffer with a higher salt content is desired, then the amount of mannitol is reduced to 160 mM and supplemented with 60 mM KCl; for yeast mitochondria the reaction buffer H*Y is composed of HY buffer supplemented with 5 mM DNP and 1.4 µM antimycin A, pH 7.2) and inverted several times to mix. The mitochondria are allowed to acclimate to room temperature for at least 5 min prior to ceramide dispersal and the volume added is less than 5% of the total volume of the reaction mixture to minimize any effect of the vehicle, typically 2-propanol for ceramides or ceramide analogs. All vehicle controls are conducted in parallel with the sample of interest. Ceramides and their analogs are dispersed very carefully while vortexing for about 15 s and the vortexing is continued, for a total of 30 s, after which the sample is incubated for 10 min at room temperature. About 27 µM reduced cytochrome *c* is added to the sample, immediately inverted 7 times to mix and read in a spectrophotometer for 2 min. The initial linear portion of the rate cytochrome *c* oxidation is measured at A_{550nm}. An illustration of this assay is presented in Fig 2.2.

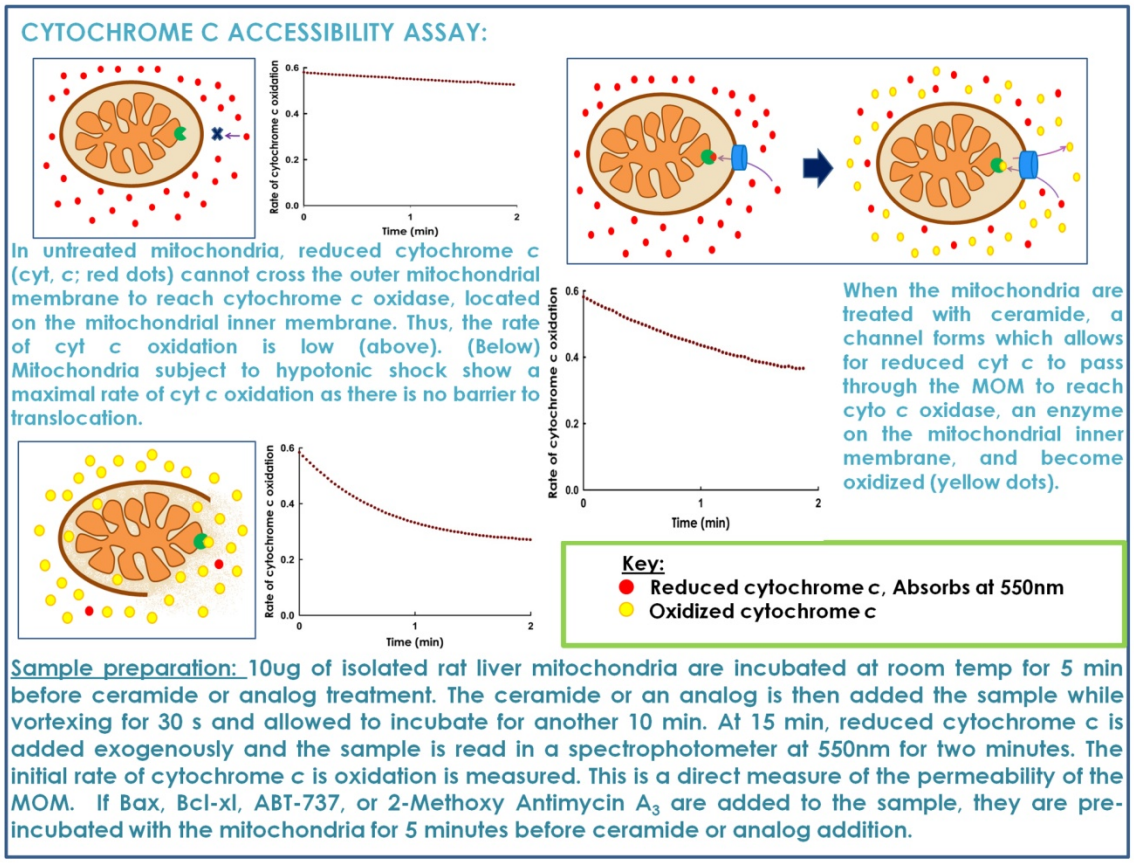

Figure 2.2 Cytochrome *c* accessibility assay.

A typical experiment is described here along with illustrations of how the rate of cytochrome *c* oxidation represents the level of permeabilization of the mitochondrial outer membrane.

2.5.1.1 Preparation of Reduced Cytochrome *C*

5mM horse-heart cytochrome *c* (Sigma) was made in 700 μL of 0.2 M J-buffer (0.2 M Tris-HCl, pH 7.5) and reduced by adding an excess of ascorbate (97 mM final). This mixture was inverted to dissolve and the ascorbate was removed from the cytochrome *c* using a Sephadex G-10 gel-filtration column. About 2.4 mL of elute is

collected in a single vial and the concentration of cytochrome *c* is determined spectrophotometrically ($\varepsilon_{550(red\text{-}ox)}$ = 18.5 mM^{-1} cm^{-1} (Margoliash & Frohwirt, 1959)). The concentration is adjusted to about 1.5 mM reduced cytochrome *c* with J-buffer; so that 10 μL of reduced cytochrome *c* added to 700 μL of J-buffer gives an absorbance reading at A_{550nm} of 0.4. This is done so that the concentrations of cytochrome *c* stocks are uniform across different preparations. Prior to freezing at -20 °C, the reduced cytochrome *c* divided into 600 μL aliquots and the microfuge tubes are flushed with argon and wrapped with Parafilm to prevent oxidation. These stocks are used within 3 months. The column is stored in J-buffer with 0.05 % sodium azide and washed with 10 column volumes of J-buffer before use.

2.5.2 Release of Adenylate Kinase

Adenylate kinase is a 24 kDa protein and, like cytochrome *c*, is located in the intermembrane space of mitochondria unless the MOM is permeabilized. This, like other release assays, allows one to determine that the mitochondria have been permeabilized at some point during the assay, as well as determine the percent of mitochondria that have been permeabilized. This assay is conducted as described earlier by (Sottocasa et al., 1967) and modified by (Siskind et al., 2002). After mitochondria have been isolated, a working stock of mitochondria is made (1.6 mg mitochondrial protein/mL FH buffer). 100 μL of this is added to 900 μL of incubation buffer (60 mM potassium lactobionate, 180 mM mannitol, 0.1 mM EGTA, and 2 mM HEPES pH 7.4) so that the final mitochondrial concentration is 160 μg/mL. This concentration of mitochondrial protein is about 3 times that used for the cytochrome *c* accessibility assay in order to obtain higher

rates and increase signal to noise. Ceramide and proteins are added as done for the cytochrome *c* oxidation assay and incubated in a 30 °C water bath for 30 min. The mitochondria are sedimented at 14k RCF for 5 min at 4 °C and placed on ice. 300 µL of supernatant is added to 700 µL of room temperature Adenylate Kinase Reaction Buffer (50 mM Tris, 5 mM $MgSO_4$, 10 mM glucose, 5 mM ADP, 0.2 mM NADP, pH 7.5) that has been pre-incubated for 2 min with 5 µL of the enzyme mixture (2.5 U of hexokinase and 8.7 U of glucose-6-phosphate dehydrogenase; 50-100 µL aliquots of this mixture are stored at -20 °C and are only thawed on ice shortly before use; the enzyme should remain ice cold until it is added to the sample and any left over enzyme should be discarded). The sample is inverted to mix and the absorbance is recorded immediately at 340 nm for 5 min. The initial rate is used as a measure of the adenylate kinase activity as an increase in absorbance at 340 nm. Maximal release was observed when mitochondria are exposed to hypotonic shock: 160 µg mitochondria protein, directly from the concentrated stock, not the working dilution, is added to 1 mL of ddH_2O and incubated on ice for 10 min.

2.5.3 Permeabilization of Planar Phospholipid Membranes

This technique allows one to observe ceramide channel behavior and the direct effects of proteins on ceramide channels in a defined system. Planar phospholipid membranes were generated by the monolayer method described by (Montal & Mueller, 1972) and modified by (Colombini, 1987a). A Saran partition (polyvinylidene chloride (PVDC)), containing a 100 µm diameter hole, separates two halves of a Teflon chamber (Fig 2.3). The hole is coated on both sides of the partition with a moderate application of petrolatum (2 % petrolatum (w/v) in petroleum ether) and allowed to dry for 15 min. To

generate a solvent free membrane, both sides of the chamber are filled with an aqueous solution (typically 1 M KCl, 1 mM $MgCl_2$, 5 mM PIPES pH 6.95) to a level below the partition. 30 to 60 μL of a lipid solution (0.5 % (w/v) 1,2-diphytanoyl-*sn*-glycero-3-phosphocholine, 0.5% (w/v) asolectin, and 0.05% (w/v) cholesterol dissolved in hexane) is layered on the aqueous solution on either side of the chamber and the solvent is allowed to evaporate for 5 min. Then, the solution on the *trans* side is raised to a level above the hole in the partition, forming a monolayer across the hole, followed by raising the solution on the *cis* side to match the level solution on the *trans* side, to complete the formation of a bilayer. Calomel electrodes are used to interface the aqueous solutions on either side of the membrane with the electronics. The voltage is clamped at 10 mV and the current is recorded. Only membranes that displayed less than 0.05 nS in conductance, were stable at increased voltage and stirring were used for experiments. All experiments are conducted at room temperature.

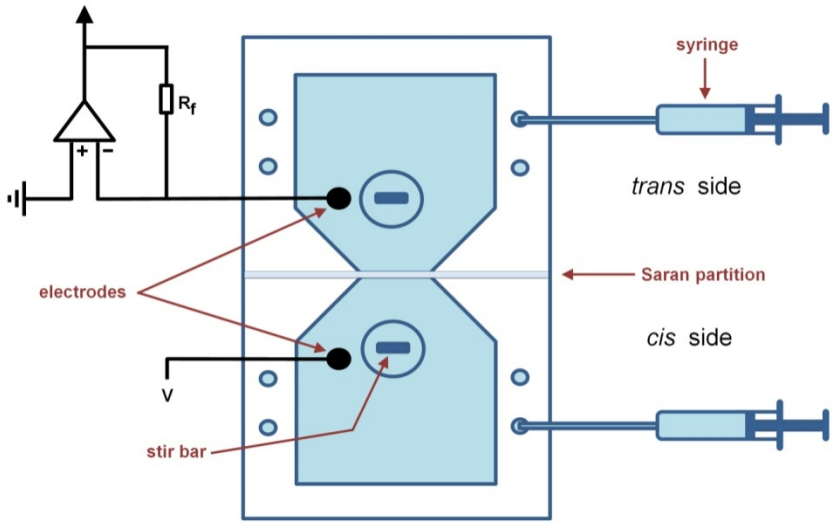

Figure 2.3 Schematic diagram of the experimental setup used for planar membrane studies.

A Teflon chamber is separated into the *cis* and *trans* sides by a Saran partition. A monolayer is formed on the surface of the aqueous solutions on either side of the membrane and a bilayer is formed across a 100 μm hole in the partition. The amplifier (►) is wired in the inverted mode and the feedback resistance (R_f) is usually $10^8\Omega$.

To generate a ceramide channel, or that of a structural analog of ceramide, 5-15 μL of a ceramide solution (typically 0.05 mg/mL in isopropanol) is added to the *cis* side of the chamber while stirring both *cis* and *trans* solution for 15 seconds. These additions are repeated in 15 min intervals between additions until a ceramide conductance is observed. The time to generate a channel is typically variable but once a channel is nucleated, the channel will often grow rapidly until a stable level is reached. Proteins are typically added to the *cis* side while stirring both compartments. When $LaCl_3$ is used to

disassemble ceramide channels, about 5-10 μL of 10 mM $LaCl_3$ if a high dose is desired and 10 μL of 1 mM $LaCl_3$ is used if a low dose is desired.

CHAPTER 3:

CERAMIDE CHANNELS:

INFLUENCE OF MOLECULAR STRUCTURE ON CHANNEL FORMATION IN MEMBRANES

3.1 ABSTRACT

The sphingolipid, ceramide, has been demonstrated to self-assemble in the mitochondrial outer membrane (MOM), forming large channels capable of translocating proteins. These channels are believed to be involved in protein release from mitochondria, a key decision-making step in apoptosis. Synthetic analogs of ceramide, bearing modifications in each of the major structural features of ceramide were used to probe the molecular basis for the stability of ceramide channels. Channel stability and mitochondrial permeabilization were disrupted by methylation of the C1-hydroxyl group whereas modifications of the C3 allylic hydroxyl group were well tolerated. A change in chirality at C2 that would influence the orientation of the C1-hydroxyl group resulted in a strong reduction of channel-forming ability. Similarly, methylation of the amide nitrogen is also detrimental to channel formation. Many changes in the degree, location and nature of the unsaturation of ceramide had little effect on mitochondrial permeabilization. Competition experiments between ceramide and analogs resulted in synergy with structures compatible with the ceramide channel model and antagonism with incompatible structures. The results are consistent with ceramide channels being highly organized structures, stabilized by specific inter-molecular interactions, similar to the interactions responsible for protein folding.

3.2 INTRODUCTION

The sphingolipid, ceramide, has been shown to be able to form channels in planar membranes (Siskind & Colombini, 2000), liposomes (Stiban et al., 2006) and the mitochondrial outer membrane (Siskind et al., 2002; Siskind et al., 2006). In mammalian mitochondria, channel formation occurs at physiologically relevant ceramide levels (Siskind et al., 2006); levels measured in mitochondria from cells early in the apoptotic process (García-Ruiz et al., 1997; Rodriguez-Lafrasse et al., 2002; Birbes et al., 2005). In addition, the propensity to form channels and their size is influenced by Bcl-2 family proteins (Siskind et al., 2008; Ganesan et al., 2010). These channels are large, stable and capable of allowing proteins to cross membranes (Siskind et al., 2002; Siskind et al., 2006). The size was determined from the molecular weight of proteins released from mitochondria (Siskind et al., 2002), from the conductance of single channels formed in planar membranes (Siskind et al., 2003), and from visualization of the pores by electron microscopy (Samanta et al., 2011). A range of sizes was reported with a typical channel having an estimated pore diameter of 10 nm (Siskind et al., 2003; Samanta et al., 2011). Thus hundreds of ceramide molecules must spontaneously self-assemble in the 2-dimensional liquid phase of the membrane. Unlike the fluid and transient toroidal pores or lipidic pores formed when lamellar lipids are disturbed by amphipathic molecules such as peptides or synthetic structures (Bechinger, 1997; Sansom, 1998; Qian et al., 2008), whole proteins (Basanez et al., 2002; Schafer et al., 2009), or at the phase transition (Blicher et al., 2009), the channels formed by ceramide seem to be highly structured and rigid. The disassembly of channels formed by short-chain ceramide shows a quantization of conductance with a strong preference for large conductance drops to be multiples of 4

nS (Siskind et al., 2003). This finding not only supports the notion that ceramide channels are highly-organized cylindrical structures, but is also consistent with a modification of the originally-proposed barrel-stave structure (Siskind & Colombini, 2000). Each stave of the barrel is proposed to consist of a stack of ceramide molecules held together by intermolecular hydrogen-bonding through the amide and carbonyl groups of the amide linkage. These span the membrane forming a cylinder when arranged in an anti-parallel fashion (Fig. 1.4) (Siskind et al., 2003). Molecular dynamic simulations indicate that this structure is stable (Anishkin et al., 2006).

The working structure of the ceramide channel is fundamentally a barrel-stave structure similar to the structure, both proposed and solved, for many channels. The main difference is that for all other channels described to date, there is a strong preference for a fixed number of monomers forming a channel. Forming channels with one stave more or less is highly unfavored. If the ceramide channel has such a preference, it is not a strong preference. Perhaps this unexpected feature is due to the large size of pore needed to allow the translocation of proteins resulting in a large radius of curvature. Thus relatively small changes in this radius of curvature, as more staves are added to the barrel, may be accommodated by relatively small changes in the conformation of the polar headgroup. Alternatively, the structure of the polar region may allow enough flexibility to adapt to changes in the radius of curvature. The difficulty observed in initially forming a ceramide channel and the rapid growth following initial formation [11] may indicate that a small radius of curvature is energetically unfavorable.

The ability of ceramide to form channels must, at least in part, be attributed to the structural features of the ceramide molecule. The polar head group of ceramide (Fig.

3.1), with its amide linkage and two hydroxyl groups located in close proximity, constitutes a tridentate hydrogen-bonding donor/acceptor center and is capable of generating an effective network of directed hydrogen bonding interactions. These structural features may partly explain its ability to form large, stable channels in membranes. However, it is not known if the location and orientation of the interacting

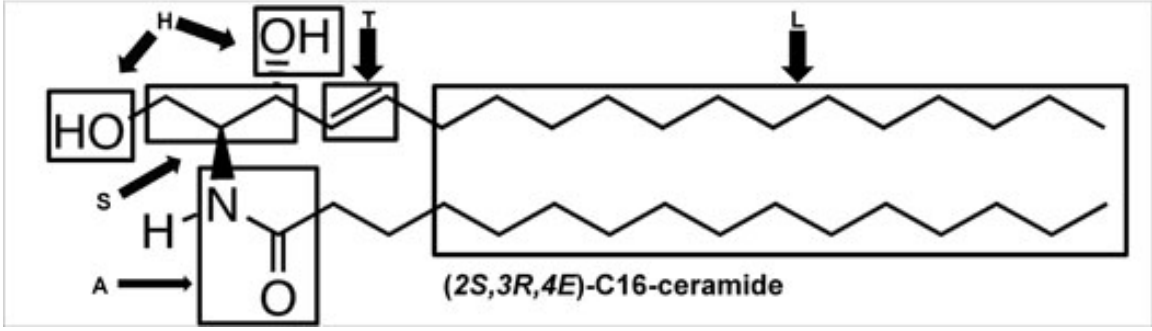

Figure 3.1 Structure of *N*-palmitoyl-D-*erythro*-sphingosine (D-e-C_{16}-ceramide or C_{16}-Cer) showing the major features of the molecule and the codes used for the synthetic analogs: H for changes to the hydroxyl groups, **S** for changes in stereochemistry, **A** for changes to the amide group, **T** for changes to the trans double bond and **L** for changes to the chain length.

groups are critical to achieve a stable structure. In addition, other structural features (such as the length of the hydrocarbon chains and the number and configuration of the double bonds) may be important. Therefore, we have undertaken a study of synthetic ceramide analogs (Table 3.1, Fig. 3.2) to determine (a) if naturally occurring ceramides are uniquely suited to form large aqueous pores and (b) the structural and stereochemical features in ceramide that are necessary for the formation of large channels.

Table 3.1 Ceramide analogs.

Code	Structural Change	Type/Location of Change
S1	enantiomer: 2*S*,3*R* to 2*R*,3*S*	Stereochemical
S2	diastereomer: 3*R* to 3*S*	
A1	C_{16}-ceramine (conversion of amide chain to amine-linked chain)	amide linkage
A2	C_8-ceramine	
A3	*N*-methylation of amide chain	
A4	urea-ceramide	
A5	α-methoxy group in amide chain of C_8-ceramide	
H1	*O*-methylation of C1-hydroxyl group	hydroxyl group
H2	*O*-methylation of C3-hydroxyl group	
H3	oxidation of C3-OH to keto group; no double bond	
T1	translocation of double bond on sphingoid base	
T2	phytoceramide: double bond replaced by OH at C4	
T3	double bond converted to triple bond	
T4	allene: adjacent double bonds	
T5	4,6-diene: conjugated *trans* double bonds in C_8-ceramide	
T6	*trans* double bond converted to *cis* in C_8-ceramide	
T7	translocation of double bond and C3-OH in C_8-ceramide	
L1	C_{10}-ceramide	hydrocarbon chains
L2	truncation of sphingoid base	
L3	C_8-ceramide	
L4	NBD-ceramide	
L5	*N*-palmitoyl-serinol	
L6	*N*-oleoyl-ceramide ($C_{18:1}$)	

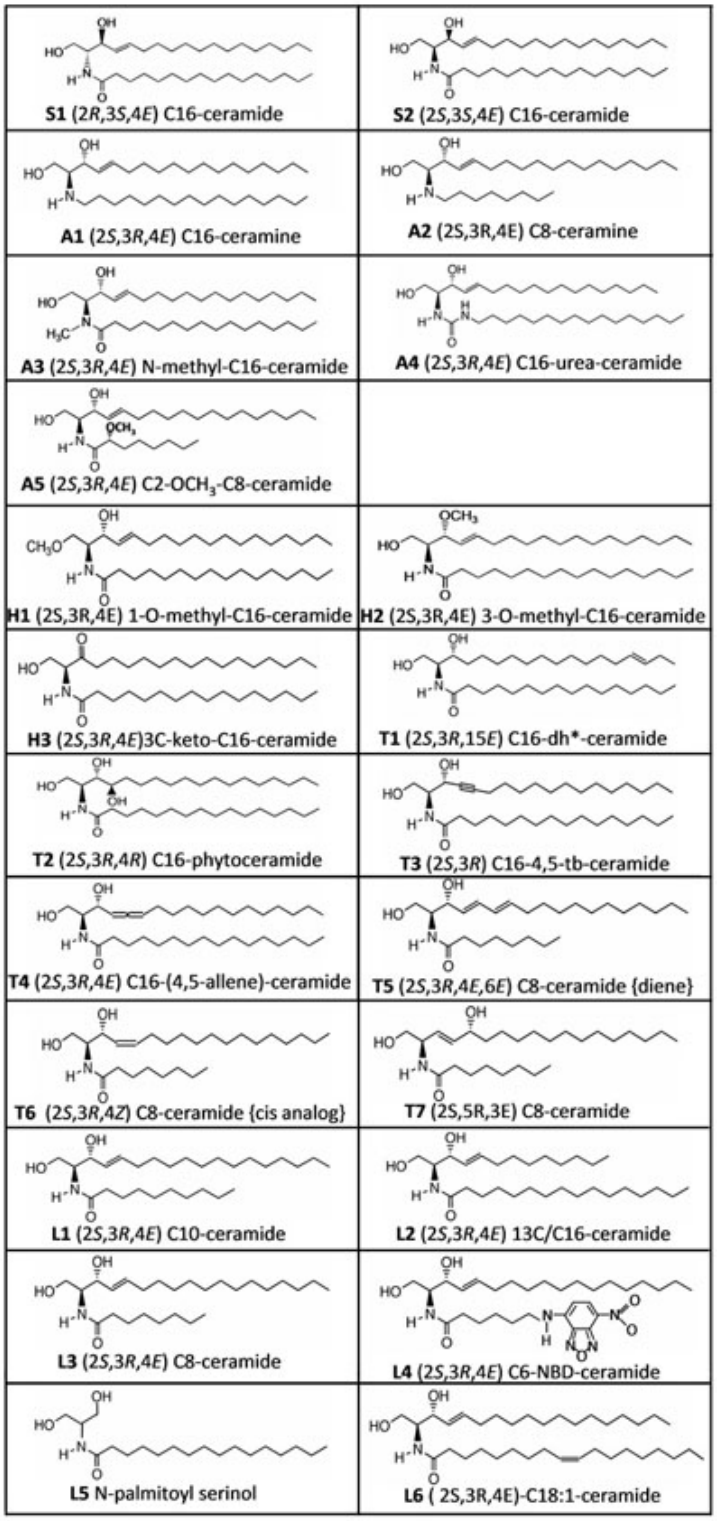

Figure 3.2 Chemical structures of the analogs used.

3.3 MATERIALS AND METHODS

3.3.1 Reagents:

N-Palmitoyl-D-*erythro*-sphingosine (D-e-C_{16}-ceramide or C_{16}-Cer) and *N*-oleoyl-D-*erythro*-sphingosine (D-e-$C_{18:1}$-ceramide or $C_{18:1}$-Cer) were obtained from Avanti Polar Lipids (Alabaster, AL). The analogs of C_{16}-Cer and D-e-C_8-ceramide (C_8-Cer) and **(T1, T4)** (Fig. 3.2) were synthesized as described previously (Karasavvas et al., 1996; He et al., 2000a; He et al., 2000b; Usta et al., 2001; Chun et al., 2002; Chun et al., 2003; Brockman et al., 2004; Chalfant et al., 2004). Antimycin A, 2,4-dinitrophenol (DNP), horse heart cytochrome c, and fatty acid depleted bovine serum albumin (BSA) were purchased from Sigma (St. Louis, MO). DPX (p-xylene-bis-pyridinium bromide) was purchased from Molecular Probes (Invitrogen). 5(6)-carboxyfluorescein was purchased from Acros Organics.

3.3.2 Preparation of rat liver mitochondria:

Rat liver mitochondria were isolated by differential centrifugation of tissue homogenates as described previously (Parsons et al., 1966) as modified (Siskind et al., 2002). Briefly, male Sprague Dawley rats were fasted overnight and sacrificed by decapitation. The liver was excised and minced in cold isolation medium, H buffer (70 mM sucrose, 210 mM mannitol, 0.1 mM EGTA, 5.0 mM HEPES, pH 7.5), supplemented with 0.5% (w/v) fatty-acid depleted BSA followed by homogenization in a motorized Potter-Thomas Teflon-glass homogenizer (two passes). The homogenate was subjected to 10-min cycles of low speed (600 g) and high speed (8600g) centrifugations in the same medium (twice each) at 4^{o}C in a Sorvall SS-34 rotor. After the low speed spin, the supernatant was collected and spun at high speed. The pellet obtained after the high

speed centrifugation was resuspended in the medium of the same composition and centrifuged. BSA was removed by centrifugation at 8600g in BSA-free medium. The final mitochondrial pellet was resuspended in an ice cold sucrose free isotonic buffer FH (280 mM mannitol, 0.1 mM EGTA, 2 mM HEPES, pH 7.4). The mitochondrial intactness was determined from the rate of cytochrome *c* oxidation (vide infra) compared with the rate measured after mild hypotonic shock (Douce et al., 1987).

3.3.3 Preparation of cytochrome *c*:

Horse heart cytochrome *c* (2 mM) was reduced by an excess of reducing agent, ascorbate (40 mM), 0.2 M Tris-Cl (pH 7.5). The reduced cytochrome *c* was separated from ascorbate by using Sephadex G-10 gel filtration (Siskind et al., 2002). The concentration of reduced cytochrome *c* was determined spectrophotometrically from the absorbance at 550 nm.

3.3.4 Cytochrome *c* oxidation assay as a measure of mitochondrial outer membrane permeability:

The rate of oxidation of exogenously-added reduced cytochrome c by cytochrome oxidase in isolated mitochondria is a measure of the permeability of the outer membrane to cytochrome c because translocation of cytochrome c through the outer membrane is a rate limiting step (see Fig. 3.2). The procedure previously described (Wojtczak et al., 1972) was modified to improve reproducibility. As the mitochondria were found to be more stable at higher concentrations, mitochondria were diluted in H buffer at 4 ^{o}C to a concentration of 0.2 mg/mL, in small batches just before the assay. Then, 50 µL aliquots were dispersed in 650 µL of room temperature H buffer supplemented with 5 mM DNP

and 5 μM antimycin A. The final protein concentration was 14.3 μg/mL. The mitochondria were allowed to acclimate at room temperature (10 min) in a microfuge tube. Then ceramide or one of the analogs (dissolved in 2-propanol at 1 mg/mL) was delivered to the mitochondria while the suspension was vortexed for 30 s to achieve effective dispersal of the sphingolipid. After dispersal, the mixture was incubated for 10 min at room temperature followed by addition of cytochrome *c* (20 μL; final concentration, approx. 25 μM) and immediate measurement of the absorbance at 550 nm for a period of 2 min. The initial rate of decline of absorbance of reduced cytochrome *c* was used as a measure of the permeability of the outer membrane to cytochrome *c*; ε_{550} (red-ox) = 18.5 mM^{-1} cm^{-1}. Vehicle controls were treated in an identical way. The percent of mitochondria with intact MOMs in these experiments was greater than 85%. Rates were corrected for the rate of oxidation observed with vehicle alone and this was very close to the untreated rate arising from a small number of damaged mitochondria.

The sensitivity of isolated mitochondria to permeabilization by added ceramide or analogs varied from one preparation to another. Therefore experiments with analogs were always performed in parallel with experiments with C_{16}-Cer. In this way the permeabilization produced by the analog (measures as the rate of cytochrome c oxidation) could be compared to that of C_{16}-Cer, either directly by reporting both rates or by expressing the result as a percent of that observed with C_{16}-Cer (Table 3.2).

Table 3.2 Relative potency of analogs to permeabilize the mitochondrial outer membrane. MOM was permeabilized by the addition of the indicated amount of analog (nmoles of analog per µg of mitochondrial protein) and the degree of permeabilization, as measured by the rate of cytochrome c oxidation is expressed as a percent (± S.E. of at least 3 trials) of the permeabilization measured in parallel experiments with C_{16}-Cer. The P values indicate the statistical significance of the permeabilization compared to that observed with C_{16}-Cer using the Student's T test. N/D means not done. N/S means not significantly different at the 95% confidence level.

Compound	Code	% of C_{16}-Cer permeabilization at 0.5-1nmol/µg protein	P Value	% of C_{16}-Cer permeabilization at 3nmol/µg protein	P value	% of C_{16}-Cer partitioning from Table 3.3
(2*R*,3*S*,4*E*) C_{16}-ceramide	S1	No effect (P = 0.32 relative to vehicle control)	<0.01	16 ± 4	<0.01	40
(2*S*,3*S*,4*E*) C_{16}-ceramide	S2	40 ± 60	N/S	80 ± 9	<0.05	--
(2*S*,3*R*,4*E*) *N*-methyl-C_{16}-ceramide	A3	No effect (P = 0.41 relative to vehicle control)	<0.02	21 ± 4	<0.01	75
(2*S*,3*R*,4*E*) C16-urea-ceramide	A4	236 ± 35	N/S	229 ± 7	<0.005	--
(2*S*,3*R*,4*E*) 3-*O*-methyl-C_{16}-ceramide	H2	125 ± 3	N/S	107 ± 15	N/S	60
(2*S*)-3-keto-C_{16}-dh-ceramide	H3	N/D		320 ± 82	<0.01	--
(2S,3R,15*E*) C_{16}-dh-ceramide	T1	76 ± 4	<0.03	385 ± 59	<0.001	30
(2*S*,3*R*,4*R*) C_{16}-phytoceramide	T2	429 ± 27	<0.03	230 ± 50	<0.05	460
(2*S*,3*R*) C_{16}-4,5-tb-ceramide	T3	N/D		120 ± 20	N/S	--
(2*S*,3*R*,4*E*) C_{16}-(4,5-allene)-ceramide	T4	N/D		303 ± 26	<0.02	--
(2*S*,3*R*,4*E*) C_{10}-ceramide	L1	46 ± 17	<0.02	662 ± 26	<0.005	90
(2*S*,3*R*,4*E*) 13C/C_{16}-ceramide	L2	1310 ± 104	<0.005	606 ± 27	<0.005	--
N-palmitoyl-serinol	L5	N/D		306 ± 92	<0.01	--
(2*S*,3*R*,4*E*) $C_{18:1}$-ceramide	L6	100 ± 19	N/S	113 ± 4	N/S	--

The degree of cooperativity between an analog and C_{16}-Cer was determined by averaging the rate of cytochrome c oxidation achieved with a specific amount of each agent alone (called the "expected average") and comparing this with the rate observed with half the amount of each agent added combined (called the "combined effect"). The degree of cooperativity is expressed as the ratio of the combined effect to the expected average. A result not significantly different from "1" means no cooperativity; greater than "1" is synergy; less than "1" is antagonism.

3.3.5 Measurement of adenylate kinase release:

The assay was performed as described earlier (Wieckowski et al., 2001). Mitochondrial suspensions containing 160 μg of mitochondrial protein were resuspended in isotonic buffer to a final volume of 1 mL. After the mitochondria were acclimated at room temperature for 10 min, ceramide or the analog was added, while vortexing. The mitochondria were incubated for 10 min at room temperature followed by centrifugation (14000 g) for 5 min at 4 ^{o}C (Beckman Coulter Microfuge 22R Centrifuge). A portion of the supernatant (300 μL) was combined with adenylate kinase reaction mixture (700 μL; 50 mM Tris, 5 mM $MgSO_4$, 10 mM glucose, 5 mM ADP, 0.2 mM NADP, pH 7.5) that had been preincubated for 2 min with enzyme mixture (5 μL; 2.5 units of hexokinase and 8.7 units of glucose 6-phosphate dehydrogenase) to consume ATP present in the reaction mixture prior to addition of the supernatant. The absorbance increase at 340 nm, from the generation of NADPH, was measured over 2 min. The maximal release was determined by measuring the activity of the supernatant obtained from an equal amount of osmotically shocked mitochondria. Measurement of adenylate kinase release does not measure the mitochondrial outer membrane (MOM) permeability but rather detects that,

at some point after treatment, the MOM was made permeable (perhaps transiently) to this 26 kDa protein.

3.3.6 Measurement of lipid insertion into mitochondria:

C_{16}-Cer, one of the analogs, or a combination of both was added to a 0.7 mL mitochondrial suspension containing 160 μg of mitochondrial protein in H buffer. In each experiment 30 μL of a 1 mg/mL 2-propanol solution of the lipid(s) was added while vortexing as described above. The suspension was then layered on 0.7 mL of ice-cold solution of 15% (w/v) sucrose, 5mM HEPES pH 7.5 and centrifuged at 18,000 g for 5 min at 4 ^{o}C. (Beckman Coulter Microfuge 22R Centrifuge). The mitochondria sedimented and the uninserted lipid remained out of the sucrose layer(prior experiments showed that dispersed ceramide floats at this density (Samanta et al., 2011)). Most of the supernatant was aspirated gradually and the tube inverted and any liquid wiped off with paper wipe. The pellets were used for lipid extraction and measurement of the mitochondria incorporated ceramide and analogs by LC-MS/MS as previously described (Bielawski et al., 2006; Bielawski et al., 2009).

3.3.7 Liposome permeabilization:

Single-walled liposomes (93% asolectin and 7% cholesterol, by weight) were prepared by the extrusion method as previously described (Stiban et al., 2006). In summary, lipids (total mass, 5 mg) were hydrated in a buffer containing 1.5 mM carboxyfluorescein (CF), 6 mM DPX, 38.8 mM NaCl, 10 mM HEPES, and 1 mM EDTA, pH 7.0. The mixture was vortexed and subjected to 4 cycles of freeze-thaw-sonication followed by freeze-thawing and extrusion through a polycarbonate membrane (13 times)

to form uniform single walled vesicles (100 nm diameter). A Sephacryl S200 gel filtration column (1.5 cm×30 cm) was used to separate the liposomes from untrapped fluorophore using an isoosmotic elution buffer lacking carboxyfluorescein and DPX (50 mM NaCl, 10 mM HEPES, 1 mM EDTA, pH 7.0). Aliquots (100 μL; containing approximately 0.1 mg of lipid) of the liposome suspension were diluted into 2 mL of the eluting buffer. CF was excited at 495 nm and the emitted light was detected at 520 nm in a Deltascan spectrofluorometer (Photon Technology Instruments). The fluorescence intensity was measured as a function of time under constant stirring and the test compound was added. The increase in fluorescence intensity was the result of the release of CF from the liposomes and its dilution from the quenching agent, DPX. The maximal increase in fluorescence intensity was measured after the addition of 150 μL of 5% Triton-X 100. The liposome permeabilization was plotted as % release of CF relative to maximal release.

3.3.8 Channel formation in planar membranes:

Electrophysiological studies were conducted on some of the analogs to determine whether they were able to permeabilize planar phospholipid membranes devoid of proteins or other mitochondrial factors. Planar phospholipid membranes were generated using the monolayer method as previously described (Montal & Mueller, 1972) and modified (Colombini, 1987b). The lipids comprising the monolayers were 1,2-diphytanoyl-sn-glycero-3-phosphocholine, asolectin, and cholesterol at a 1:1:0.1 ratio by weight. The aqueous solutions were 1.0 M KCl, 1mM $MgCl_2$, 5mM PIPES pH 6.9 on both sides of the chamber. The bilayer was formed across a 100μm diameter hole in a Saran (polyvinylidene chloride) partition Calomel electrodes were used to interface with

the aqueous solution, the voltage was clamped at 10 mV and the current recorded using a Digidata 1322A digitizer by Axon Instruments and Clampex 9.0 software by Axon Laboratories. To form a channel, successive additions of 5-20 μL of 0.05 mg/mL of the analog in 2-propyl alcohol were stirred into the aqueous solution (5 mL) on one side of the membrane. The vehicle has no effect and its final concentration was less that 1% (v/v).

3.4 RESULTS

The analogs were tested for their ability to permeabilize the outer membrane of isolated rat liver mitochondria to proteins, using the cytochrome *c* oxidation assay (Fig. 3.2). Permeation through the MOM limits the rate of oxidation of exogenously-added cytochrome *c* by cytochrome oxidase in the inner membrane and thus the initial rate of oxidation of cytochrome c was utilized as a measure of the permeabilization of the MOM to proteins. Sample dose-response curves are shown in Fig. 3.3. Note that the shapes of these curves vary from rectangular hyperbola to sigmoid, making rigorous comparisons difficult. Generally a dose of 30 nmoles per 10 μg of mitochondrial protein was chosen as the common dose for comparison because it was low enough to avoid pronounced saturation by some analogs but high enough to detect permeabilization by the less-effective analogs. Results with lower doses are also reported. The sensitivity of mitochondria to MOM permeabilization varied from one isolation to the next so the permeabilization results summarized in Table 3.2 are expressed as a percentage of the permeabilization achieved by ceramide in the same mitochondrial preparation, either C_{16}-Cer or C_8-Cer, as appropriate.

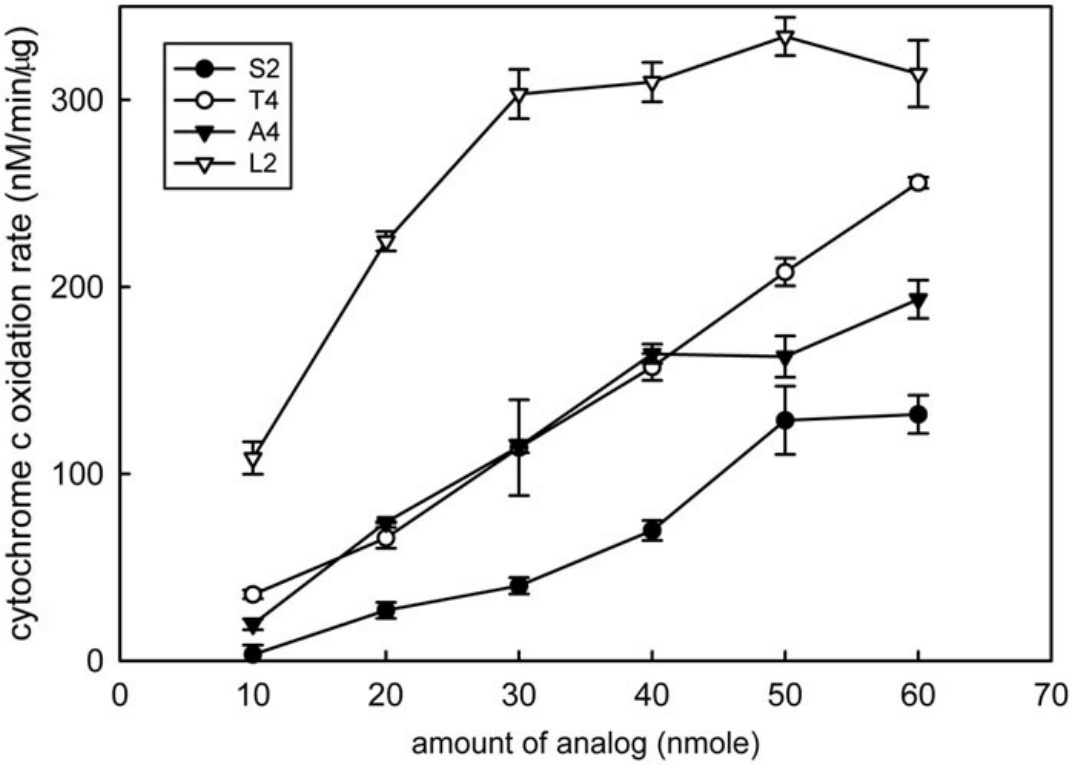

Figure 3.3 Examples of dose-response curves of the analogs used. The cytochrome *c* oxidation rate was used to assess the permeability of the MOM to proteins. The indicated amount of analog was added to 0.7 mL of a mitochondrial suspension (see section 4.3.4).

An indication of MOM permeabilization was also obtained by measuring the extent of release of adenylate kinase. This is not a measure of MOM permeabilization but rather an indication of the fraction of mitochondria that have been permeabilized. With one notable outlier (vide infra) the MOM permeabilization assay and the adenylate kinase release assay yielded similar results for the analogs when compared to the effect of ceramide (Fig. 3.4). The permeabilizing ability of the analog is expressed as a fraction of the ability of the corresponding ceramide, either C_{16}-Cer or C_8-Cer. The line drawn is not

fit to the data but is a theoretical line for a 1:1 correlation between the two experimental results.

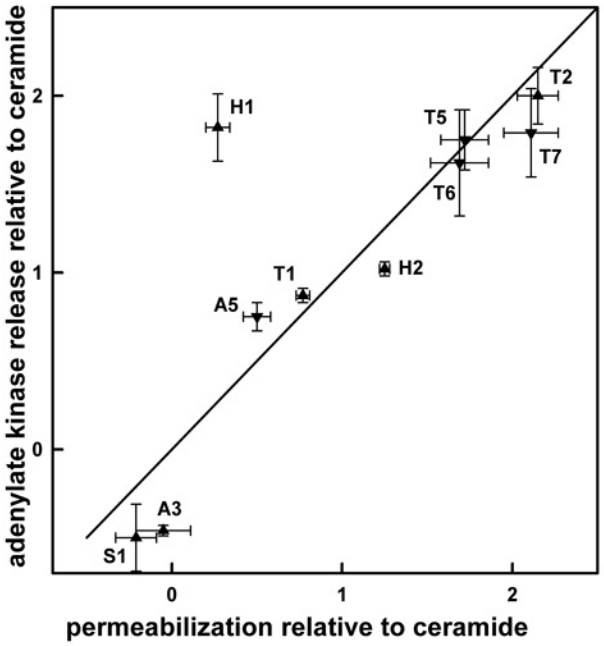

Figure 3.4 Correlation between changes in MOM permeability and adenylate kinase release by analogs. The "permeabilization relative to ceramide" is the rate of cytochrome *c* oxidation induced by the analog divided by that induced by ceramide (C_{16}-Cer for triangles and C_8-Cer for inverted triangles) under the same conditions. "adenylate kinase release relative to ceramide" is the activity of adenylate kinase released from mitochondria by analog addition divided by that released by ceramide. The error bars are standard error of at least three experiments.

The MOM permeabilization is dependent on the extent of insertion of the analog into the mitochondria, the propensity for channel formation, and the stability of the channels. Typically, only 0.3 to 1% of the added analog actually inserted into the mitochondrial membranes (Table 3.3). Phytoceramide was the exception with nearly 5% insertion. The extent of insertion helped to interpret the observed ability of an analog to permeabilize the MOM.

Table 3.3 Extent of delivery of ceramide and its analogs to mitochondrial membranes. The indicated amount of lipid was added to a mitochondrial suspension (160 μg protein). The percent of the added lipid that incorporated into mitochondria is shown as mean ± S.E. of 4 trials or the values of individual trials. Column 4 shows the extent of analog insertion when added with equal amounts of C_{16}-Cer. The insertion of C_{16}-Cer was not affected by the presence of the analog. Column 5 is the T-test probability value obtained when comparing results in column 3 and 4.

Compound	nmoles added	% incorporation	% incorporation in the presence of C_{16}-Cer	P value
D-C_{16}-Cer	56	1.04 ± 0.23		
L-C_{16}-Cer (S1)	56	0.41 ± 0.06		
C_{10}-Cer (L1)	66	0.95 ± 0.07	2.45 ± 0.34	0.01
Phytoceramide (T2)	54	4.78 ± 0.80	1.64 ± 0.36	0.004
N-Me-C_{16}-Cer (A3)	54	0.74, 0.85		
1-O-Me-C_{16}-Cer (H1)	54	1.00, 1.25		
3-O-Me-C_{16}-Cer (H2)	54	0.35, 0.95		
15E-C_{16}-Cer (T1)	56	0.23, 0.42		

3.4.1 Ability of analogs to permeabilize the MOM to proteins

Changes in the non-polar portions of ceramide did not interfere with channel formation. The analogs of ceramide having a shorter *N*-acyl chain **(L1)** or a shorter sphingosine backbone **(L2, L5)** were more potent in permeabilizing the MOM than C_{16}-Cer (Table 3.2). For C_2-ceramide (Siskind et al., 2006) the additional potency was attributed to an enhanced ability to incorporate into the mitochondrial membrane. That is not the case for C_{10}-ceramide **(L1)** (Table 3.2, column 5) as the permeabilization was increased 6 fold despite no difference in the degree of incorporation into the MOM**.** Increasing the effective bulk of the hydrocarbon chain by using fluorescently labeled C_6-

NBD-ceramide **(L4)**, or $C_{18:1}$-Cer **(L6)** with a *cis* double bond in the middle of the acyl chain, inhibited cytochrome oxidase activity. After correction for the inhibition, channel formation by $C_{18:1}$-Cer **(L6)** was indistinguishable from that of C_{16}-Cer (Table 3.2).

Major alterations in ceramide's *trans* double bond were also well tolerated (Table 3.2 and 3.5). Some of these were analogs of C_8-ceramide. Under identical treatments, C_8-Cer **(L3)** permeabilized the MOM to cytochrome c 36% of the maximal permeabilization, whereas the *cis* isomer **(T6)** resulted in a 61% of maximal permeabilization (Table 3.5). An analog with an extra double bond (6*E*) in conjugation with the first **(T5)** permeabilized the outer membrane to the same extent as the *cis* isomer **(T6)**. Moving the 4*E* double bond to a position between the two hydroxyl groups by putting it at the C3 position and moving the C3-hydroxyl group to the C5 position **(T7)** did not prevent MOM permeabilization. Similar results were obtained with analogs of C_{16}-Cer. C_{16}-phytoceramide **(T2)**, where the 4*E*-double bond is replaced by a C4-hydroxyl group, had a 2-fold higher ability to permeabilize the MOM as compared to C_{16}-Cer but this can be more than accounted for by an enhanced ability to insert into the MOM (Table 3.3). Replacing the 4*E*-double bond by a C4, C5-triple bond **(T3)** also did not significantly affect the ability of the molecule to permeabilize the MOM. Moving the double bond farther down the chain **(T1)** to a position that does not form an allylic system results in an enhanced MOM permeabilization, despite a substantial reduction in its ability to insert into mitochondria. Hence the location, conformation, and degree of unsaturation do not have significant effects on channel-forming ability.

The amide linkage in ceramide is proposed to have similar organizing effects as the amide linkages in proteins (Bittman, 2009). The hydrogen-bonding ability of this

linkage was proposed to organize ceramide monomers into columns. We found that increasing the hydrogen-bonding ability of this region by introducing a "urea" linkage **(A4)** resulted in an enhanced ability to permeabilize the MOM (Table 3.2). Moreover, reducing the hydrogen-bonding capacity by using C_8- and C_{16}-ceramines **(A1, A2),** which differ from ceramide by having an amino instead of an amide group, eliminated the molecule's ability to permeabilize MOM to proteins. Since both of these ceramines strongly inhibit cytochrome oxidase activity, release of adenylate kinase from the mitochondrial intermembrane space was measured. The ceramines caused no significant release of adenylate kinase. For C_{16}-ceramine, kinase release was -0.6 ± 7% for the highest dose tested (8 nmol/μg mitochondrial protein). C_8-ceramine was much more effective at releasing carboxyfluorescein from liposomes than C_8-Cer (Table 3.4) showing that it readily forms channels but these are very small. Methylation of the amide nitrogen, affording *N*-methyl-C_{16}-Cer **(A3)**, drastically reduced but did not completely eliminate the ability of the molecule to permeabilize the MOM to cytochrome *c* (Table 3.2). The partitioning of **(A3)** into mitochondria was slightly reduced, however the reduced insertion into the membrane of this analog could not account for the extent of its loss of function.

Table 3.4 Comparison of channel-forming activity in mitochondria and liposomes. Liposomes and mitochondria were treated with ceramide analogs to assess the latter's ability to permeabilize membranes. For the liposomes (column 3) the % release of contents was performed at 2 different doses: 87 and 147 nmoles per 2.5 mL of liposome suspension. For the MOM permeabilization (column 4) results are expressed as a % permeabilization achieved by hypotonic shock. The dose used was 0.19 nmoles/μg protein. Measurements of adenylate kinase release (column 5) are expressed as percent of the kinase activity released following treatment with 0.25 nmoles/μg protein.

Compound	Code	Liposome % release	MOM % perm.	Adenylate Kinase % release
(2*S*,3*R*,4*E*) C_8-ceramide	L3	17 ± 2 22 ± 3	36 ± 4	24 ± 2
(2*S*,3*R*,4*E*) C_8-ceramine[a]	A2	100	N/D	none
(2*S*,3*R*,4*E*) C2-OCH_3-C_8-ceramide	A5	18 ± 2 24 ± 3	18 ± 3	18 ± 2
(2*S*,3*R*,4*E,6E*)C_8-ceramide (diene)	T5	32 ± 3 40 ± 3	62 ± 5	42 ± 4
(2*S*,3*R*,4*Z*) C_8-ceramide (*cis* analog)	T6	37 ± 3 47 ± 4	61 ± 6	39 ± 7
(2*S*,5*R*,3*E*) C_8-ceramide	T7	36 ± 3 46 ± 4	76 ± 6	43 ± 6

[a] Release from liposomes was complete with as little as 15 nmoles per 2.5 mL of liposome suspension. MOM permeabilization could not be done (N/D) because of strong inhibition of cytochrome oxidase.

The ability of **(A3)** to form channels, even at a much reduced potency raises a severe problem with the working model of the ceramide channel where the hydrogen bonding from the amide nitrogen is essential to the overall structure. In the model, the amide nitrogen of one ceramide molecule forms a hydrogen bond with the carbonyl group of another to form ceramide columns. Methylation of the amide nitrogen as in **(A3)** would effectively prevent such interactions. However, in molecular dynamic simulations

performed by Andriy Anishkin (Anishkin et al., 2006), whereas the working model of the ceramide channel is the predominant form arising from such simulations, other, minor forms were also detected. In some of these the carbonyl oxygen is not hydrogen bonding with the amide hydrogen of the adjacent ceramide but hydrogen bonding with a C1-hydroxyl through a water bridge (e.g. Fig. 3.5). Thus it may be possible for **(A3)** to form a similar structure.

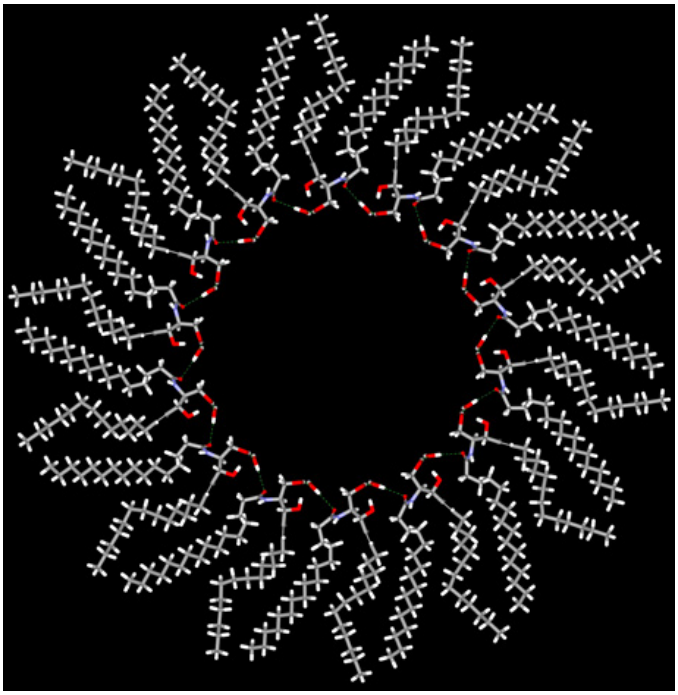

Figure 3.5 The top view of a ceramide channel structure. This figure, which was obtained by Andriy Anishkin as part of the structures formed by simulated annealing, is one of a few structures in which the carbonyl oxygen forms a hydrogen bond with one of the hydroxyl groups rather than forming a hydrogen bond with the amide group of an adjacent ceramide molecule. In this structure, the ceramide columns are arranged in parallel rather than anti-parallel.

The C1 and C3 hydroxyl groups have been proposed to stabilize channel structure via hydrogen bonds with the corresponding functional groups on adjacent ceramide molecules. Analogs of these functional groups were utilized to determine the contribution of these groups to the channel structure. *O*-Methylation of the C1-hydroxyl group **(H1)** was chosen because the methyl group should prevent this hydroxyl group from participating in a hydrogen bond. The methylation of the C1 hydroxyl resulted in an almost complete loss of any stable MOM permeabilization despite no change in ability to insert into mitochondria (Table 3.4). When the ability of **(H1)** to release adenylate kinase was tested, it was almost double that observed with C_{16}-Cer indicating that twice as many mitochondria were permeabilized, if only transiently, by **(H1)**. When reconstituted into planar membranes, **(H1)** produced conductances that were transient (vide infra) as opposed to the growing conductances observed with C_{16}-Cer. These were similar to those published for sphingosine (Elrick et al., 2006) except that these are large enough to allow the release of adenylate kinase (Fig. 3.4).

Unlike **(H1),** methylation at the C3-hydroxyl **(H2)** produced functional properties very similar to those of C_{16}-Cer (Table 3.2). Both the cytochrome c oxidation assay and the adenylate kinase release assay produced results indistinguishable from those of C_{16}-Cer. The importance of the location of the C3-hydroxyl group and the stereochemistry of the adjacent chiral center were tested by relocating the hydroxyl to the C5 position **(T7)** and by changing configuration from (2*S*,3*R*)-C_{16}-Cer to (2*S*,3*S*)-C_{16}-Cer **(S2)**, respectively. Neither of these alterations had a large effect on the ability of these molecules to permeabilize MOMs of isolated mitochondria (Table 3.2). Thus the location and orientation of the C3-hydroxyl can be changed with minimal consequences.

By sharp contrast, converting the (2*S*,3*R*)-C_{16}-Cer to (2*R*,3*S*)-C_{16}-Cer **(S1)** (i.e. an additional change in the chirality at C2) greatly reduced its ability to permeabilize MOMs, consistent with the importance of the C1-hydroxyl group (Table 3.2). Unlike the results with **(H1)**, **(S1)** was unable to permeabilize the MOM or release adenylate kinase at 1 nmole/μg protein and produced only 16% of the permeabilization of C_{16}-Cer at 3 nmoles/μg protein. The amount of insertion was reduced by a little over half but not enough to account for the large reduction in ability to permeabilize the MOM. Thus, the stereochemistry of ceramide that limits the possible and preferred positions of its polar groups (Bittman, 2009), can also influence the propensity for channel formation in the MOM.

3.4.2 Interactions between D-e-C_{16}-ceramide and its analogs

Isolated mitochondria were treated with either C_{16}-Cer alone or the analog alone, or an equimolar mixture of C_{16}-Cer and the analog at half the dose. Thus, the total amount of sphingolipid added was kept constant. The ability of each of the three treatments to permeabilize the MOM to cytochrome *c* was measured. Examples of the results are shown in Fig. 3.6. For **(A4)** and **(L2)** the simultaneous presence of both lipids

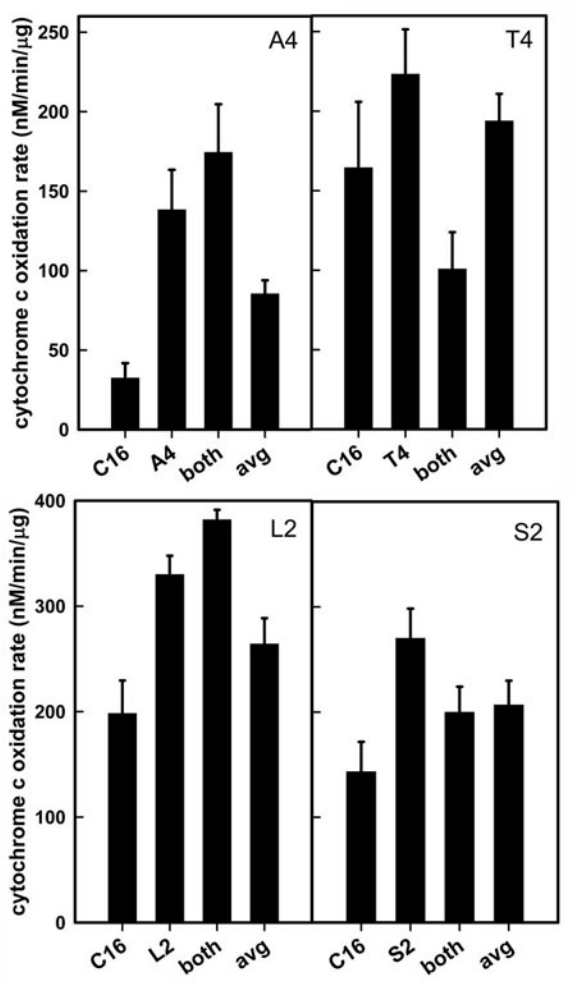

Figure 3.6 Cooperativity between analogs and C_{16}-Cer. For an individual addition, a total of 40 nmol was used. For combined additions (both), 20 nmol of each was used. The average bar (avg) shows the average of the results obtained with each lipid alone. The statistics are shown in Table 3.5. The individual and combined additions for each analog were performed with the same batch of mitochondria under the same conditions to avoid the variability in sensitivity to ceramide found among mitochondrial preparations.

(designated as both) yielded a higher rate of cytochrome c oxidation (and therefore a higher permeability) than the average of the individual treatments (avg), thus indicating synergy. The converse was true for **(T4)**, indicating antagonism. For **(S2)** there was no

significant difference, indicating neutrality or no cooperativity. Depending on the experimental set, 40 nmol or 60 nmol of lipids were utilized (as indicated in Table 3.5). The permeability resulting from the combined treatment ("combined effect" in Table 3.5) was compared to the "expected average" which is the average of the permeabilities observed with the individual sphingolipid treatments. The ratio is reported in Table 3.5 along with the P values of statistical significance and the interpretation of the results. Ratios significantly greater than 1 indicate synergy and ratios significantly less show antagonism.

A subtle change, such as the replacement of the 4*E* double bond of ceramide with a C4,C5-triple bond **(T3),** resulted in a neutral effect when combined with C_{16}-Cer (Table 3.5). Experiments with the diastereomer **(S2)** (2*S*,3*S* as opposed to 2*S*,3*R* for C_{16}-Cer) were also consistent with simple neutrality (Fig. 3.6 and Table 3.5).

Treating mitochondria with a mixture of C_{16}-Cer and the shorter chain analog, 13C/$C_{16:0}$ **(L2)** resulted in a permeabilization that was greater than the average of treatments with individual compounds (Fig. 3.6). Similar results were obtained with other short-chain analogs **(L1, L5)** (Table 3.5) and with urea-ceramide **(A4).**

Mitochondria treated with an equimolar mixture of ceramide and phytoceramide **(T2)** achieved a much reduced level of permeabilization than expected from averaging the individual treatments (Fig. 3.6, Table 3.5). This inhibition was also found between phytoceramide **(T2)** and L-e-C_{16}-Cer **(S1)** (data not shown). A similar antagonistic interaction was found between C_{16}-Cer and either *N*-methyl-C_{16}–Cer **(A3)** or the enantiomer, (2*R*,3*S*) **(S1)**.

Table 3.5 Cooperativity between C_{16}-ceramide and its analogs. The analog was mixed in equimolar quantities with C_{16}-Cer and the permeabilization of the MOM was compared to the average permeabilization observed with equal total amounts of either C_{16}-Cer or the analog alone. At least 3 experiments were performed for each condition and P values for the t-tests are listed. Using 95% confidence, ratios significantly greater than 1 are labeled synergistic; significantly less than 1, antagonistic; not significantly different, neutral.

Compound	Code	Combined effect / Expected average	P value	Nature of interaction
(2*R*,3*S*,4*E*) C_{16}-ceramide	S1	0.33	0.0005	Antagonistic
(2*S*,3*S*,4*E*) C_{16}-ceramide	S2	1[a]	0.36	Neutral
(2*S*,3*R*,4*E*) *N*-methyl-C_{16}-ceramide	A3	0.21	0.003	Antagonistic
(2*S*,3*R*,4*E*) C_{16}-urea-ceramide	A4	1.5[a]	0.015	Synergistic
(2*S*,3*R*,4*E*) 3-O-methyl-C16-ceramide	H2	1.0	0.25	Neutral
(2*S*)-3-keto-C_{16}-dh-ceramide	H3	1.0	0.41	Neutral
(2S,3R,15E) C_{16}-dh-ceramide	T1	1.3	0.15	Neutral
(2*S*,3*R*,4*R*) C_{16}-phytoceramide	T2	0.52[a]	0.009	Antagonistic
(2*S*,3*R*) C_{16}-4,5-tb-ceramide	T3	0.95[a]	0.33	Neutral
(2*S*,3*R*,4*E*) C_{16}-(4,5-allene)-ceramide	T4	1.3	0.06	Neutral
(2*S*,3*R*,4*E*) C_{10}-ceramide	L1	1.5[a]	0.04	Synergistic
(2*S*,3*R*,4*E*) 13C/C_{16}-ceramide	L2	1.4[a]	0.02	Synergistic
N-palmitoyl-serinol	L5	1.4	0.002	Synergistic

[a] The increase in MOMP resulting from the addition of a total of 3.6 nmoles/μg protein of an equimolar mixture of C_{16}-Cer and the specified analog was compared to 3.6 nmoles/μg protein of either C_{16}-Cer or the analog alone. In the other experiments, 5.6 nmoles/μg protein were used.

The type and degree of cooperativity correlates with the channel-forming ability of the analog. A plot of the channel-forming potency relative to that of C_{16}-Cer versus the cooperativity ratio from Table 3.5 shows the strong correlation (Fig. 3.7). The upper

right quadrant contains data from the analogs showing synergy and higher propensity for channel formation whereas the lower left quadrant contains data from those displaying antagonism and lower channel-forming propensity. Analogs showing no cooperativity and essentially similar channel-forming propensity to C_{16}-Cer tend to cluster at the "origin". The other two quadrants are essentially vacant.

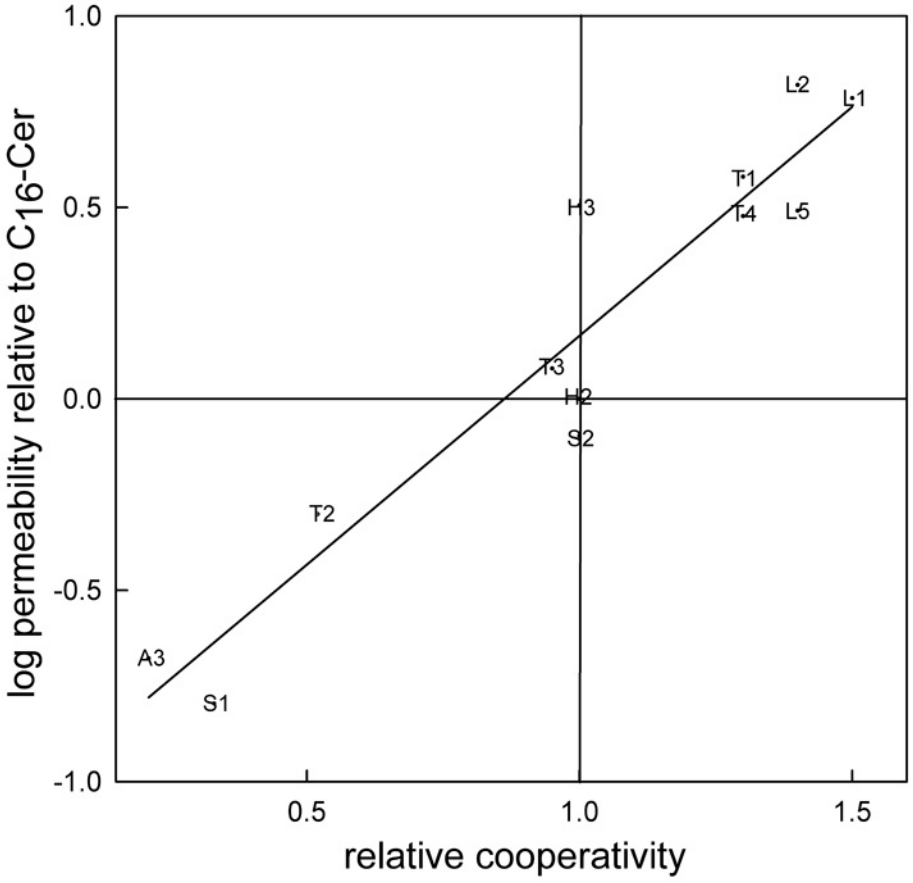

Figure 3.7 Correlation between degree of cooperativity and ability of an analog to permeabilize the MOM. Relative cooperativity is from column 3 of Table 3.5. The permeability relative to C_{16}-Cer is from Table 3.2 column 3 after dividing by 100 and taking the log.

The permeabilization of the MOM following the dispersal of ceramide or an analog must involve at least two processes: insertion and self-assembly. The cooperativity could take place at one or both of these. The influence of combined delivery on the insertion of the sphingolipids was assessed for one analog showing synergy **(L1)** and one showing antagonism **(T2)** (Table 3.3). The presence of C_{16}-Cer influenced the ability of the analogs to insert into the MOM in harmony with the observed cooperativity. The amount of **(T2)** that inserted when combined with C_{16}-Cer was one third of that measured following its individual addition whereas the insertion of **(L1)** doubled. The insertion of C_{16}-Cer was not significantly affected by the presence of the analog.

The antagonism observed in mitochondrial experiments was also evident in experiments with liposomes, showing a direct interaction between these lipids. Premixing C_{16}-Cer and C_{16}-phytoceramide **(T2)** resulted in a much smaller permeabilization of liposome membranes than phytoceramide **(T2)** alone (Fig. 3.8).

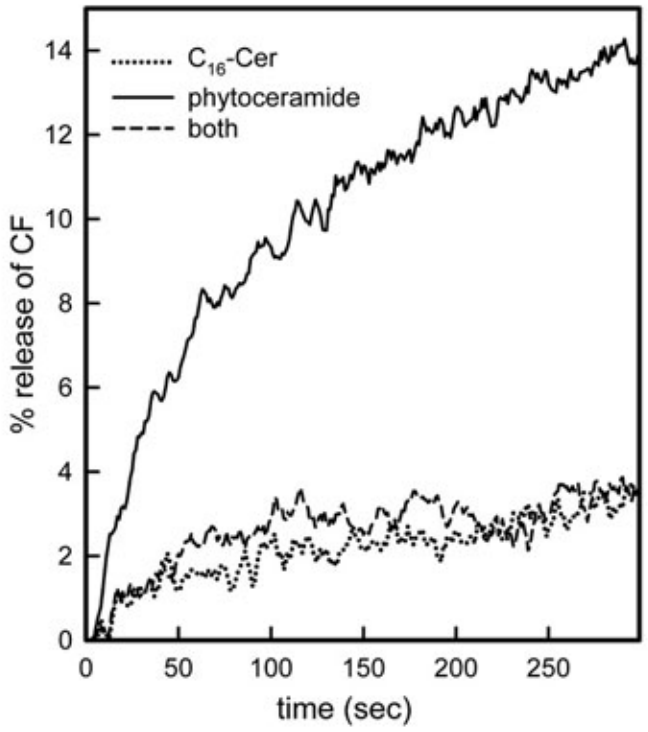

Figure 3.8 Permeabilization of liposomes by C_{16}-Cer, C_{16}-phytoceramide (T2), or the two together.

3.4.3 Channel formation in phospholipid membranes

To directly observe channel formation by ceramide analogs and to gain insight into their stability and dynamics, experiments were performed in defined systems consisting of phospholipid membranes: planar membranes and liposomes. In planar membranes, channel formation was monitored as changes in conductance to K^+ and Cl^- ions. In liposomes, the release of carboxyfluorescein and the quenching agent, DPX, was used to assess the permeabilization of single-walled liposomes by the analogs. In both of these experimental systems, the analogs that were able to permeabilize the MOM were also able to permeabilize phospholipid membranes that were free of proteins,

demonstrating that the analogs form channels rather than inducing MOM proteins to form channels.

Most of the analogs that could permeabilize the MOM produced conductances in planar membranes with similar characteristics to those of C_{16}-Cer. Examples for phytoceramide **(T2)** and urea-ceramide **(A4)** are shown in Fig. 3.6. Channel formation occurred after a lag phase and usually required a few separate additions. Fig. 3.9A shows how a sustained conductance developed after a final addition of 1 nmole of **(A4)**. The conductance increased in steps of varying size until it reached a plateau. Sometimes the increase was rapid, reaching a high conductance (Fig. 3.9B). At the reduced gain required to observe the total conductance the increase appears to be very smooth. Addition of La^{+3} resulted in channel disassembly after a variable delay (Fig. 3.9B), which is similar to the effect of La^{+3} on a C_{16}-ceramide channels as previously reported (Siskind et al., 2003). The variable delay is characteristic of a stochastic process (Siskind et al., 2003) and is also consistent with the formation of a single channel that enlarges in size. Most of the analogs appear to form a single large channel in the planar membrane (data not shown), as was demonstrated for ceramide (Siskind et al., 2003).

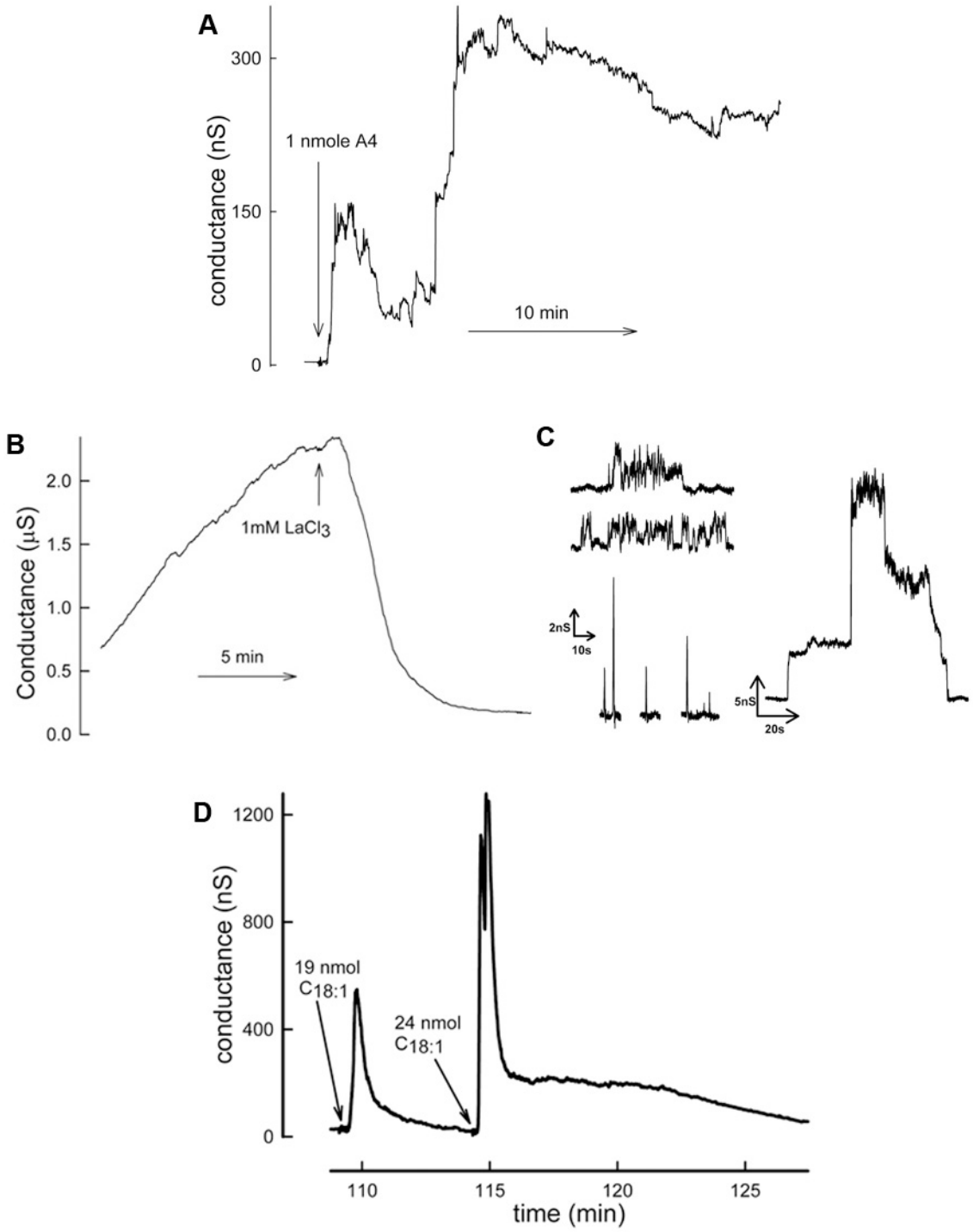

Figure 3.9 Electrophysiological recording of conductances formed by ceramide analogs in planar phospholipid membranes. A. The formation of a channel by urea ceramide **(A4)**. Equal amounts of the analog were added at intervals (for a total of 4.6 nanomoles) with the last shown in the figure. B. The formation of a C_{16}-phytoceramide **(T2)** channel and its partial disassembly

by the addition of $LaCl_3$. Channel formation followed the addition of 0.46 nmoles of C_{16}-phytoceramide **(T2)**. C. Segments of conductance transients observed after addition of 1 nmole of ceramide methylated at the C1-hydroxyl **(H1)**. The bursts shown were observed over a 40 min time period. D. Transient channels formed by **(L6)** $C_{18:1}$-ceramide. A total of 25nmol of $C_{18:1}$ was added at intervals and similar patterns of channel growth and disassembly were seen after each addition. In all cases the transmembrane voltage was clamped at 10 mV.

Marked exceptions were the behaviors of the conductances produced by 1-O-methyl-C_{16}-ceramide **(H1)**, *N*-methyl-C_{16}-ceramide **(A3)** and $C_{18:1}$-Cer **(L6)**. With these compounds, the conductance rose rapidly but was transient, declining and returning to the baseline shortly thereafter. This behavior was often observed multiple times in the same membrane. Only occasionally would a prolonged conductance form. The analog with the shortest conductance bursts was **(H1)** (Fig. 3.9C). The figure shows samples of conductance burst recorded within a 40 min period of activity. **(L6)** was at the other end of the spectrum, producing greater conductances but these also tended to decay (Fig. 3.9D). The addition of more sample produced a second transient conductance. **(A3)** was intermediate between these (data not shown). The behavior of these analogs is consistent with a less stable structure and in agreement with the observations made with isolated mitochondria. **(H1)** produced virtually no permeability; **(A3)** had a much diminished permeabilizing ability (21% of that induced by C_{16}-cer, Table 3.2); **(L6)** produced an effective permeabilization similar to C_{16}-Cer. Clearly the channel dynamics are not detectable in mitochondrial experiments and only the average permeability to cytochrome c is assessed.

In general, liposome permeabilization experiments and adenylate kinase release experiments produced results in agreement with mitochondrial permeability measurements (Table 3.4 and Fig. 3.4). **(H1)** and the ceramines **(A1)** and **(A2)** were the exception. **(A2)** induced the maximal release of liposomal contents, but did not facilitate the release of adenylate kinase from the mitochondrial intermembrane space (Table 3.4). The fact that ceramine can permeabilize liposomes to carboxyfluorescein, but did not permeabilize the MOM to adenylate kinase is consistent with its formation of small channels capable of allowing small molecules to cross membranes, but not large enough to allow the passage of proteins. These conductances resemble those published for sphingosine (Elrick et al., 2006). Like **(H1)**, these conductances did not grow in size but returned to the baseline and were likely the result of the formation of small pathways such as the toroidal structures induced by amphipathic structures (Bechinger, 1997; Sansom, 1998; Qian et al., 2008). Unlike **(H1)** the transient conductances did not become large enough to release adenylate kinase from mitochondria.

3.5 DISCUSSION

The data presented show that the structure of ceramide can be altered in a number of ways without losing the ability of the molecule to permeabilize membranes in a manner that is consistent with self-assembly into large channels capable of translocating proteins through membranes. The mitochondrial and planar membrane experiments suggest that many of the analogs form large, stable channels. The results indicate the relative importance of specific structural features of ceramide for channel formation,

namely the differential importance of the hydroxyl groups, the role of the *trans* double bond, and the importance of the stereochemistry.

3.5.1 Ceramide channel formation is minimally affected by apolar chain length

Physiologically, the length of the *N*-acyl chain of ceramide is clearly very important (Megha et al., 2007; Pruett et al., 2008). For example, the ceramide synthases show strong specificity for different acyl-CoA substrates (Venkataraman et al., 2002; Mizutani et al., 2005; Laviad et al., 2008; Menuz et al., 2009). Some preferentially produce long-chain ceramides such as C_{16}-Cer, whilst others preferentially produce very long-chain ceramides such as C_{24}-Cer (Venkataraman et al., 2002; Mizutani et al., 2005). Many enzymes that metabolize ceramide do not recognize C_2-Cer (El Bawab et al., 2002; Wijesinghe et al., 2005). Yet, with regard to the ability to form channels, the length of the *N*-acyl chain was found to be relatively unimportant (Siskind & Colombini, 2000; Siskind et al., 2002). After compensating for the difference in delivery to the mitochondrial membranes, the potency of C_{16}-Cer and C_2-Cer were found to be indistinguishable (Siskind et al., 2006). Here we tested analogs having shorter *N*-acyl chains **(L1, L3)** and shorter sphingoid base backbones **(L2, L5)**. The results indicate that these can also form permeability pathways in membranes in a manner consistent with channels and interact synergistically with ceramide. For **(L1)**, the synergy arises from the ability of C_{16}-Cer to aid in the insertion of **(L1)** into mitochondria.

It is important to note that the minimal ceramide analog, N-palmitoyl-serinol **(L5)**, functions very well with only one aliphatic chain. Thus, one might ask why natural ceramides have such a large amount of apolar mass. The simplest answer would be that

the extra bulk anchors the lipid in the membrane, limiting spontaneous, uncatalyzed motion between membranes of different organelles.

3.5.2 C1- hydroxyl group is critical to stable ceramide channel formation; modifications to the *trans* double bond are well tolerated

An important feature in the ceramide structure is the C4,C5-*trans* double bond in the sphingoid base backbone (Bittman, 2009; Phillips et al., 2009). For permeabilization of the MOM, many changes were well tolerated, namely conversion of *trans* to *cis*, displacement of the double bond relative to the adjacent hydroxyl, and replacement of the double bond by a third hydroxyl. Thus, a variety of structures are capable of permeabilizing membranes in a manner consistent with the channels formed by C_{16}-ceramide.

The ability to form stable channels was lost by *O*-methylation of the C1-hydroxyl group **(H1)**. It forms transient pores capable of allowing adenylate kinase release but too short-lived to significantly increase the overall MOM permeability to proteins. The transient conductances were evident in planar membrane experiments. By contrast, *O*-methylation of the C3-hydroxyl group **(H2)** was well tolerated. Similar results with the C3-keto **(H3)** analog provide additional evidence that C3-hydroxyl modifications are well tolerated. Further evidence for a difference in the importance of these two hydroxyl groups comes from results obtained with stereochemical isomers. The diastereomer studied in which "3R" was changed to "3S" **(S2)** showed no change in MOM permeabilizing properties despite a change in orientation of the C3-hydroxyl. However, the enantiomer, with the same change at the C3 position and an additional change from "S" to "R" at the C2 position **(S1)**, was much weaker in its capacity to permeabilize

mitochondria. Thus the presence and orientation of the free hydroxyl at C1 is critical to the stability of the channels, indicating that this hydroxyl forms part of a highly organized structure.

3.5.3 Amide linkage provides stabilizing structural support for the ceramide channel

The importance of the amide linkage as an organizing unit is supported by the finding that the conversion of an amide chain to an amine-linked chain in ceramine **(A1, A2)** prevents the permeabilization of the MOM to proteins. If the ceramides are arranged in the channel as proposed by the structural model (Siskind et al., 2003; Anishkin et al., 2006), then the conversion of the amide linkage to an amine would indeed destabilize the structure by eliminating the hydrogen bonding that has been proposed to be the basis for the columns that make up the channel. By contrast, the greater hydrogen-bonding and ordering ability of a urea linkage according to the structural model would be expected to stabilize the channel, and indeed this analog **(A4)** forms channels (Fig. 3.9A). The introduction of a methoxy group in the amide region **(A5)** still allowed channel formation, indicating that the modification is tolerated.

N-methyl C_{16}-Cer **(A3)** can still form channels, which is in apparent contradiction to the structural model because the methyl group that replaces the C3 hydroxyl cannot participate in hydrogen bonding. Whilst its ability to permeabilize the MOM is much reduced as compared to C_{16}-Cer and in planar membranes it forms unstable channels, the ability to form channels at all seems to invalidate the structural model of the ceramide channel. However, channel formation by **(A3)** is antagonistic with that of C_{16}-Cer, indicating that structural incompatibilities were introduced by *N*-methylation. Molecular modeling studies show that a channel can be formed with the carbonyl group hydrogen-

bonding with the C1-hydroxyl group through a water bridge as shown by the example structure in Fig. 3.5. This structure is quite different from the working model of the ceramide channel (Anishkin et al., 2006).

3.5.4 Cooperativity between ceramide and analogs

Combined addition of C_{16}-Cer and an analog showed cooperativity in membrane permeabilization in certain cases: either synergy or antagonism. The cooperativity correlates well with the ability of individual lipids to permeabilize the MOM. Surprisingly, the cooperativity seems to involve the insertion into the MOM. Insertion may be catalyzed by structures formed by sphingolipids in the membrane. Perhaps ceramide forms phases or domains in the membrane that could engage or exclude other analogs depending on the compatibility or incompatibility of the molecular structures (i.e. their ability to bind to each other). Organized structures composed of many sphingolipids would require that each component fit well sterically and in bonding interactions. Thus very similar structures would be interchangeable, complementary structures would show synergy and poorly compatible structures would show antagonism. Without structural information it will be difficult to understand the molecular basis for the cooperativity.

3.5.5 Influence of structural changes on channel function

The ability of ceramide to self-assemble and form membrane channels is remarkably resistant to changes in molecular structure. However, structural changes in specific regions such as the C1-hydroxyl and the amide linkage do decrease channel stability or form channels too small to release proteins. These changes would reduce or eliminate the ability of the channel to release proteins from mitochondria. A reduction in

the rate of release and amount of protein release does result in a failure to initiate apoptosis. The use of lasers to damage mitochondria in live cells (Khodjakov et al., 2004) failed to induce apoptosis presumably because of insufficient protein release and thus failure to achieve a critical cytosolic concentration of pro-apoptotic proteins such as cytochrome c. Thus natural selection pressure maintains the structure of ceramide and the ability to form large and stable channels.

3.6 CONCLUSIONS

The results of previously published work on ceramide channels strongly suggests that these channels have a highly organized structure, one in which an altered configuration of the polar lipid head region would disrupt the structure. The results presented here identify key functional groups important for ceramide channel formation and structural aspects where changes are tolerated. The C1-hydroxyl is indispensable for channel stability whereas C3-hydroxyl is not critical for channel formation. It is interesting that further elaborations of ceramide in cells involve additions to the C1-hydroxyl rather than the C3-hydroxyl, thus interfering with the propensity to form channels. The amide linkage is also highly important for channel stability. Reducing the length of the hydrocarbon chains favors channel formation and indeed a single chain is sufficient. The allylic system is not necessary and the *trans* double bond does not seem important to the ability to form channels. The sensitivity of channel stability to the stereochemistry at C2 further supports the notion of ceramide channels being highly-organized structures.

NOTE:

This work was accomplished in collaboration with Vidyaramanan Ganesan who made an equal contribution to this work. Dr. Leah J. Siskind conducted the experiments with C_8-ceramide whereas Vidyaramanan Ganesan and I tested all other analogs together. Dr Szulc, Dr. Bielawska, and Dr. Bittman provided the analogs.

CHAPTER 4:

CERAMIDE AND ACTIVATED BAX ACT SYNERGISTICALLY TO PERMEABILIZE THE MITOCHONDRIAL OUTER MEMBRANE

4.1 ABSTRACT

A critical step in apoptosis is mitochondrial outer membrane permeabilization (MOMP), releasing proteins critical to downstream events. While the regulation of this process by Bcl-2 family proteins is known, the role of ceramide, which is known to be involved at the mitochondrial level, is not well-understood. Here, we demonstrate that Bax and ceramide induce MOMP synergistically. Experiments were performed on mitochondria isolated from both rat liver and yeast (lack mammalian apoptotic machinery) using both a protein release assay and real-time measurements of MOMP. The interaction between activated Bax and ceramide was also studied in a defined isolated system: planar phospholipid membranes. At concentrations where ceramide and activated Bax have little effects on their own, the combination induces substantial MOMP. Direct interaction between ceramide and activated Bax was demonstrated both by using yeast mitochondria and phospholipid membranes. The apparent affinity of activated Bax for ceramide increases with ceramide content indicating that activated Bax shows enhanced propensity to permeabilize in the presence of ceramide. An agent that inhibits ceramide-induced but not activated Bax induced permeabilization blocked the enhanced MOMP, suggesting that ceramide is the key permeabilizing entity, at least when ceramide is present. These and previous findings that anti-apoptotic proteins disassemble ceramide channels suggest that ceramide channels, regulated by Bcl-2-family proteins, may be responsible for the MOMP during apoptosis.

4.2 INTRODUCTION

Apoptosis, a type of programmed cell death, is a regulated process where unwanted or damaged cells are eliminated. The permeabilization of the mitochondrial outer membrane (MOM) to key intermembrane space (IMS) proteins such as cytochrome *c*, Smac/Diablo, and apoptosis-inducing factor, is an irreversible and decision-making step in apoptosis, which leads to the execution phase involving effector caspase activation. Ceramide, a pro-apoptotic sphingolipid, has been reported (Pettus et al., 2002; Hannun & Obeid, 2008) to act as a second messenger in several cellular processes, including apoptosis. It can also form channels (Siskind et al., 2002) and thus can directly permeabilize the MOM without the aid of ancillary proteins (Siskind et al., 2008). Physiological studies show that ceramide is both an extracellular stimulus and intracellular mediator (Pettus et al., 2002; Hannun & Obeid, 2008) of mitochondrial apoptosis. Several lines of evidence indicate that cellular levels of ceramide become elevated (Thomas et al., 1999; Charles et al., 2001; Kroesen et al., 2001; Rodriguez-Lafrasse et al., 2001; Ardail et al., 2009), most importantly in mitochondria (Vance, 1990; Matsko et al., 2001; Dai et al., 2004; Birbes et al., 2005; Siskind et al., 2006; Ardail et al., 2009). We have shown that Bcl-xL and Bcl-2 can inhibit permeabilization induced by ceramide in isolated rat liver mitochondria (Siskind et al., 2008). This is achieved by the anti-apoptotic proteins inhibiting ceramide channel formation and disassembling pre-formed ceramide channels.

The mechanism by which Bax increases MOMP is cause for much debate (Roucou et al., 2002; Antonsson, 2004; Guihard et al., 2004; Zhou & Chang, 2008). Bax is located in the cytosol or loosely associated with the MOM in the monomeric form.

Upon an apoptotic signal, Bax inserts into the MOM and becomes activated and oligomerized. Activated Bax and/or Bak are proposed to be directly responsible for the release of intermembrane space proteins by forming channels in cells and indeed, in phospholipid membranes, Bax treated with β-octyl glucoside (activated Bax) is capable of forming channels (Antonsson et al., 1997; Schlesinger et al., 1997). Yet whether these channels are large enough to allow for the release of all the IMS proteins is unclear (Roucou et al., 2002). In yeast cells that lack the mammalian apoptotic machinery, expression of Bax still leads to leads to cytochrome c release and cell death indicating that Bax channels may suffice despite the presence of ceramide. However the effect of Bax is inhibited by co-expression of sphingomyelin synthase, which consumes ceramide (Yang et al., 2006). In mammalian cells, ceramide-induced cytochrome c release does not require Bax (Neise et al., 2008; Siskind et al., 2008) but Bax enhances apoptosis induced by ceramide (von Haefen et al., 2002). Also, ceramide has been found to activate monomeric Bax in the presence of the MOM (Birbes et al., 2005; Kashkar et al., 2005). When combined, these publications can be interpreted to indicate that Bax and ceramide may interact cooperatively to generate the MOMP. This is clearly not the view of most investigators in the field but it is a logical conclusion from published experiments. The present work provides direct evidence of a synergistic interaction between activated Bax and ceramide resulting in enhanced MOMP to proteins. We also provide mechanistic insights into this interaction.

4.3 MATERIALS AND METHODS

4.3.1 Reagents

C_{16}-ceramide was bought from Avanti Polar Lipids. Antimycin A, 2, 4-dinitrophenol (DNP), horse heart cytochrome *c*, fatty acid-depleted bovine serum albumin (BSA), and sodium ascorbate were bought from Sigma Chemical Co. Other chemicals were reagent grade.

4.3.2 Isolation of mitochondria

Rat liver mitochondria were isolated essentially as previously described (Siskind et al., 2002). The isolation buffer was 210 mM mannitol, 70 mM sucrose, 0.1mM EGTA, 0.05% fatty acid free BSA, 5mM HEPES, pH 7.4. To achieve a high level of intactness, mitochondria were sedimented at 5600 RCF (average). Finally, the BSA was removed by sedimenting the mitochondria in isolation buffer without BSA. These were suspended in sucrose-free medium (280 mM mannitol, 0.1 mM EGTA, 2 mM HEPES, pH 7.4), typically to a protein concentration of 9-10 mg/mL and stored on ice.

Yeast mitochondria were prepared and isolated as previous described (Lee et al., 1998) until the washed spheroplast pellet was obtained. Twice, the pellet was resuspended in H-medium (0.6 M mannitol, 0.1 mM EGTA, 10 mM HEPES, pH 7.2) and spun at 700 RCF for 5 min to yield the mitochondrion-containing supernatants. The supernatants were spun at 5600 RCF for 10 min and the pellets were retained. The pellets were resuspended in H-Medium, combined and spun at 700 RCF for 5 min. The supernatant was spun at 5600 RCF for 10 minutes yielding the final mitochondrial pellet which was resuspended in H-medium.

The intactness of the mitochondria, as measured by comparing their rate of cytochrome *c* oxidation with that of osmotically shocked mitochondria (Siskind et al., 2002), was more than 85% for rat mitochondria and over 93% for yeast mitochondria.

4.3.3 Preparation of Bax

Recombinant human Bax was produced as described previously (Suzuki et al., 2000) except the Bax eluted from the chitin column (New England Biolabs Inc) was dialyzed in 12000 M.W. cut-off dialysis membranes at 4^{o}C for 24 hours in 3L (1mM EDTA and 20mM Tris-HCl pH 8.0) and then changed into 5L (20mM Tris-HCl pH 8.0) for 48 hours. The Bax was then filter sterilized through a 0.2 μm filter and 0.5 mL aliquots were made. Glycerol (10%) was added to some of these and they were rapidly shell-frozen in ethanol and dry ice and stored at -80^{o}C. The protein content was typically 10-25μg/mL, assayed by the Micro BCA Protein Kit (Pierce Chemical Co), and SDS/PAGE analysis showed a 95% pure m-Bax band. No detergents were used during the protein isolation. It must be noted that monomeric Bax, when stored in solution at 4^{o}C shows a tendency to oligomerize over time, which is why most of the protein was immediately frozen after purification and only thawed on ice just before use. This method of freezing did not alter protein activity. The native Bax was oligomerized by adding 10% β-octyl glucoside to a final concentration of 0.7% and incubated for 30 min on ice. The proper folding of the detergent treated Bax was confirmed by its partial resistance to trypsin (Fig. 2.1), as published elsewhere (Lucken-Ardjomande et al., 2008). Note that the concentrations of activated Bax reported in the paper were based on the molecular weight of monomeric Bax (21 kDa) because the activated form is heterogeneous.

4.3.4 Purification of N/C Bid

Recombinant N/C Bid (cleaved human Bid) was purified as previously described (Kuwana et al., 2002). Once the Bid was bound to the glutathione-sepharose beads, 50U/ml thrombin in PBS was loaded onto the column and allowed to incubate overnight at room temperature. The addition of thrombin directly to the column allowed us to elute only N/C Bid without the contamination of the GST tag in one step. The elution was then dialyzed overnight against 50mM Tris-HCl pH 8.0, filter sterilized, aliquotted and rapidly frozen as described above. The yield was typically 3 mg/mL as assayed by the Micro BCA Protein Kit (Pierce Chemical Co.) and SDS/PAGE analysis showed an over 95% pure N/C Bid band. Wherever N/C Bid was used, protease inhibitors were added to prevent any deterioration of protein activity. The final concentration of the protease inhibitors was: 1.5μM pepstatin, 16.5μM chymostatin, 2.2μM leupeptin, .6μM aprotinin and 20μM PMSF.

4.3.5 Cytochrome c accessibility assay

Shortly before use, mitochondria were diluted in the isolation buffer to 0.5 mg protein/mL and stored on ice. Once diluted, mitochondria lose function more rapidly and so the diluted suspension is used within an hour. In a typical experiment, 50μL of this dilution was dispersed in 650μL of room temperature incubation buffer (the sucrose-free buffer supplemented with 5mM DNP and 5μM antimycin A and pH 7.25 (Siskind et al., 2002) to final protein content of 25 μg in 700μL). Unless otherwise stated, this was done for all experiments. In most experiments, when Bax was added, it was added immediately. Then the mitochondria were incubated for 10 min at room temperature to

allow them to acclimate and interact with Bax. In experiments where N/C Bid and monomeric Bax were used, the mitochondria were incubated with the permeabilizing agents for 30 minutes at 30^{o}C in a rotary shaker set for gentle mixing. Ceramide was generally added at this point from a 1 mg/mL solution in isopropanol. It was added while simultaneously vortexing the microfuge tube vigorously so as to achieve rapid and effective dispersal of the sphingolipid (controls show that this does not damage the outer membrane). After dispersal, the mixture was incubated for 10 min followed by measurement of the outer membrane permeability. Reduced cytochrome c (Siskind et al., 2002) was added to the mitochondrial suspension (10μL; final concentration approx 25μM) and the absorbance at 550nm was measured immediately for 2 min. The initial rate was used to assess the permeability of the MOM to cytochrome c. The extinction coefficient of 18.5 $mM^{-1} \cdot cm^{-1}$ ($\Delta\in_{Red.-Ox.}$) was used to convert absorbance units to μM units.

4.3.6 Assessment of apparent dissociation constant of ceramide channels for activated Bax

The oxidation rate was used as the functional parameter to evaluate the apparent dissociation constant of ceramide channels for activated Bax. The data was plotted using the Hill formalism for cooperative binding.

$$\log \frac{rate_{Bax}}{rate_{\max}} = \log(K) + n \log[Bax]$$

where the rates are the initial activated Bax-stimulated rates of oxidation at a specific ceramide concentration, above the rate observed with ceramide alone. $rate_{Bax}$ is the rate at any (activated Bax) and $rate_{max}$ is the maximal rate. K and n are the parameters of the Hill

formalism. The inherent variability in the experiments forced us to combine these parameters into one. Since K and n increased simultaneously with amount of ceramide used, we found it more informative to combine these two parameters into one term:

$K_{0.5} = [1/K]^{1/n}$

$K_{0.5}$ is the Bax concentration at which the extent of permeabilization (as measured by the rate of cytochrome *c* oxidation) is half-maximal. It is a measure of the apparent dissociation constant, the reciprocal of the apparent affinity.

4.3.7 Electrophysiological Experiments

The monolayer method was used as described previously (Colombini, 1987a) to make planar phospholipid membranes. Calomel electrodes were used to interface with the aqueous solutions (1.0 M KCl, 1mM $MgCl_2$, 5mM PIPES pH 6.95] on either side of the membrane. The voltage was clamped and the current recorded. The lipid solution contains 0.5% (w/v) 1,2-diphytanoyl-*sn*-glycero-3-phosphocholine, 0.5% (w/v) asolectin, and 0.05% (w/v) cholesterol dissolved in hexane. To form a ceramide channel, a stock solution of 0.05 mg/ml C_{16}- ceramide was made in isopropanol and 10-20μL amounts were added to the cis side of the membrane while stirring for 15 seconds to induce an initial conductance. The channel was then allowed to enlarge and stabilize before the addition of proteins or other compounds. To obtain an activated Bax conductance, activated Bax was added to the cis side of the membrane only.

4.3.8 Adenylate Kinase Assay

As described earlier (Siskind et al., 2002), mitochondria were resuspended in the incubation buffer (50mM potassium lactobionate, 180mM mannitol, 0.1mM EGTA and

2mM HEPES and pH 7.4) to a final mitochondrial protein concentration of 160μg/mL. After adding ceramide and Bax, as done for cytochrome *c* oxidation assay, to 1 mL aliquots, mitochondria were incubated at 30^{o}C for 30 min. The mitochondria were sedimented at 14,000 RCF for 5 min at 4^{o}C and 300μL of the supernatant was combined with 700μL adenylate kinase reaction buffer (50mM Tris, 5mM $MgSO_4$, 10mM glucose, 5mM ADP, 0.2mM NADP pH 7.5) that had been preincubated for 2 min with 5μL of enzyme mixture (2.5 units of hexokinase and 8.7 units of glucose-6-phosphate dehydrogenase). The absorbance of the mixture at 340nm was recorded immediately and the initial rate used as a measure of the adenylate kinase activity. Maximal release of adenylate kinase was achieved by exposing the mitochondria to an osmotic shock. An aliquot of the mitochondrial suspension (usually 10-20 μL containing 160 μg mitochondrial protein) was added to in 1mL distilled H_2O (50 to 100 fold shock) and incubated on ice for 10 min.

4.3.9 Statistics

The Student's t test was used to determine the probability values.

4.4 RESULTS

4.4.1 Activated Bax enhances ceramide-induced MOMP

To evaluate the influence of Bax on ceramide permeabilization of the MOM, we used a dynamic cytochrome *c* accessibility assay, as previously described (Siskind et al., 2002). This is a dynamic measurement of permeability and permeability changes in the MOM to cytochrome *c* in real-time. While treatment of isolated mitochondria with low

levels of ceramide or N/C Bid-monomeric Bax induced a small amount of membrane permeabilization, when the same amounts were added together, there was a synergistic increase in MOMP (Fig. 4.1A). This synergistic induction of permeabilization was also observed using the adenylate kinase release assay that evaluates release of proteins from the intermembrane space. (Fig. 4.1B). N/C Bid alone did not have any effect on ceramide-induced MOMP at these levels. It must be noted that processed Bid itself is capable of permeabilizing mitochondria (Kluck et al., 1999), possibly by acting on Bak. Also, the degree of Bax activation varies with the amount of N/C Bid. In order to eliminate the effects of N/C Bid alone on ceramide and differences in degree of Bax activation at different concentrations of N/C Bid, we used chemically activated Bax for subsequent experiments. Bax activated chemically with detergent has been found to permeabilize the MOM in similar manner to physiologically activated Bax (Kuwana et al., 2002; Ivashyna et al., 2009) and shows similar restricted accessibility to trypsin (Lucken-Ardjomande et al., 2008). A similar synergistic enhancement of permeabilization was also observed with ceramide and chemically activated Bax (Fig. 4.1C). Under these conditions, there was no swelling of the mitochondria and thus the permeabilization was not secondary to inner-membrane swelling.

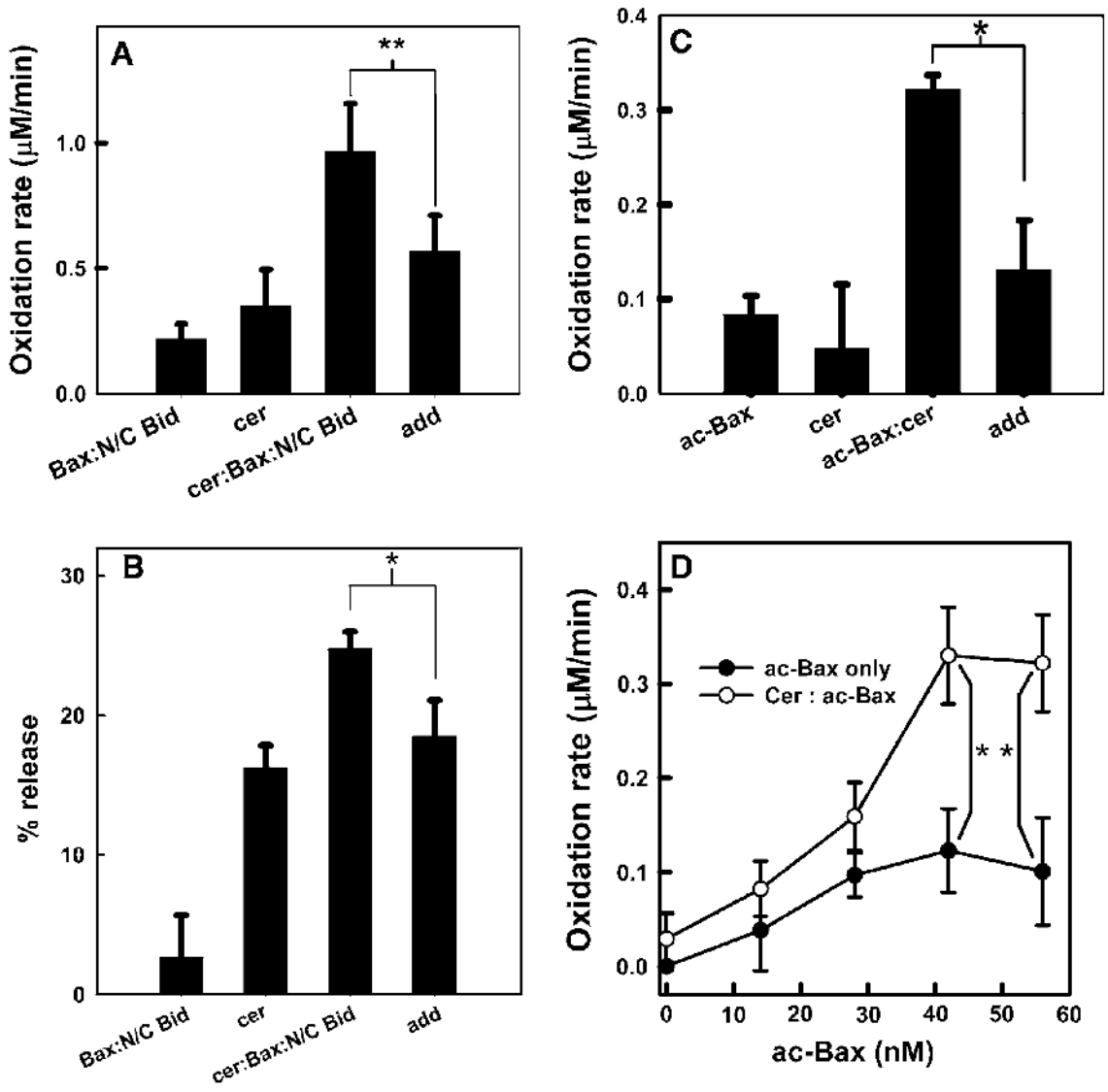

Figure 4.1 Ceramide (cer) and activated Bax increase the MOMP in a cooperative fashion assessed by the cytochrome *c* accessibility assay (A, C, D) or adenylate kinase release (B). **A** Isolated rat liver mitochondria diluted to 250μg protein/mL were pre-treated with both 45nM N/C Bid and 40nM monomeric Bax. Sub-aliquots containing 25μg of mitochondria were either treated with 5 μL isopropanol (as a vehicle control) or 5μL of 1 mg/mL ceramide (in isopropanol) and incubated at room temperature for 10 min before assaying for cytochrome *c* accessibility. Respective vehicle controls were subtracted from the data shown. The "add" bar is the sum of the rates measured with ceramide alone and Bid/Bax alone. The results are the means ± S.D. of 3 experiments. The respiration rate of the combined treatment differed from the sum of the individual rates with $p < .01$. **B** Rat liver mitochondria were treated either with 10 μg ceramide or a combination of 40nM monomeric Bax and 245nM N/C Bid or both and the released adenylate

kinase activity was measured. The "add" bar is the sum of the results of individual treatments minus their product divided by the maximal possible release (to correct for both agents acting on the same mitochondrion). The combined treatment exceeded the sum of individual treatments, "add", with $p < .05$. **C** Isolated rat liver mitochondria were treated with either 1 μg ceramide, 15nM detergent activated Bax (ac-Bax), or both. The results are mean ± S. E. of 3 experiments. The combined treatment exceeded the sum of individual treatments, "add", with $p < .05$. **D** Mitochondria isolated from wild-type *S. cerevisiae* were used and treated with 2 μg of ceramide and activated Bax as shown. The results are means ± S.E. of 3-5 experiments. Statistical tests yielding $p < .05$ compared the results of the combined treatment of ceramide and ac-Bax with the numerical addition of the results of treatments with ceramide alone and ac-Bax alone.

One possible interpretation for the synergistic interaction between ceramide and activated Bax is that activated Bax could be binding to anti-apoptotic proteins thus removing any inhibitory effect on ceramide induced MOMP. To test if the anti-apoptotic Bcl-2 proteins are involved in this interaction, ceramide induced MOMP enhancement by activated Bax was tested using yeast mitochondria, which are devoid of Bcl-2 family proteins. We found that activated Bax and ceramide interact synergistically to induce MOMP in yeast mitochondria also, suggesting that their interaction could be direct and not indirectly mediated by elimination of inhibition by anti-apoptotic members (Fig. 4.1D). This also suggests that the interaction between activated Bax and ceramide does not require processed Bid or Bak.

4.4.2 Bax-mediated enhancement of ceramide-induced permeabilization can be inhibited by trehalose, a disaccharide that disassembles ceramide channels

Since both Bax and ceramide are channel formers and each of them is capable of permeabilizing the MOM in the absence of the other, we wanted to test whether, in this

synergistic interaction, Bax is enhancing ceramide channels or vice versa. Some insight was gained by using trehalose, a disaccharide that inhibits ceramide channels causing partial disassembly. The same dose of trehalose inhibited both the ceramide induced MOM permeabilization and the enhancement of this permeabilization induced by activated Bax (Fig. 4.2A). In this experiment, activated Bax alone had essentially no effect. Using a higher concentration of activated Bax (inset) a significant MOMP was achieved and trehalose had no effect on this MOMP induced by activated Bax alone. The simplest interpretation is that the enhanced MOMP has the properties of ceramide channels. Activated Bax could be acting by enhancing the permeabilization induced by ceramide, perhaps by favoring the growth of ceramide channels. This observation can also be explained by a complex structural assembly of ceramide and activated Bax that is sensitive to trehalose. However, this observation is inconsistent with the possibility that ceramide is simply enhancing Bax activation. In addition, if the enhanced MOMP were the result of ceramide monomers enhancing channels formed by activated Bax then it is hard to see how trehalose could interfere with this process because trehalose cannot remove ceramide from the membrane.

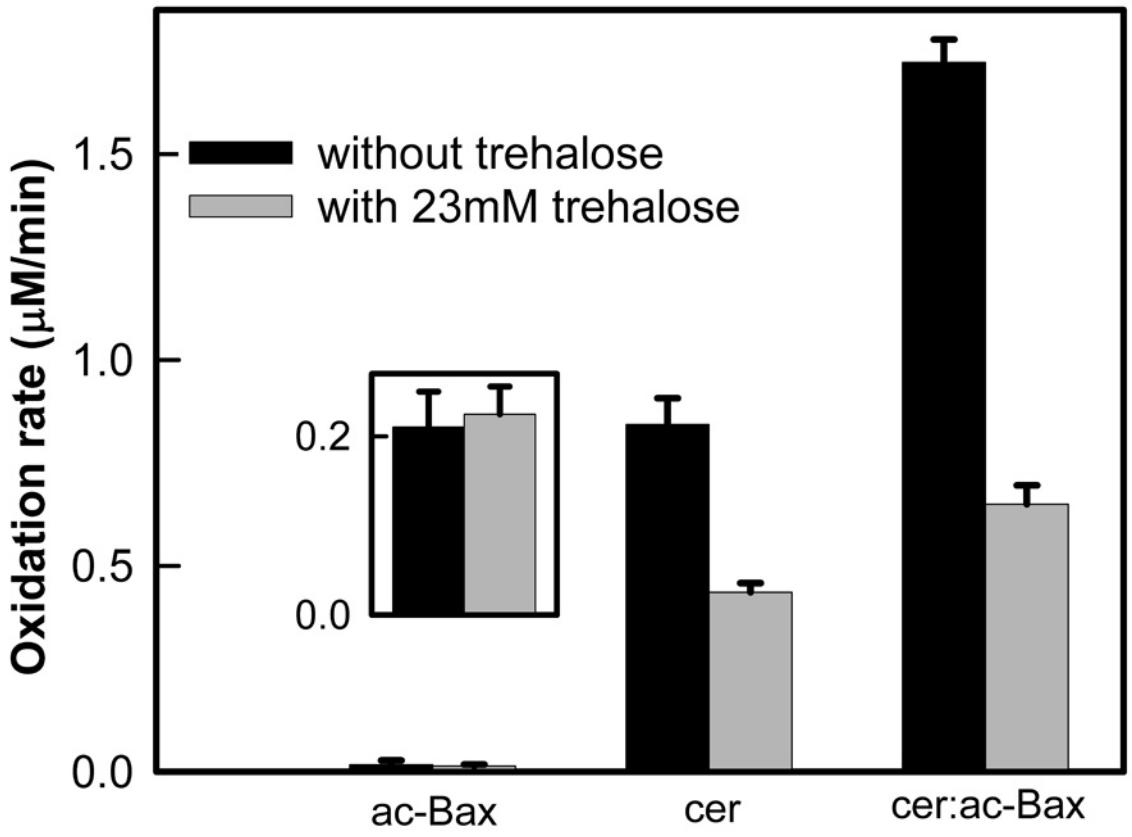

Figure 4.2 Trehalose (23 mM final) inhibits MOMP induced by ceramide alone and that induced by the combination of ac-Bax and ceramide.

In the main figure, samples were treated with 30 μg of ceramide and 10 nM ac-Bax as indicated. In the inset 43 nM ac-Bax was used to obtain a high enough MOMP. The cytochrome *c* oxidation rates are means ± S. E. of 3 to 4 experiments. ** represents $p < .01$ and *** represents $p < .001$.

4.4.3 Bax expands ceramide-induced conductance in planar phospholipid membranes

Planar phospholipid membranes are membranes consisting only of phospholipids and cholesterol. Being a defined system, one can clearly demonstrate interactions

without the influence of other constituents found in natural membranes. The ability of ceramide to form channels in planar membranes has been established (Siskind & Colombini, 2000). To assess the effect of activated Bax on ceramide channels in an environment free of other membrane components, ceramide channels were formed in the planar membranes and then activated Bax was added. Activated Bax caused a large increase in conductance while monomeric Bax (m-Bax) did not significantly affect the channel (Fig. 4.3A). This is typical of many experiments. These show that the interaction between activated Bax and ceramide is a direct one and does not require other proteins.

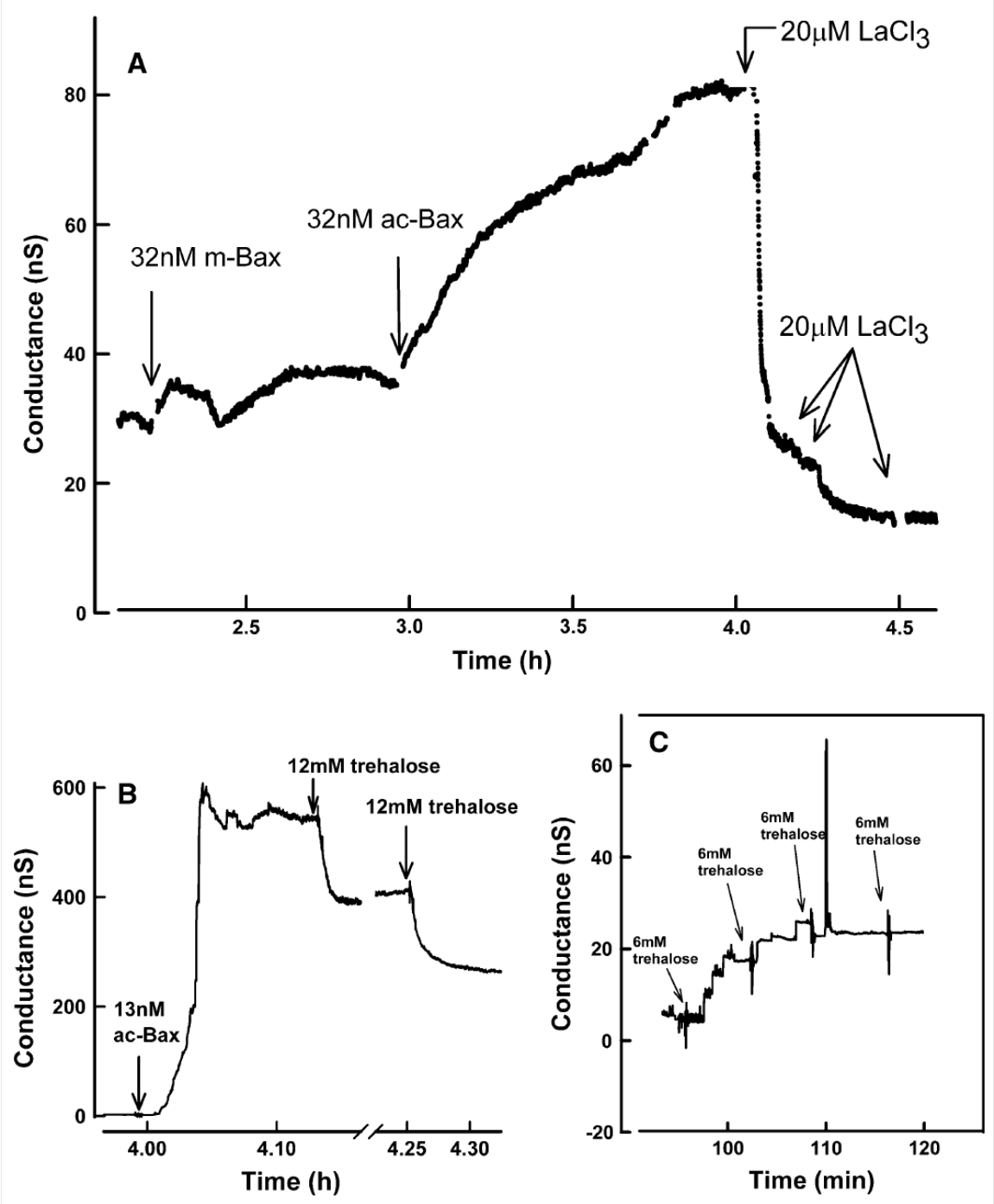

Figure 4.3 Addition of activated Bax to a ceramide channel in a planar phospholipid membrane causes it to enlarge.

A. The initial conductance was formed by the addition of 16 μg ceramide to a high-resistance phospholipid membrane. Once the conductance had stabilized first monomeric Bax then activated Bax were added to both sides of the membrane. Once the conductance rise had restabilized at a higher level $LaCl_3$ was added to the final concentrations indicated in the figure.

The $LaCl_3$ additions were added to one side in the sequence: cis, cis, trans, trans. The experiment shown is representative of more than 8 experiments. Amounts of added ceramide and ac-Bax were different between experiments. Bax enhancement of a ceramide channel was seen in over 50 experiments. **B.** A small ceramide channel was formed followed by the addition of ac-Bax at the indicated final concentration. Trehalose was added as indicated. **C** Activated Bax conductances were induced in a planar phospholipid membrane in the experiment illustrated in the figure. The total amount of activated Bax added was equivalent to 42 nM. Trehalose was added as indicated stepping up the final concentration by 6 mM at each addition. This is typical of more than 3 experiments.

Trehalose also inhibited the conductance of a ceramide channel formed in a phospholipid membrane (data not shown). In Fig. 4.3B, a small ceramide conductance was greatly increased by the addition of activated Bax to a final calculated size of 50 nm. At the reduced scale used to show the experiment, the initial ceramide conductance is barely visible. Once the conductance stabilized, trehalose was added resulting in an immediate decline in conductance. Thus the activated Bax-enhanced conductance was reduced by trehalose (Fig. 4.3B). Trehalose has no effect on the conductance produced by activated Bax alone (Fig. 4.3C). Thus, trehalose is useful to effectively distinguish between a permeability formed by activated Bax and one formed by ceramide. When the Bax/ceramide conductance was inhibited using lanthanum ions, there was stochastic delay in channel disassembly, suggesting that a singular structure is responsible for the conductance observed. Ceramide and activated Bax may be forming a unified structure or activated Bax might enhance the size of the ceramide channel. These experiments also suggest that metabolism of ceramide to other sphingolipids like sphingosine is not necessary for interaction with activated Bax and the consequent changes in permeability.

4.4.4 The influence of activated Bax on MOMP depends on the amount of added ceramide

At a low level of added ceramide 0.5 μg/mL, the amount of activated Bax needed to enhance the MOMP to half maximal was 20 nM. At a higher dose of 1.0 μg ceramide, less activated Bax was needed to achieve a half-maximal effect (12nM) (Fig. 4.4A). Both of these results were obtained on the same mitochondrial preparation, eliminating variability between mitochondrial isolations. This difference can be interpreted as a change in apparent affinity between activated Bax and a ceramide channel as the size of the ceramide channel increases. In a separate set of experiments (Fig. 4.4B) low levels of ceramide still show a dose-dependence but at high levels (10 μg), the enhancement by activated Bax was not observed (Fig. 4.4B). The lack of further stimulation was not due to the achievement of maximal cytochrome *c* accessibility to cytochrome oxidase because higher levels of ceramide did produce still higher rates of cytochrome *c* oxidation, closer to those observed with hypotonically-shocked mitochondria. This indicates that the effect of activated Bax on ceramide induced-MOMP is a saturable function of the amount of ceramide. This saturation could be interpreted as activated Bax favoring an optimal size of the ceramide channel and if the channel is already at the optimal size there is no further change in MOMP. A Hill plot revealed changes in both the measure of

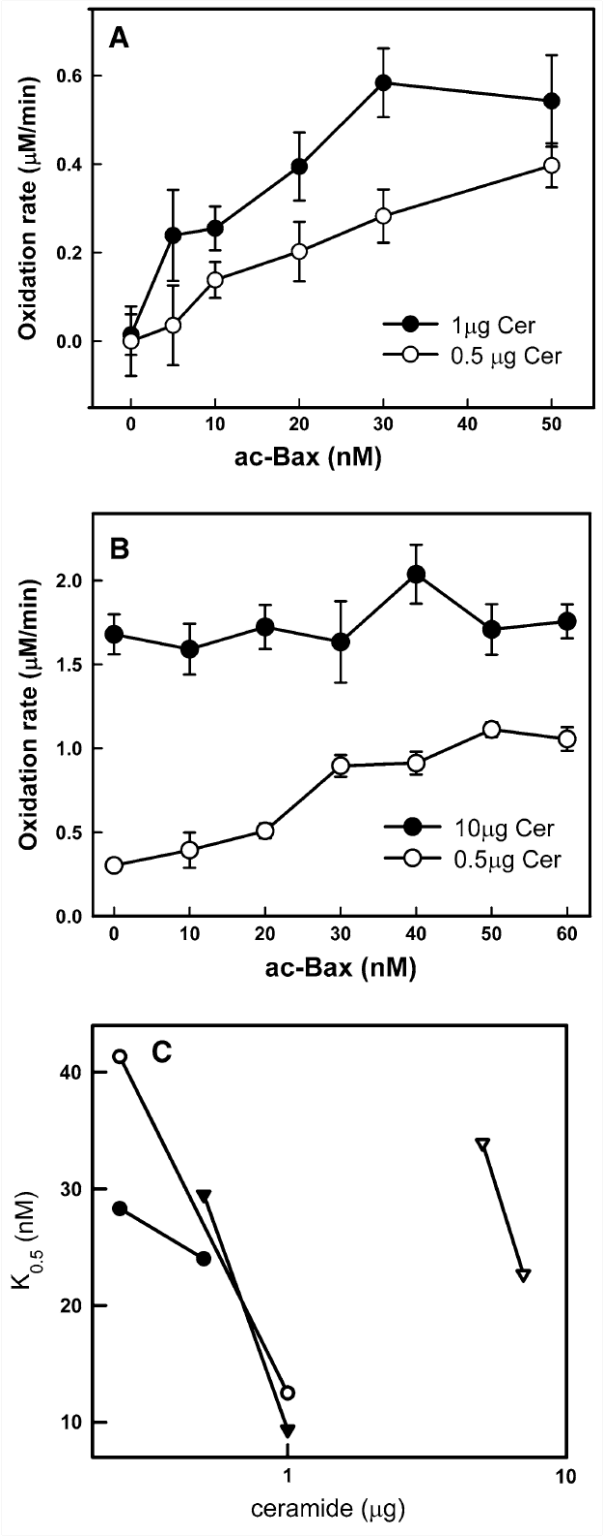

Figure 4.4 Dose-response curves of the enhancement of ceramide mediated MOMP by the addition of activated Bax to rat liver mitochondria. A, B Experiments were performed by preincubating the mitochondria with the indicated amount of activated Bax for 10 min followed

by addition of the indicated amount of ceramide. **A** 0.5μg and 1μg of ceramide were used. These results are mean ± S. E. of 4 experiments. **B** 0.5μg and10μg of ceramide were used. These results are mean ± S. E. of 3-4 experiments. Experiments within one panel were performed on the same batch of mitochondria. **C** Summary of the results of 4 independent experiments. Each set of data points defining each line was determined from a set of experiments performed on the same mitochondrial isolation. The figure shows the increase in apparent affinity of activated Bax for ceramide channels with increase in ceramide content. $K_{0.5}$ is defined in the method section. These results were obtained from experiments such as those illustrated in **A** and **B.**

cooperativity, *n*, and the constant, *K*. The Hill parameters were combined (see methods) to evaluate the apparent dissociation constant, $K_{0.5}$ (the Bax concentration at which half-maximal enhanced permeabilization is achieved). The resulting apparent dissociation constant of activated Bax for ceramide channels in the MOM decreases as the ceramide concentration increases (Fig. 4.4C). This is highly reproducible, despite the variation in intrinsic sensitivity of isolated mitochondria to added ceramide. Each line represents the results of sets of experiments performed on one isolated batch of mitochondria. These results indicate a relationship between the structure of activated Bax and the structure formed in the presence of ceramide. An increase in affinity indicates a better fit. The increase in MOMP may result from an increase in diameter of the Bax-ceramide assembly resulting is a better match to the structure of activated Bax. In this way activated Bax could result in the formation of a channel of a particular size.

4.5 DISCUSSION

The release of proteins from mitochondria is a critical, decision-making step in apoptosis and thus the identification of the structure responsible for this release has many important implications. A favorite candidate for the release pathway is activated Bax since Bax is pro-apoptotic, can form channels and its activation on the MOM leads to protein release. Interestingly, ceramide is also pro-apoptotic, can self-assemble to form channels (Siskind & Colombini, 2000; Pettus et al., 2002; Hannun & Obeid, 2008) and its delivery to the MOM leads to protein release (Birbes et al., 2001; Pettus et al., 2002; Di Paola et al., 2004; Birbes et al., 2005) Here we show that activated Bax and ceramide act synergistically to permeabilize the MOM.

The nature of the channels formed in the presence of both ceramide and activated Bax is not known and could be a structure fundamentally different from that formed by either substance alone. Some findings in this work, however, are easily interpreted in terms of activated Bax controlling the structure of ceramide channels. The apparent affinity of activated Bax for ceramide-induced MOM permeability increases with the amount of ceramide added. In other words, as the amount of added ceramide was increased, lesser amounts of Bax were required to achieve half-maximal permeabilization. This could be due to more ceramide increasing the degree of Bax activation but at high levels of ceramide, where ceramide by itself produced a large permeability, there was no further stimulation by activated Bax (even though additional amounts of ceramide would have increased MOMP). This observation is not easily compatible with ceramide activating Bax or the two channels mutually enhancing each

other. It is more naturally explained by activated Bax favoring the growth of a ceramide channel up to a size designated by the structure of activated Bax.

Activated Bax seems to enhance the size of ceramide channels up to some critical level, probably an optimum channel size. The increased radius of curvature may offer a better fit for activated Bax. Regardless of the site of interaction, if the interaction energy increases with channel size, then the binding of activated Bax to a smaller channel could generate stress on the channel that would be relieved by the channel growing in size (Fig. 4.5). The dynamic equilibrium between ceramides in the channel and non-conducting

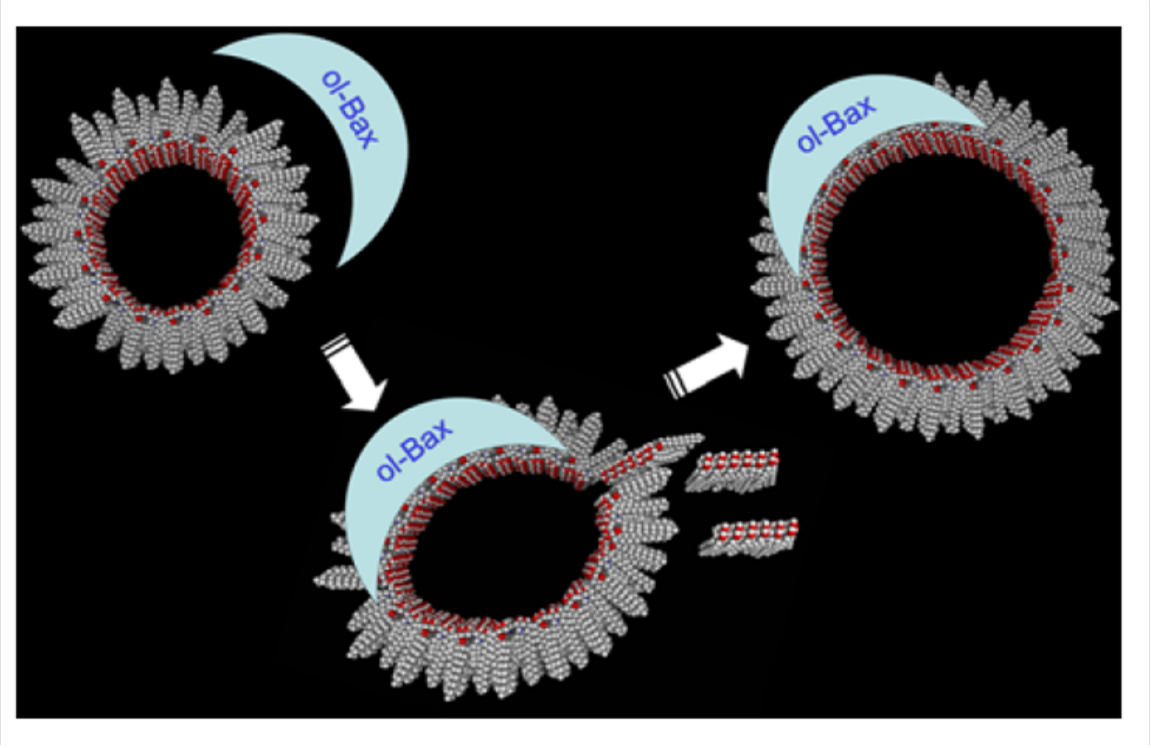

Figure 4.5 Illustration of how activated Bax might increase the size of the ceramide channel.

On the left, a 32-column ceramide channel has a small radius of curvature than ac-Bax. When ac-Bax binds (center) it distorts the channel disturbing the equilibrium between ceramide aggregates on the monolayer and ceramides forming the channel. The insertion of more ceramide

columns increases the channel size until its curvature matches that of activated Bax (right), forming a 48-column channel.

ceramide in the membrane would be shifted toward ceramide insertion into the channel and thus growth of the channel size. Once the optimal size is achieved, activated Bax would have no further effect and this was observed. It is possible that the physical shape of the activated Bax in the membrane might act as a molecular mold to drive the ceramide channel to an optimum size.

The results obtained with phospholipid membranes argue that the interaction between activated Bax and ceramide channels must be direct. Furthermore, these demonstrate that activated Bax increases the size of the single existing ceramide channel because the disassembly of the resulting enhanced permeability shows stochastic properties consistent with a unified structure. If the added Bax were to form a separate structure then the disassembly would show two separate processes rather than just one. This is in harmony with the natural interpretation of the mitochondrial experiments that measured the apparent affinity of activated Bax as described above.

Experiments on isolated mitochondria raise the possibility of indirect effects. Ceramide could act on another mitochondrial component and thus indirectly influence the ability of activated Bax to permeabilize the outer membrane. Indeed, a product of ceramide metabolism could be the active species. Mitochondria have ceramidases that could convert ceramide to sphingosine (Bionda et al., 2004; Siskind, 2005). Although the conversion rate was shown to be minimal under the conditions of our experiments (Siskind et al., 2005), even a small conversion might be important. Sphingosine was shown to be capable of interacting with and influencing the formation of ceramide

channels (Siskind et al., 2005) and thus might influence the channel-forming ability of activated Bax. Although this possibility cannot be excluded, the experiments performed in planar membranes demonstrate a direct functional synergism between ceramide and activated Bax in terms of channel formation. The close parallelism between the results obtained with the two experimental approaches provides strong confidence that both are reporting the same synergistic permeabilization.

It is not clear whether the release of IMS proteins *in vivo* is due to transient openings or sustained permeability. Many publications (Jurgensmeier et al., 1998; Kluck et al., 1999) have reported a Bax-induced release of cytochrome c from isolated mitochondria over a period of hours without significant increases in the MOM permeability to cytochrome c. Transient channel openings are a likely explanation. Does this mean that the Bax/ceramide sustained permeabilization of the MOM and thus rapid release of protein is unnecessary or unphysiological? It seems unlikely that the Bax/ceramide synergism is an interaction that is not specific and not maintained by natural selection, especially since anti-apoptotic proteins act precisely in the opposite manner (Siskind et al., 2008). Further, Kluck et al. (Kluck et al., 1999), have shown that, in the presence of a putative apoptotic component of the cytosol (which would be expected to be available to apoptotic mitochondria *in vivo)*, Bax induces sustained enhancement of permeability. Munoz-Piendo et al. (Munoz-Pinedo et al., 2006) report that a non-specific pore showing prolonged permeability is responsible for protein release during apoptosis. Thus the sustained permeability observed in the presence of activated Bax and ceramide is not an aberration.

It must be emphasized that the experiments were performed with physiologically relevant doses of ceramide and Bax. The ceramide used in this study is C_{16}-ceramide which is one of the common, naturally occurring, long-chain ceramides. The amounts of ceramide used seem high but, only about 5% of the ceramide added to isolated mitochondria inserts into mitochondrial membranes (Siskind et al., 2006), requiring the addition of larger amounts of ceramide to the mitochondrial suspension to achieve MOMP. Nevertheless, as shown previously (Birbes et al., 2005; Siskind et al., 2006), we are working at mole fractions of ceramide typically found in mitochondria early in apoptosis. The amount of activated Bax used in these experiments is also at physiological levels. Enhancement of ceramide induced MOMP was achieved with levels of activated Bax in the low nM range. At these levels, activated Bax often has little or no effect on MOMP, indicating that its action on ceramide channels may be more important.

Activation of Bax in cells is thought to be mediated by N/C Bid in cells. Apart from N/C Bid, non-ionic detergents, at their CMC, have also been found to activate Bax (Hsu & Youle, 1997; Lucken-Ardjomande et al., 2008). This detergent-activated Bax shows similar reactivity to conformation specific antibody (Hsu & Youle, 1997) and restricted accessibility to trypsin digestion (Lucken-Ardjomande et al., 2008). We have used detergent activated Bax for most of our experiments to focus on the Bax/ceramide interaction. This is just part of a bigger, more complicated, picture. For example, Bcl-2 family proteins have been shown to regulate the formation of ceramide also, during apoptosis (Sawada et al., 2006).

These and earlier studies with the anti-apoptotic Bcl-2 family proteins (Siskind et al., 2008) underscore that natural selection has favored mechanistic interactions between

some Bcl-2 family proteins and ceramide resulting in functional outcomes. These functional interactions could be pivotal in regulating MOMP under circumstances where both ceramide and the Bcl-2 family proteins are present.

4.6 CONCLUDING REMARKS

Experiments with isolated mitochondria and phospholipid membranes show that low levels activated Bax and ceramide interact to enhance the membrane permeability to a level greater than each agent alone. The results are best interpreted as activated Bax enhancing ceramide channels but other interpretations are not excluded. These results are in harmony with published results showing that anti-apoptotic proteins disassemble ceramide channels. These show that the Bcl-2 family of proteins that regulate protein release from mitochondria early in apoptosis also interact with ceramide and ceramide channels to influence MOMP. This result is consistent with an emerging picture that ceramide channels may be a pathway by which proteins are released from mitochondria, initiating the execution phase of apoptosis.

NOTE:

This work was completed in collaboration with Vidyaramanan Ganesan who made an equal contribution to this work. The following students assisted me with experiments on planar membranes: Kirti Chadha, David Colombini, Raksha Bangalore, Dipkumar Patel, Kevin Yang and Chiemezie Onyewuchi.

CHAPTER 5:

BAX, BCL-XL EXERT THEIR REGULATION ON DIFFERENT SITES OF THE CERAMIDE CHANNEL

5.1 ABSTRACT

This study demonstrates the important structural features of ceramide required for proper regulation, binding and identification by both pro-apoptotic and anti-apoptotic Bcl-2 family proteins. The C4:C5 *trans* double bond has little influence on the ability of Bax and Bcl-xL to identify and bind to these channels. The stereochemistry of the head group and access to the amide N-H group of ceramide is indispensible for Bax binding indicating that Bax may be interacting with the polar portion of the ceramide channel facing the bulk phase. On the contrary, Bcl-xL binding to ceramide channels is tolerant of stereochemical changes in the head group. This study also revealed that Bcl-xL has an optimal interaction with long-chain ceramides that are elevated early in apoptosis while short-chain ceramides are not well regulated. Inhibitors specific for the hydrophobic groove of Bcl-xL including 2-methoxyantimycin A_3, ABT-737, and ABT-263 provide insights into the region of Bcl-xL involved in binding to ceramide channels. Molecular docking simulations of the lowest energy binding poses of ceramides and Bcl-xL inhibitors to Bcl-xL were consistent with the results of our functional studies and propose potential binding modes.

5.2 INTRODUCTION

The intrinsic pathway of apoptosis, a type of programmed cell death, is regulated at the mitochondrial level by the Bcl-2 family of proteins. Permeabilization of the mitochondrial outer membrane (MOM) leads to the release of key intermembrane space (IMS) proteins, such as cytochrome *c*, which irreversibly commit the cell to the execution phase of apoptosis. The Bcl-2 proteins have pro-survival members, such as Bcl-xL, Bcl-2, and Mcl-1, that maintain the integrity of the MOM in normal cells and pro-apoptotic members, like Bax, Bak and Bid that initiate the apoptotic process and facilitate IMS protein release when the cell is damaged or an apoptogenic signal is delivered. Whether the anti-apoptotic or pro-apoptotic Bcl-2 proteins prevail will determine whether IMS proteins are released by a pore through the MOM and thus the fate of the cell. There are multiple pathways proposed for the release of IMS proteins from mitochondria (Dejean et al., 2005; Siskind et al., 2006; Chiara et al., 2008; Montessuit et al., 2010), and even Bax itself is able to form channels (Terrones et al., 2004; Lovell et al., 2008). Whatever the nature of the pathway, it must be tightly regulated to prevent unwanted cell death. One such proposed pathway for IMS protein release is formed by the bio-active sphingolipid ceramide.

The involvement of ceramide in apoptosis is widely recognized and in response to many different apoptotic stimuli intracellular ceramide levels increase; specifically, it is the elevation of ceramide in mitochondria that is pro-apoptotic (Birbes et al., 2001; Matsko et al., 2001; Dai et al., 2004; Birbes et al., 2005). Elevation of ceramide in mitochondria can occur in a number of ways (Siskind, 2005; Mullen & Obeid, 2011), including transfer of ceramides from mitochondrial associated membranes (Stiban et al.,

2008). In fact, while Bax/Bak knockout cells are known to be highly resistant to apoptosis (Wei et al., 2001; Zong et al., 2001), it was shown recently that this resistance is accompanied by a deficit in ceramide generation, as Bak regulates ceramide metabolism by activating a critical ceramide synthase to elevate mitochondrial ceramide levels (Siskind et al., 2010). Moreover, while metabolism of ceramide to other forms, such as glucosylceramide, can render cells less susceptible to cytotoxic agents (Komori et al., 1999; Liu et al., 2001; Itoh et al., 2003), blocking ceramide metabolism can sensitize multi-drug resistant cells to death (Lavie et al., 1997; Patwardhan et al., 2009; Liu et al., 2011). Thus, the steady-state level of ceramide is an important step in the apoptotic program in a variety of cell types (Komori et al., 1999; Chapman et al., 2010), and cytotoxic stimuli (Lavie et al., 1997; Dai et al., 2004; Birbes et al., 2005) and ceramide channel formation can be demonstrated at these physiological levels of ceramide in mammalian mitochondria and yeast mitochondria (Siskind et al., 2002; Siskind et al., 2006; Siskind et al., 2008). Ceramide channels have also been visualized in liposomes using transmission electron microscopy (Samanta et al., 2011). These structures are stable and have been shown to be large enough for the release of all known IMS proteins released from mitochondria during apoptosis (Siskind et al., 2002).

The current model of the ceramide channel highlights the structural features that are important for channel formation ((Anishkin et al., 2006), see Table 5.1 for structure of ceramide and analogs). The amide nitrogen and carbonyl group allow for the formation of ceramide columns. Adjacent ceramide columns are held together by the C1 and C3 hydroxy groups forming the lumen of the channel. The length of the hydrocarbon chains of ceramide, though physiologically important (Megha et al., 2007; Pruett et al., 2008), is

relatively unimportant for channel formation (Siskind et al., 2003). The sphingoid base is typically 18 carbons in length with a *trans* double bond at the C4:C5 position. The ceramide species in mammalian cells have fatty-acyl chains that range from 12 to 24 carbons in length. It is important to note that ceramide channels are highly stable, rigid structures that are held together by a vast network of hydrogen bonds (Anishkin et al., 2006; Ganesan et al., 2010) and not simply lipidic pores of a transient, non-specific nature.

It was found that ceramide channels are regulated by the Bcl-2 family of proteins. The pro-survival Bcl-2 members, Bcl-xL and Ced-9 (the *C. elegans* homolog of Bcl-2) were shown to antagonize channel formation and disassemble ceramide channels (Siskind et al., 2008). Conversely, a pro-apoptotic Bcl-2 member, Bax, can directly enhance ceramide channels (Ganesan et al., 2010). The regulation of ceramide channels was demonstrated by the addition of purified Bcl-2 family proteins to isolated mammalian mitochondria (which have other Bcl-2 family proteins naturally present in those membranes), yeast mitochondria (which do not have potentially interfering Bcl-2 family proteins), and planar phospholipid bilayers (which are devoid of any proteins or specialized lipids). These results highlight the ability of Bcl-2 family proteins to identify and regulate ceramide channels. These interactions are highly specific and do not require other proteins or specialized lipids, demonstrating for the first time that a channel formed of lipids can be regulated by a protein. Remarkably, this regulation was in accordance with the known physiological function of these Bcl-2 proteins.

In this study, we set out to further understand the interaction of ceramide channels and Bcl-2 family proteins. We provide insights into the specific sites on the ceramide

channel where Bax and Bcl-xL exert their regulatory effects. Moreover, to investigate the binding site on Bcl-xL for ceramide, we tested specific inhibitors of Bcl-xL that bind to a known location on the protein. Molecular docking studies were conducted with ceramides and Bcl-xL inhibitors to probe for the ceramide binding site and reveal the lowest energy binding modes of these molecules to Bcl-xL. We offer mechanistic insights as to how the specific interactions we discovered could lead to the regulation of ceramide channels and discuss the implications of these results.

5.3 MATERIALS AND METHODS

5.3.1 Reagents

N-Acetyl-D-*erythro*-sphingosine (C_2-Cer), *N*-butyryl-D-*erythro*-sphingosine (C_4-Cer), *N*-octanoyl-D-*erythro*-sphingosine (C_8-Cer), N-palmitoyl-D-*erythro*-sphingosine (C_{16}-Cer), *N*-oleoyl-D-*erythro*-sphingosine ($C_{18:1}$-Cer), *N*-arachidoyl-D-*erythro*-sphingosine (C_{20}-Cer), and *N*-lignoceroyl-D-*erythro*-sphingosine (C_{24}-Cer) were obtained from Avanti Polar Lipids (Alabaster, AL). Antimycin A, 2,4-dinitrophenol (DNP), and fatty acid depleted bovine serum albumin (BSA) were purchased from Sigma (St. Louis, MO). The analogs of D-*e*-C_{16}-ceramide and the analog **T4** and **L5** (Table 5.1) were synthesized as previously described (He et al., 2000a; He et al., 2000b; Usta et al., 2001; Bieberich et al., 2002; Brockman et al., 2004). Horse heart cytochrome *c* was purchased from Acros, 2-methoxyantimycin A_3 was purchased from Enzo Life Sciences (Plymouth Meeting, PA), and ABT-737 and ABT-263 were purchased from Chemie Tek (Indianapolis, IN).

5.3.2 Preparation of rat liver mitochondria

Rat liver mitochondria were isolated from male Sprague Dawley rats by differential centrifugation of tissue homogenates as described previously (Parsons et al., 1966) and modified (Siskind et al., 2002). BSA medium was used to wash the liver during the excision and initial centrifugation steps and was removed by centrifugation at 8700 RCF (twice) in BSA-free medium. The final mitochondrial pellet was resuspended in ~3-5mL of ice cold sucrose free isotonic buffer FH (280 mM mannitol, 0.1 mM EGTA, 2 mM HEPES, pH 7.4). The mitochondrial intactness was determined from the rate of cytochrome *c* oxidation (*vide infra*) compared with the rate measured after mild hypotonic shock (Douce et al., 1987) as described below. The animal use protocols were approved by the Institutional Animal Care and Use Committee. The animals were euthanized by a procedure consistent with the Panel on Euthanasia of the AVMA. The animal facility used to house the animals is accredited by AAALAC.

5.3.3 Purification of recombinant proteins

Recombinant human Bax was purified as described previously (Suzuki et al., 2000) and modified (Ganesan et al., 2010). One change made was to reduce the Tris concentration from 20mM to 10mM in both dialysis steps; this change had no effect of the activity of the protein. The protein was shell-frozen in small aliquots in thin-walled glass tubes using ethanol/dry ice and stored at -84ºC. A fresh monomeric Bax sample was thawed before each experiment. Standardizing the concentration of Bax to 5-10μg/mL with FH buffer (10mM Tris-HCl pH 8.0 solution could also be used) before activation improved reproducibility between different Bax preparations. This monomeric Bax was

activated using 10% β-octyl glucoside to a final concentration of 1% and incubated for 30 min on ice; this activated Bax was used in the experiments throughout this study. Full length recombinant Bcl-xL was isolated as previously described (Basañez et al., 2001) and the following changes are recommend. Only 5mL overnight culture was inoculated into 1 L of LB media and this was allowed to incubate with shaking until OD_{600}=0.600. The culture was then induced with 0.01mM isopropyl β-D-1-thiogalactopyranoside (IPTG) for 2h at 37^{o}C. After the cells were harvested by centrifugation, the pellet was resuspended in 40 mL of PBS and incubated on ice for 20 min with 140 U of lysozyme and 35 μM PMSF (final concentration). The cells were then subjected to two passes through a French press and centrifuged to remove cell fragments. The lysate was then incubated with glutathione-agarose beads for 2 h at 4^{o}C and packed into a column. The beads were washed with 10 column volumes of cold PBS containing 35 μM PMSF and another 10 column volumes of 20 mM Tris-HCl, pH 8.0. 10 mL of the same buffer supplemented with 5 U of biotinylated thrombin were added to the column and allowed to incubate overnight at 4^{o}C. The protein was eluted, and 80 μL of streptavidin beads were added to remove the remaining thrombin. After a 30 min incubation with rotation, the beads were removed by centrifugation and the sample was filter sterilized. Glycerol (10%) was added to the protein and 100 μL aliquots were rapidly shell frozen in ethanol/ dry ice. The published method included the addition of Triton-X100 to the cells along with the PMSF and lysozyme prior to French pressing of the cells. This greatly increased the yield (1.4 mg/mL with Triton vs. 165 μg/mL without Triton). Both methods resulted in proteins with identical function in our assays.

5.3.4 Cytochrome *c* oxidation assay

The ability of cytochrome *c* to translocate through the MOM and become oxidized by cytochrome *c* oxidase (found on the mitochondrial inner membrane) is the rate limiting step thus this assay is a measurement of the permeability of the MOM. While measurements from mitochondrial release assays indicate that mitochondria were permeabilized at some time point, perhaps transiently, one of the advantages of using this dynamic cytochrome *c* oxidation assay is that real-time permeability of the MOM can be measured. Thus, this assay allows us to garner more information about the nature and stability of the channels in question. This assay was performed as previously described (Wojtczak et al., 1972) with the following modifications to optimize reproducibility as mitochondria were found to be more stable at higher concentrations. In a typical experiment, unless otherwise noted in the figure legends, mitochondria were diluted in FH buffer at 4^{o}C to a concentration of 0.5 mg/mL, in small batches just before the assay. Then, 50 μL aliquots were dispersed in 650 μL of room temperature reaction buffer (160mM mannitol and 60mM KCl, 5 mM DNP and 1.3 μM antimycin A (antimycin A was tested in our system with Bcl-xL and ceramide and no effect was seen at the highest concentration tested which was 2.7 μM), pH 7.25). The final mitochondrial protein concentration was 36 μg/mL. The mitochondria were allowed to acclimate at room temperature for 5 min in a microfuge tube. Then ceramide or a ceramide analog (dissolved in 2-propanol at 1 mg/mL) was delivered to the mitochondria while the suspension was vortexed for 30 s to achieve effective dispersal of the sphingolipid. After dispersal, the mixture was incubated for 10 min at room temperature followed by addition of cytochrome *c* (12 μL; final concentration 27 μM) and immediate measurement of the

absorbance at 550 nm for a period of 2 min. The initial rate of decline of absorbance of reduced cytochrome *c* was used as a measure of the permeability of the outer membrane to cytochrome *c*; ε_{550} (red-ox) = 18.5 mM^{-1} cm^{-1}. The amount of vehicle added was less than 4% of the sample volume and all vehicle controls were treated in an identical way. Rates were corrected for the rate of oxidation observed with vehicle alone and this was very close to the untreated rate arising from a small number of damaged mitochondria. The maximal rate of cytochrome c oxidation was assessed by subjecting the mitochondria to mild hypotonic shock as previously described (Douce et al., 1987) with the following modifications. Briefly, mitochondria were diluted in double distilled water to 1mg/ml and incubated on ice for 10 minutes before adding 2xFH buffer (FH buffer with double the amount of additives) to restore the isotonic conditions. 50uL of this 0.5mg/mL mitochondrial stock is then added to the reaction buffer and tested for cytochrome c oxidation as described below. In these experiments, the intactness of the mitochondrial preparations was greater than 85%. The rate of cytochrome *c* oxidation was converted to % permeabilization of mitochondria by taking this rate as a percentage of the maximal rate of oxidation obtained by subjecting the mitochondria to mild hypotonic shock. The permeabilization induced by ceramide alone is given for each experiment in the figure legends. It is important to note that even a relatively low % permeabilization of mitochondria, as seen with our Bax experiments, is physiologically relevant (Kluck et al., 1999; von Ahsen et al., 2000; Siskind et al., 2006) and even low levels of cytochrome c release are sufficient to induce apoptosis in whole cells (Li et al., 1997a; Zhivotovsky et al., 1998).

It should be pointed out that unlike liposomes, mitochondria are complex organelles whose function decays with time. Thus we are limited in what experiments can be performed within the functional time window. Also, it is necessary to monitor the state of the mitochondria. Before experiments are performed the mitochondria are tested for the ability of C_{16}-Cer to permeabilize the MOM and for the ability of the Bcl-2 family proteins to alter this permeabilization. These tests are repeated as time passes to ensure that any results obtained in the experimental trials are meaningful. The disadvantages of using a "living" organelle are more than compensated for by performing experiments in the natural membrane environment. Clearly, the greatest level of understanding is reached by performing experiments at various levels of complexity, from the intact cell to the pure components in a defined system.

5.3.5 Testing Bcl-2 proteins on channels formed by ceramide and its analogs

The sensitivity of isolated mitochondria to permeabilization by added ceramide or analogs varied from one preparation to another. Therefore experiments with analogs were always performed in parallel with experiments with C_{16}-Cer. Furthermore, the amounts of C_{16}-Cer and analog added were adjusted (dilutions were made to keep the volume added to the sample constant at 10 μL) so as to induce approximately the same extent of mitochondrial outer membrane permeabilization (MOMP). This was done because some analogs of ceramide may insert more or less readily into mitochondria or have a different propensity for channel formation. By finding conditions that result in the same degree of MOMP, we achieve the same level of channel formation. The permeabilization was measured as the rate of cytochrome *c* oxidation. Bax, Bcl-xL, 2-MeAA_3, ABT-737, and ABT-263 were added along with the mitochondria for a 5 min incubation at room

temperature prior to sphingolipid dispersal. Stock solutions of 2-MeAA$_3$ (1.9 mM in 2-propanol), ABT-737 (0.7 mM in DMSO) and ABT-263 (0.7 mM in DMSO) were diluted to the appropriate concentration with the same solvent so that the volume added to reach the concentration indicated in the figure remained constant (10 μL, 5 μL, and 5 μL respectively). Results are shown as a % change comparing the effect of adding a Bcl-2 protein in combination with ceramide (or an analog) vs. the addition of ceramide (or the analog) alone.

5.3.6 Molecular docking simulations of potential Bcl-xL inhibitors

Modeling, simulations and visualizations were performed using Molecular Operating Environment (MOE) Version 2011.10 (Chemical Computing Group Inc., Montreal, Canada). Simulations were performed on a Dell E8500 with an Intel Core 2 Duo @ 3.16 GHz using Windows XP OS. All other computational procedures were performed using a Dell XPS M1530 with an Intel Core2 Duo processor T8300@2.40 GHz w 2GB RAM using Windows Vista OS. The structural file used as input for analysis and docking simulations was pdb: 1PQ1 (PubMed: 14499110). Before analysis and simulations the main chain protein was protonated at pH 7.5 with a salt concentration of 0.2 M and the structures energy minimized using the Amber99 forcefield and Born solvation model. Simulations focused on the entire protein surface and Bcl-xL was held rigid while the ligand was flexed. Initial placement calculated 500 poses per molecule using triangle matching placement with London dG scoring, the top 250 poses were then refined using forcefield placement and Affinity dG scoring. The resulting interaction after refinement is called E score 2. This is a measure of the strength of the interaction with stronger interactions yielding a more negative number. Ligands were prepared in

MOE, protonated at pH 7.5, and chirality formalized within the ligand database. The top poses generated from each ligand were then minimized in place as a system with Bcl-xl to allow the protein to flex as well as the ligand. System minimization also used the Amber99 forcefield and Born solvation model.

5.3.7 Statistical analysis

All results shown are an average of 3-4 trials and each experiment was repeated on three separate mitochondrial preparations. Student's *t* test was performed to obtain *P*-values and identify a statistically significant change from the additive value (for Bax experiments) or individual C_{16}-Cer or analog addition (for Bcl-xL experiments). As a standard, * indicates $P<0.05$, ** indicates $P<0.01$, and *** indicates $P<0.001$. Error bars represent ± SE of 3-4 experiments.

5.4 RESULTS AND DISCUSSION

Previous results (Siskind et al., 2008; Ganesan et al., 2010) have indicated that the recognition between the ceramide channel and Bcl-2 proteins is highly specific. These findings prompted the present study in which we used a dynamic cytochrome *c* accessibility assay to assess the influence of Bax and Bcl-xL on the ability of ceramide and its analogs to permeabilize the MOM. To determine the specific site(s) of interaction of these Bcl-2 proteins on ceramide channels, we prepared ceramide analogs with changes in different functional groups thought to be important for channel formation. The analogs that retained channel-forming ability are illustrated in Table 5.1.

Experiments with ceramide and an analog were performed in parallel. Before each experiment, the amounts of ceramide or ceramide analog were adjusted so as to induce approximately the same extent of MOMP. In this way we compensated for any differences in the propensity for channel formation and tested the Bcl-2 family proteins on the same degree of channel presence. As a result the ability of the Bcl-2 family proteins to alter the MOMP induced by ceramide could be compared to that for the analog.

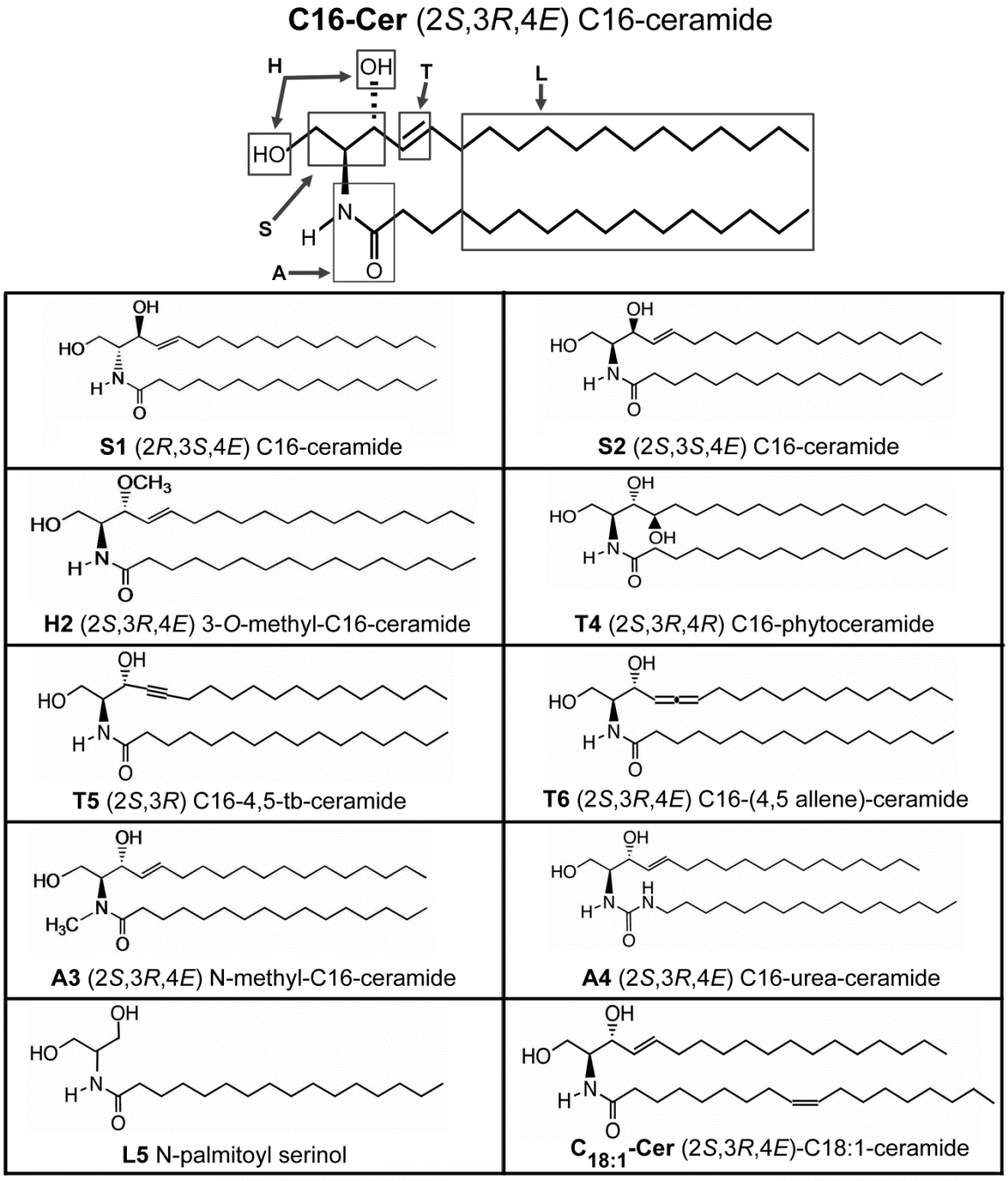

Table 5.1 Structures of Ceramides and Analogs Used.

Coded boxes highlight the key areas of the ceramide molecule that are important for ceramide channel formation (top). The codes indicate the location on the ceramide molecule where changes were introduced (**S** for stereochemistry, **H** for hydroxy group, **T** for *trans* double bond, **A** for amide linkage, **L** for hydrophobic chain length) and the analogs are named throughout the manuscript using these short codes followed by a number as indicated in the table.

When different doses of ceramide or ceramide analogs were applied to achieve a comparable degree of permeabilization, the amount of Bcl-2 family protein added was kept the same. This is because the amount of protein added greatly exceeded the number of channels present (for additional details, see Supplemental Information). Thus the binding is not of very high affinity or stoichiometry. Previous studies showed that the channels are responsive to the effective concentration of added protein in a manner consistent with a dynamic equilibrium. Thus despite adding different amounts of the sphingolipid to achieve the same degree of permeabilization, it makes sense to use the same effective dose of Bcl-2 family protein to detect differences in effect on channel-mediated permeability.

The results described were obtained at room temperature whereas apoptosis, in mammalian cells, typically takes place at 37ºC. Thus differences in rates of reaction, fluidity, etc. resulting for a difference in temperature could easily affect the reported values but are unlikely to change the fundamental conclusions about the specificity of the sites of interaction with ceramide associated with Bax and Bcl-xL. Indeed, key experiments reproduced at 37°C yield similar results as seen at 23°C (Fig 5.3A, 5.4C, 5.8A, B), indicating the physical properties of this interaction remain at physiological temperatures.

5.4.1 The Importance of the *trans*-Double Bond

The following changes were introduced to the C4:C5 *trans* double bond of the sphingoid backbone of ceramide: C_{16}-phytoceramide (**T4**), which has a hydroxy group at the C4 position instead of the double bond; C_{16}-4,5-tb-ceramide (**T5**), which has a triple

bond in place of the double bond; and C_{16}-(4,5-allene)-ceramide (**T6**), which is a 4,5-cumulated diene. Previous results showed that the addition of either detergent-activated Bax or tBid-activated Bax along with C_{16}-Cer to isolated rat liver mitochondria resulted in a much greater permeabilization of the MOM than either entity alone, indicating that Bax enhances the formation of ceramide channels (Ganesan et al., 2010). Here we look for a similar result on ceramide analogs. An example of the result of a typical paired experiment with C_{16}-Cer and an analog (**T5**) is shown in Figure 5.1A. Detergent-activated Bax ("Bax") induces a small permeabilization while C_{16}-Cer ("C16") produces a more significant permeabilization. However, when both are added together ("C16 + Bax"), the resulting permeabilization is much greater than the value obtained by adding the values of the "Bax" and "C16" bars, "Predicted C16 + Bax." The permeabilization induced by **T5** was enhanced by the addition of Bax to a similar extent indicating that the modification had not influenced the ability of Bax to act on **T5** channels. Similar paired experiments were performed with the other analogs. Fig 5.1B shows that Bax enhanced the permeabilization induced by **T4** to the same extent as **T5** but was 40% less effective on **T6**.

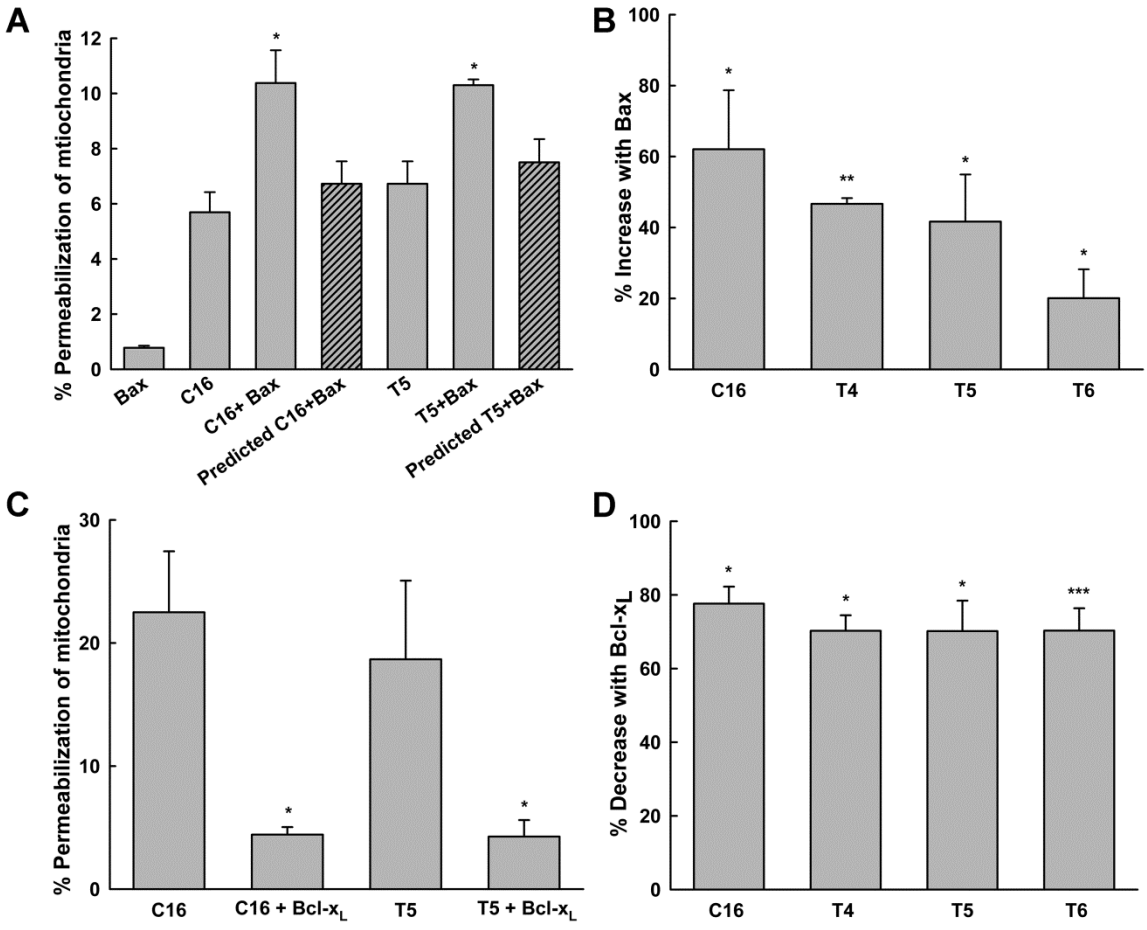

Figure 5.1 Testing the ability of Bax, Bcl-xL to regulate channels formed in isolated rat liver mitochondria by ceramide analogs with changes in the C4:C5 *trans* double bond or extent of unsaturation.

The cytochrome *c* oxidation assay was used to determine the degree of MOM permeabilization induced by the addition of ceramide or an analog and the enhancement or inhibition of this permeability in the presence of Bax or Bcl-xL respectively. **A.** A typical Bax/C_{16}-Cer/analog experiment: the amount of "C16"-ceramide (10 μg) and "T5" (5 μg) added was adjusted so that they induced approximately the same extent of MOM permeabilization when added alone. The addition of Bax (3.5 nM) along with C_{16}-Cer ("C16+Bax" column) and **T5** ("**T5**+Bax" column) resulted in enhancement of the MOM permeability induced by ceramide and the analog. These tested combinations are compared to the permeability predicted by adding the effect of the respective individual treatments ("Predicted" columns; i.e. "Bax" + "C16" = "Predicted C16 + Bax"). **B.** Bax (3.5nM) can enhance channels formed by **T4** (5 μg), **T5** (5 μg) and **T6** (5 μg) and is shown as a % increase in MOMP. **C.** A typical Bcl-xL/C_{16}-Cer/analog experiment is shown

here and is conducted similarly to panel **A**. Bcl-xL (0.4 μM) inhibits C_{16}-Cer (10 μg) channels and **T5** (6 μg) channels to a similar extent. As Bcl-xL does not induce a detectible MOMP (see Fig. 6A) the combination treatments of "C16 + Bcl-xL" and "T5 + Bcl-xL" were compared to the individual treatments of C_{16}-Cer and **T5** respectively and subject to the same statistical analysis as stated below. **D.** Bcl-xL (0.4 μM) inhibited C_{16}-Cer (10 μg), **T4** (7.5 μg), **T5** (6 μg), and **T6** (5 μg) channels to the same extent and is shown as a % decrease in MOMP. For efficiency, all experiments henceforth will be shown as % change in MOMP as in panels **B** and **D** of this figure.

In Bcl-xL experiments (Fig. 5.1C), as in the Bax experiments, the doses of ceramide and analog used were adjusted so that the extent of MOMP induced was approximately the same. When Bcl-xL is present ("C16 + Bcl-xL" and "**T5** + Bcl-xL"), the permeabilization was greatly reduced in both cases and by the same amount. The % decrease of permeabilization is shown in Fig 5.1D. Bcl-xL (0.4μM) inhibited ceramide channel formation in isolated mitochondria by nearly 80% (Fig. 5.1C). The same dose of Bcl-xL was similarly effective on **T4**, **T5,** and **T6**.

Analogs in which changes to the double bond were made by introducing a hydroxy group in its place (**T4**), changing it to a triple bond (**T5**), or adding another double bond next to it (**T6**) were well tolerated by both Bax and Bcl-xL. Thus, the location of the C4:C5 double bond and the degree of unsaturation at this position have little influence on the ability of Bax or Bcl-xL to regulate these lipid channels.

5.4.2 Importance of the C1 and C3 Polar Groups

The C1 and C3 hydroxy groups of the ceramide are thought to hold adjacent columns of ceramide together to form the lumen of the ceramide channel. 3-*O*-Methyl-

C_{16}-ceramide (**H2**) has the C3-hydroxy group blocked yet this analog can still form channels (Fig. 5.2A), suggesting that the C1-hydroxy group is sufficient to stabilize the channel. Both Bax and Bcl-xL can exert their respective effects on **H2,** indicating that the C3-hydroxy group is not a site at which either protein interacts (Fig. 5.2 A,B).

The effect of changing the configuration at C2 or C3 of ceramide was explored by using two stereoisomers: the enantiomer (2*R*,3*S*,4*E*) C_{16}-ceramide (**S1**) and the diastereomer (2*S*,3*S*,4*E*) C_{16}-ceramide (**S2**). Bax was unable to enhance channels formed by **S1** (Fig. 5.2C). **S1** is the mirror image of the natural ceramide and Bax is unable to recognize channels formed by **S1**. However, Bax was able to enhance channels formed by **S2** to a similar degree as C_{16}-Cer (Fig. 5.2D), where only the orientation of the C3-hydroxy group is altered. Bcl-xL was able to inhibit channels formed by **S1** and **S2** (Fig. 5.2E), although to a lesser degree than those formed by C_{16}-Cer. These results indicate that the ability of Bax to interact with ceramide channels does not require access to the C3-hydroxy group (**H2**), but is highly sensitive to the configuration at C2 of ceramide.

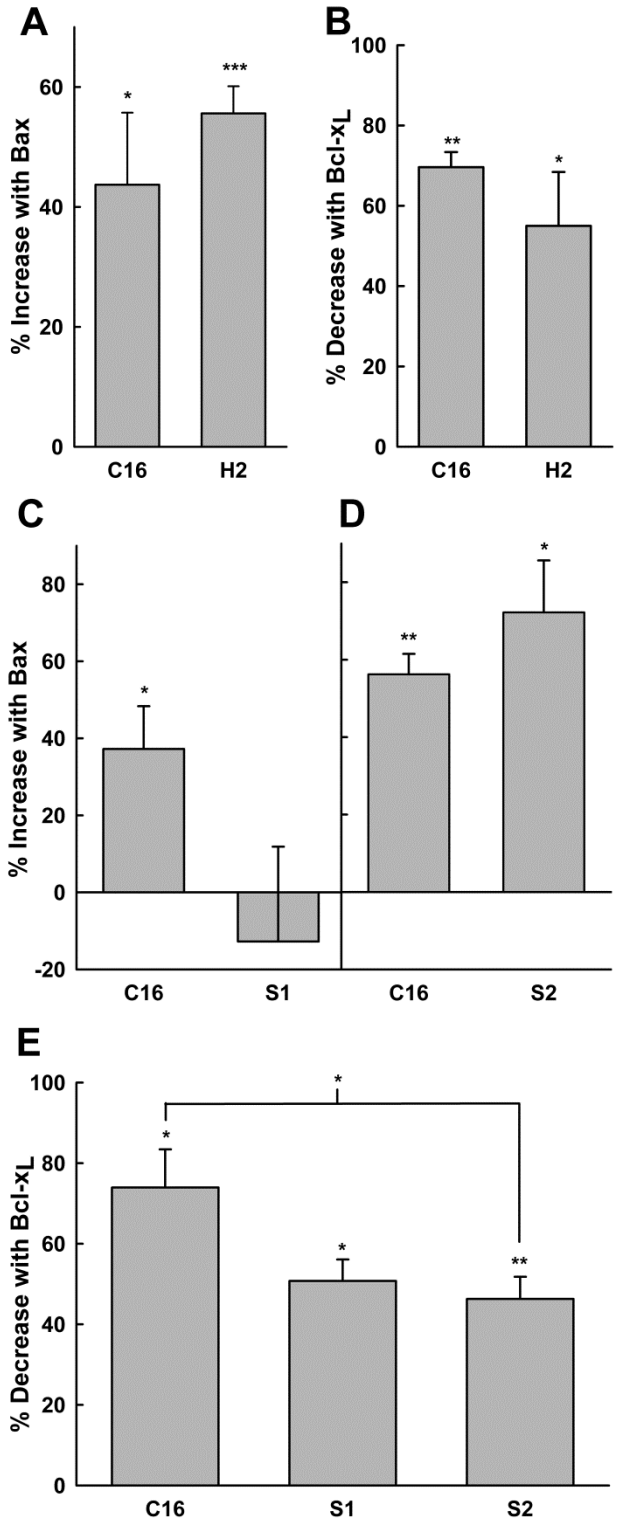

Figure 5.2 Tests of the ability of Bax, Bcl-xL to regulate ceramide analogs with changes to polar head groups or stereochemistry.A, B. Blocking the C3 hydroxy group does not reduce the channel's sensitivity to 3.5 nM Bax (5 μg C_{16}-Cer, 2 μg **H2**, yielding ~10% MOMP) or

0.4μM Bcl-xL (7.5 μg C_{16}-Cer, 5 μg **H2**, yielding ~12% MOMP). **C.** Bax (2 nM) is sensitive to changes in the stereochemistry found in analog **S1**. Mitochondria were treated with 10 μg each of **S1** and C_{16}-Cer (~20% MOMP). **D.** Channels formed by analog **S2** (5 μg) interact with Bax (3.5 nM) similarly to those formed by C_{16}-Cer (5 μg) (~8% MOMP). **E.** Bcl-xL (0.4 μM) inhibits C_{16}-Cer (3.5 μg) channels more strongly than those formed by **S1** and **S2** (10 μg and 3.5 μg resp. yielding ~10% MOMP).

5.4.3 The Importance of the Amide N-H group of Ceramide

In the current model of the ceramide channel, the amide N-H group is thought to form a hydrogen bond with the carbonyl group of another ceramide molecule (Anishkin et al., 2006). These intermolecular interactions allow for the assembly of ceramide columns. Analog **A3**, *N*-methyl-C_{16}-ceramide, features a methyl group instead of the N-H group. MOMP induced by **A3** was not enhanced by the addition of 3.5nM of Bax, whereas parallel experiments with C_{16}-Cer resulted in a 40% enhancement (Fig. 5.3A, S1A). Thus, Bax is unable to influence the structure of channels formed by **A3**, possibly due to a requirement for binding to the N-H group. Bcl-xL also has a much reduced interaction with **A3** but the effect is not completely diminished as with Bax (Fig. 5.3B). (2*S*,3*R*,4*E*)-C_{16}-urea-ceramide (**A4**) is a potent channel former as half as much is needed to permeabilize the MOM to the level achieved by a given amount of C_{16}-Cer (Fig. 5.3C). This could be attributed to the enhanced hydrogen-bonding ability afforded by the urea group and thus the potential to further stabilize ceramide columns. This change is opposite to that of A3 in terms of hydrogen bonding ability of the molecule and Bax addition resulted in a greater enhancement of **A4** channels than C_{16}-Cer channels. Perhaps the increased hydrogen-bonding ability also serves to increase the strength of the

interaction with Bax. Bcl-xL inhibits the **A4** channels to the same extent as the C_{16}-Cer channels (Fig. 5.3C, D) indicating that Bcl-xL is not sensitive to the modification.

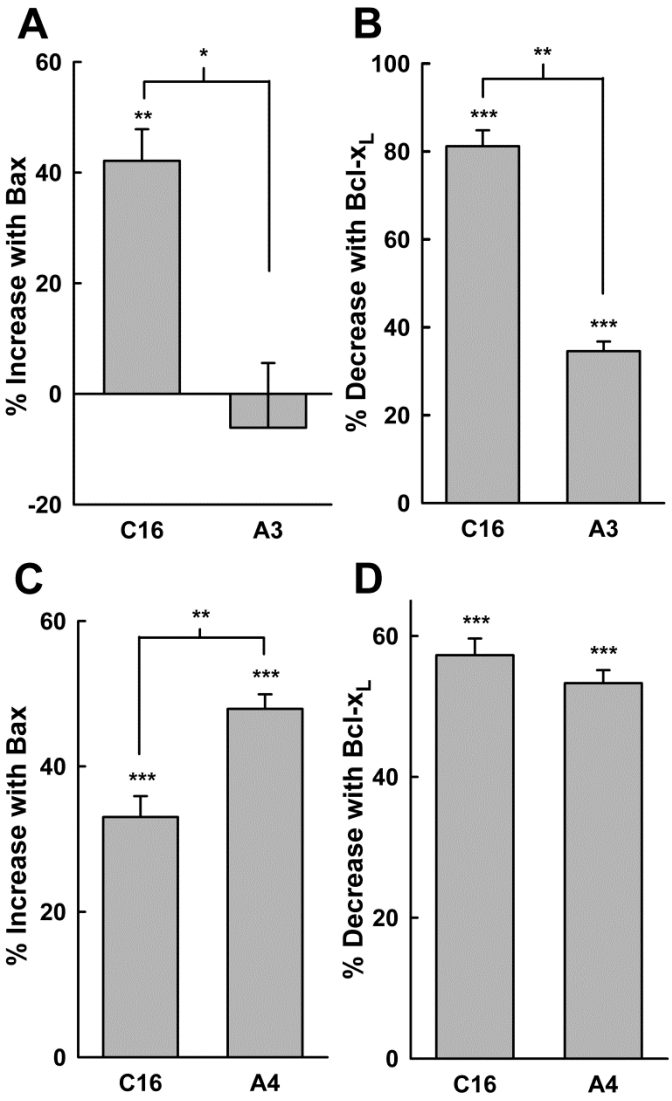

Figure 5.3 Bax is more sensitive than Bcl-xL to changes in the amide N-H group of ceramide.

A. Blocking the amide nitrogen with a methyl group prevents Bax (3.5 nM) from enhancing channels made by **A3** (10 μg of C_{16}-Cer and **A3** were added to induce approximately 10% MOMP). **B.** Bcl-xL (0.1 μM) is approximately 50% less effective on **A3** (20 μg) than C_{16}-Cer (6 μg); however, Bcl-xL can still cause about a 35% decrease in the permeability induced by **A3**

channels (~11% MOMP). **C, D.** Analog **A4** contains a urea group, which increases the hydrogen-bonding ability of the molecule. While Bax is more effective on **A4** than C_{16}-Cer, Bcl-xL is similarly effective on both. For these experiments, 3.5 nM Bax, 0.1μM Bcl-xL, and 10 μg of C_{16}-Cer and 5 μg of **A4** were used to induce approximately 22% MOMP.

5.4.4 The Importance of Tail Length and Apolar Bulk

The importance of the apolar region of ceramide for Bcl-2 protein interaction was tested with a minimal analog, N-palmitoyl serinol (**L5**). It only has one aliphatic chain. Bax was able to interact with **L5** (Fig. 5.4A) almost as well as C_{16}-Cer. Surprisingly, Bcl-xL was not able to inhibit these channels at all (Fig. 5.4B). Likewise, the permeability induced by a very short-chain ceramide analog, C_2-ceramide (C_2-Cer), was also not inhibited by Bcl-xL (Fig. 5.4C, 5.8B). To test whether this unexpected result was due to kinetic delays, the added doses of the ceramides was adjusted to achieve a similar MOMP by C_2-Cer and C_{16}-Cer alone. Fifteen and 30 min incubations with Bcl-xL resulted in the same degrees of inhibition (Fig. 5.4D). No effect of Bcl-xL on C_2-Cer was seen at either time point whereas the same substantial level of inhibition of C_{16}-Cer permeabilization occurred at each time point. Thus, the inability of Bcl-xL to inhibit C_2-Cer channels is not dependent on incubation time.

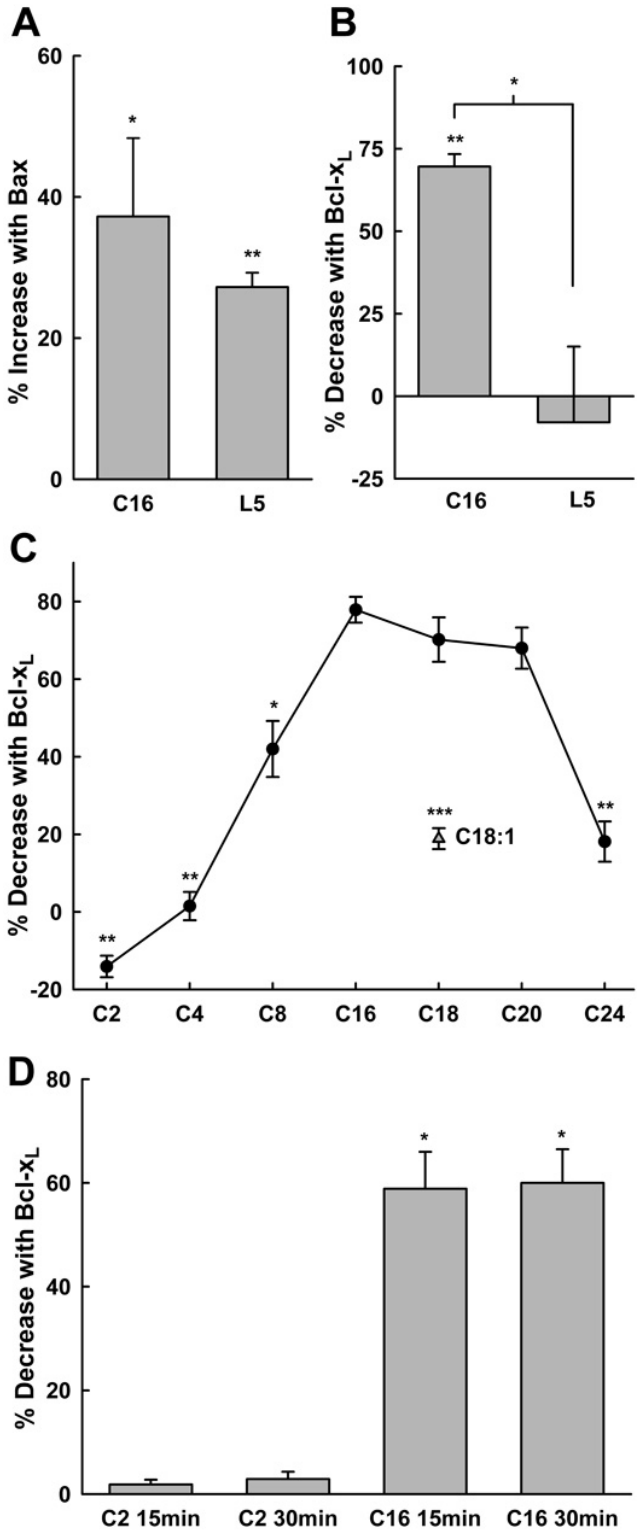

Figure 5.4 Effects of analogs with altered hydrophobic regions on the regulation by Bcl-xL and Bax. A. Bax (2 nM) enhances MOMP formed by **L5** (10μg), which has a truncated

sphingoid base (10 μg of C_{16}-Cer was used, ~30% MOMP). **B.** Bcl-xL (0.4 μM) does not inhibit channels formed by **L5** (3 μg); 7.5 μg of C_{16}-Cer was added here (~12% MOMP). **C.** Varying the length of the *N*-acyl chain of ceramide reveals an optimal acyl chain length for Bcl-xL (0.4 μM) inhibition of ceramide channels. 10 μg of C_2-Cer - C_{18}-Cer and $C_{18:1}$-Cer was used. 7.7 μg each C_{20}-Cer and C_{24}-Cer were added in a volume of 13μL. Before addition of Bcl-xL, the amount of ceramide or ceramide analog used induced approximately 19% MOMP. **D.** Analysis of the time dependence of Bcl-xL interaction. 6 μg of C_2-Cer and 12 μg of C_{16}-Cer in a volume of 12 μL were added to induce a similar level of mitochondrial permeabilization (~40%). The addition of 0.1 μM of Bcl-xL results in 60% inhibition of C_{16}-Cer channels but does not cause any change in the permeability of C_2-Cer channels during the time of a typical experiment, 15 min. Increasing the incubation time by 15 min does not abate the inability of Bcl-xL to recognize C_2-Cer channels.

Ceramide analogs with tail lengths varying between C_2-C_{24} were tested and the results show an optimal length for the acyl chain of C_{16}, C_{18} and C_{20}. Bcl-xL is known to have a hydrophobic groove and perhaps the optimal hydrocarbon bulk results in optimal binding. The introduction of an unsaturated bond in the acyl chain at C9:C10 of C_{18}-Cer ($C_{18:1}$-Cer) resulted in a large drop in sensitivity to Bcl-xL inhibition. The kink in the fatty acyl chain may interfere with binding to Bcl-xL, indicating a very specific interaction.

These results have important implications. Various long-chain and very-long chain ceramides are found in the MOM and the specific *N*-acyl chains of the naturally occurring ceramides in membranes are thought to play an important physiological role (Megha et al., 2007; Pruett et al., 2008; Grösch et al., 2011). In fact, ceramide synthases show specificity for different acyl-CoA substrates (Venkataraman et al., 2002; Riebeling et al., 2003; Mizutani et al., 2005; Laviad et al., 2008; Menuz et al., 2009), and some

preferentially generate long-chain ceramides such as C_{16}-Cer or C_{24}-Cer (Venkataraman et al., 2002; Mizutani et al., 2005). In the early stages of apoptosis, cells are reported to generate primarily C_{16}-Cer along with some C_{18}-Cer and C_{20}-Cer (Kroesen et al., 2003; Siskind et al., 2010). C_{24}-Cer generation occurs at later stages (Kroesen et al., 2003). This fits well with our observation that Bcl-xL interacts optimally with C_{16}-, C_{18}-, and C_{20}-Cer as those species are elevated when the fate of the cell is still being decided. During this initiation stage of apoptosis, before the mitochondria have become permeabilized, various apoptotic signals result in the elevation of ceramides. Anti-apoptotic Bcl-2 family proteins, like Bcl-xL and Bcl-2, could prevent these higher ceramide levels from forming channels resulting in MOMP. Bax activation and heterodimerization with Bcl-xL would relieve this inhibition and, at the same time, any excess Bax could favor ceramide channel formation and/or growth. Clearly these interactions result in many opportunities for controlling this key, decision-making step.

Many studies have been carried out with cell permeable C_2- and C_6-ceramides to trigger apoptosis in cancer cells. It is also evident that many enzymes that metabolize ceramide do not recognize C_2-ceramide (Wijesinghe et al., 2005; Phillips et al., 2009) thus allowing these molecules to act over a longer time scale. Interestingly, the ability of short and long-chain ceramides to form channels is about the same and mixtures of long and short-chain ceramides are actually more potent (Perera et al., 2012). Thus, it is possible that these short-chain ceramides may be more effective than long chain ceramides therapeutically in promoting apoptosis because Bcl-xL is unable to recognize or regulate these species while Bax retains the ability to promote channel formation by these ceramides.

5.4.5 Inhibitors provide insights into the region of Bcl-xL that binds to the ceramide channel

Cells overexpressing pro-survival proteins Bcl-xL and Bcl-2 are highly resistant to cell death and many types of cancer indeed display this phenotype. Three known small-molecule inhibitors of Bcl-xL and Bcl-2 are 2-MeAA$_3$, ABT-737, and ABT-263. These inhibitors bind to the hydrophobic groove on Bcl-2 and Bcl-xL (Manion et al., 2004; Wendt et al., 2006; Siskind et al., 2008; Tse et al., 2008), effectively neutralizing the effects of pro-survival protein overexpression and sensitizing cells to death. Since Bcl-xL interacts with the ceramide channel through the hydrophobic region, the inhibitors should interfere with the interaction if binding involves the hydrophobic groove.

Results from the 2-MeAA$_3$ experiments are shown in Figure 5.5A. Whereas the highest concentration of 2-MeAA$_3$ tested (2.7 μM) had no effect on ceramide induced permeabilization of the MOM, Bcl-xL (0.7 μM) inhibited the ceramide induced permeabilization by about 50%. 2-MeAA$_3$ produced a dose-dependent recovery of ceramide-induced permeabilization, indicating that 2-MeAA$_3$ might bind to the same site on Bcl-xL as the ceramide channel. Unlike 2-MeAA$_3$, ABT-737 displayed a strong inhibition of ceramide permeabilization at 2.5 and 5 μM whereas lower concentrations had either no effect or a slightly stimulatory effect on ceramide permeabilization (Fig. 5.5B). In the presence of 0.7 μM Bcl-xL, ABT-737 produced a dose-dependent recovery of ceramide permeabilization with 50% recovery at about 1 μM and complete recovery at 2.5 μM. A strong inhibition of ceramide channels by ABT-737 is evident at 5 μM even in the presence of Bcl-xL. ABT-263, the orally available analog of ABT-737, was also

able to cause a dose-dependent recovery of ceramide permeabilization in the presence of Bcl-xL but did not inhibit ceramide permeabilization at any of the concentrations tested when Bcl-xL was not present (Fig. 5.5C). Thus the inhibitory effects of Bcl-xL on ceramide channels can be reversed by the addition of Bcl-xL-targeted inhibitors that bind to the hydrophobic groove, suggesting competition and that the hydrophobic groove is likely the site at which Bcl-xL binds to the ceramide channel.

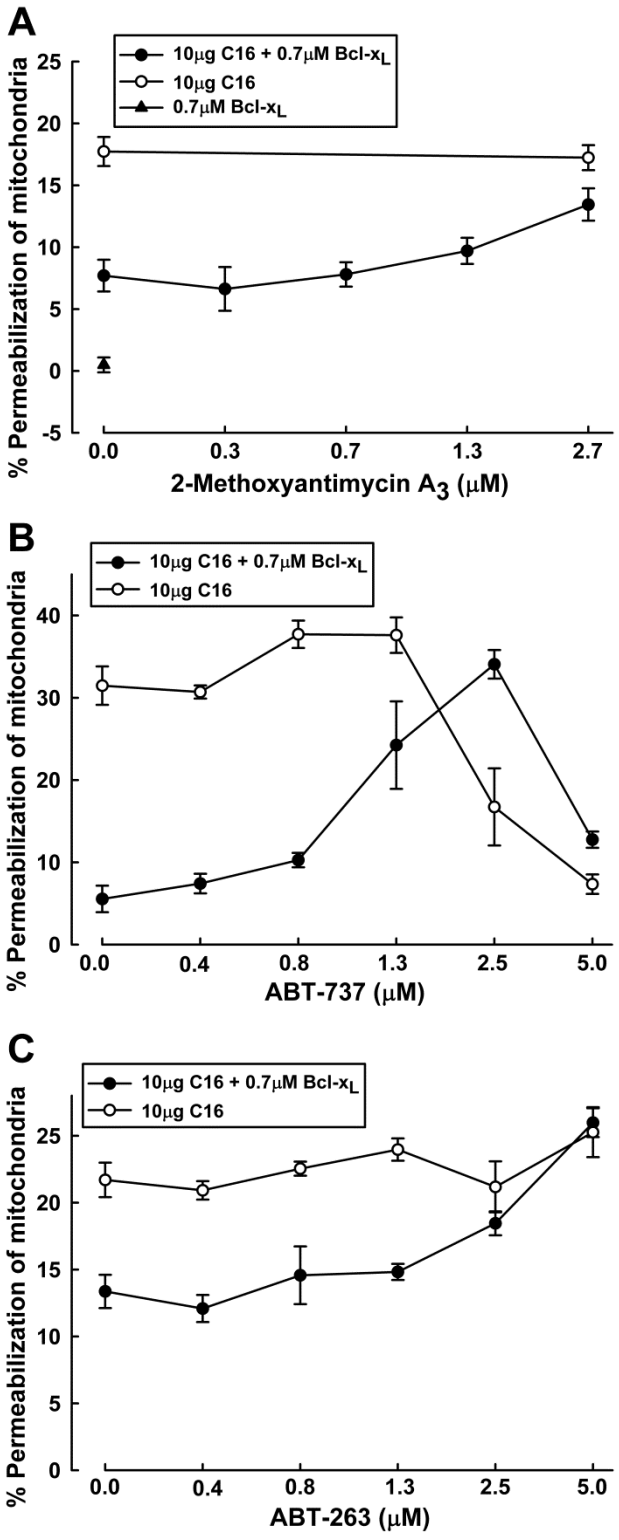

Figure 5.5. The hydrophobic groove of Bcl-xL is involved in binding to ceramide channels. Inhibitors known to bind to the hydrophobic groove of Bcl-xL were assayed for ability to prevent Bcl-xL binding to ceramide channels in isolated rat liver mitochondria. **A.-C.** Increasing

concentrations of 2-methoxyantimycin A_3 (2-MeAA_3), ABT-737 or ABT-263 were tested with C_{16}-Cer alone (10 μg) and the combination of C_{16}-Cer and Bcl-xL (0.7μM).

Molecular docking of ceramides and inhibitors to Bcl-xL were conducted to determine the lowest energy site and mode of binding on Bcl-xL. The region of lowest energy binding was first determined probing the whole surface of Bcl-xL and the hydrophobic groove was the best, or near best, scored region for all ligands tested. The top 10 poses for each of the ligands are shown in Fig. 5.6 and the average energy of these were calculated and shown as a horizontal bar. The more negative the number the stronger the interaction. ABT-737 and ABT-263 had the lowest energy score, and therefore best binding, followed by C_{16}-ceramide. Especially noteworthy is the weaker average binding of C_2-ceramide as compared to C_{16}-ceramide, consistent with the experimental results. To further explore the potential interaction between Bcl-xL and C_{16}-ceramide, the lowest energy pose was subjected to global system energy minimization to allow both the protein and the ligand to flex. These results were considered a plausible prediction of the interaction between ceramide and Bcl-xL Fig. 5.7B.

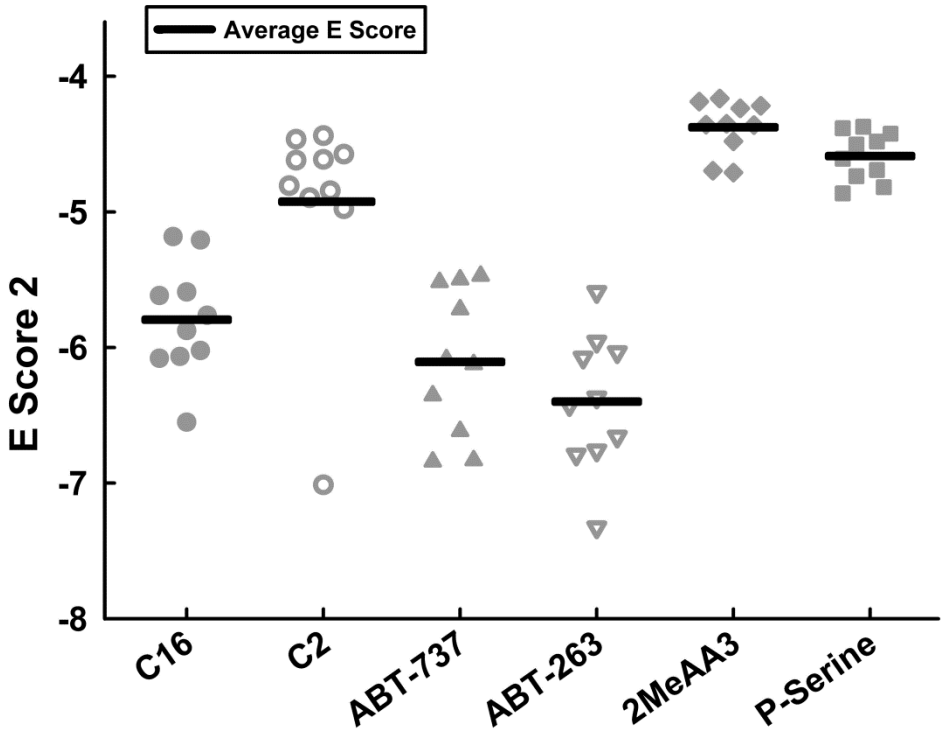

Figure 5.6 E Score 2 of ten best poses of molecular docking simulations.

Docking simulations of Bcl-xL to either C_{16}-Cer (C16), C_2-Cer (C2), ABT-737, ABT-263, 2-methoxyantimycin A_3 (2MeAA3), or palmitoyl-serine (P-Serine) yielded structures of various degrees of interaction energy. The lower the E Score, the better the interaction. The average of the 10 best interacting structures (poses) for each ligand is shown as a horizontal line.

One of the top 10 poses shows ceramide binding to Bcl-xL with only one chain (Fig. 5.7A). When this is placed on top of a segment of the model of a ceramide channel, this provides mechanistic support for a hypothetical mechanism by which Bcl-xL destabilizes a ceramide channel.

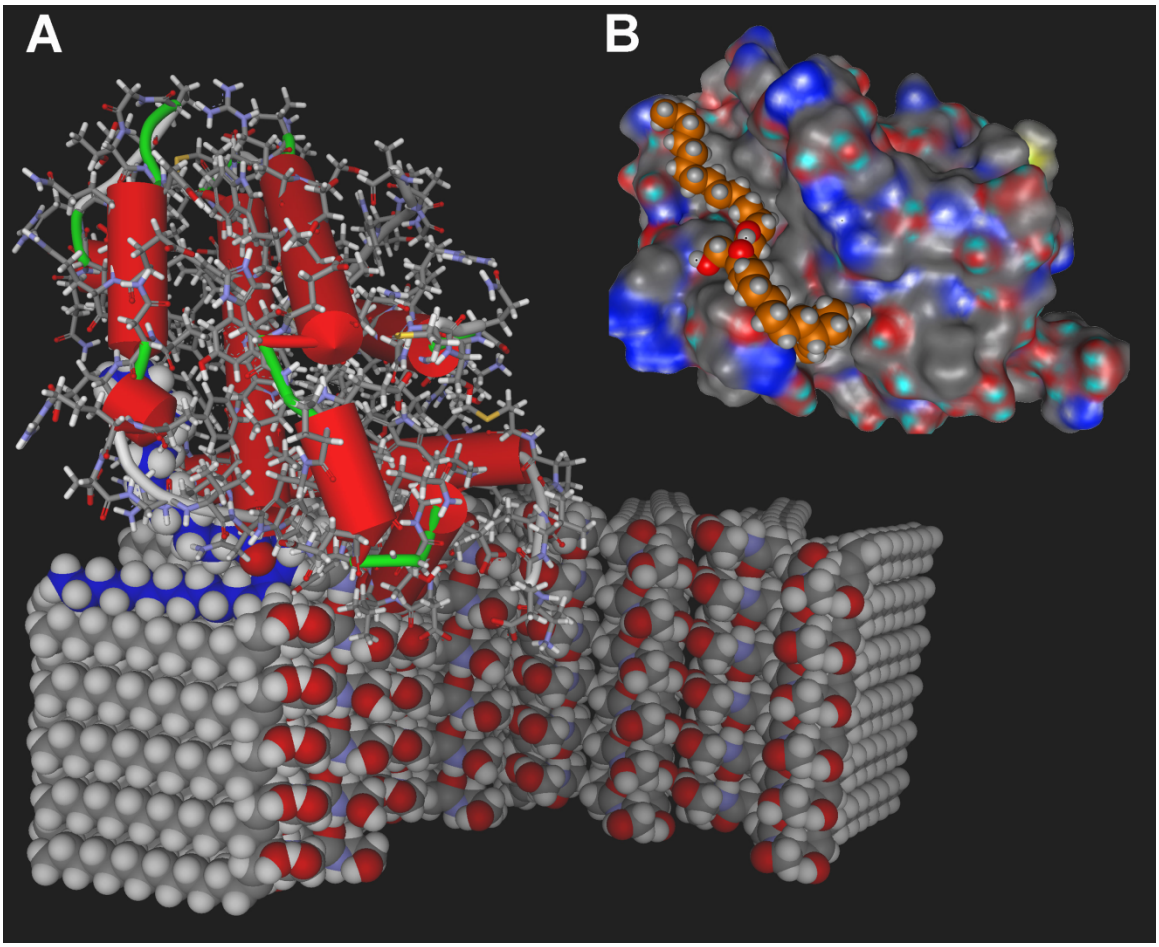

Figure 5.7 Molecular structures of C_{16}-Cer bound to Bcl-xL from docking simulations and possible interaction with a ceramide channel.

A. How Bcl-xL might bind to a ceramide molecule at the end of a ceramide column that is part of a ceramide channel. One of the top poses of C_{16}-Cer bound to Bcl-xL leaves one chain free. This was lined up with a segment of the proposed structure of a ceramide channel, showing how Bcl-xL might bind to the end of one ceramide column, disrupting the column's interaction with the adjacent phospholipid bilayer. B. C_{16}-Cer nestled in the hydrophobic grove of Bcl-xL. This is one of the top ten poses after energy minimization.

Molecular dynamics simulations (Anishkin et al., 2006; Samanta et al., 2011) indicate that the ceramide channel forms an hourglass shape in the membrane, allowing the channel to properly interface with the phospholipid bilayer and thus avoiding exposure of apolar chains to the aqueous environment (Fig. 5.9, 5.10). This results in a

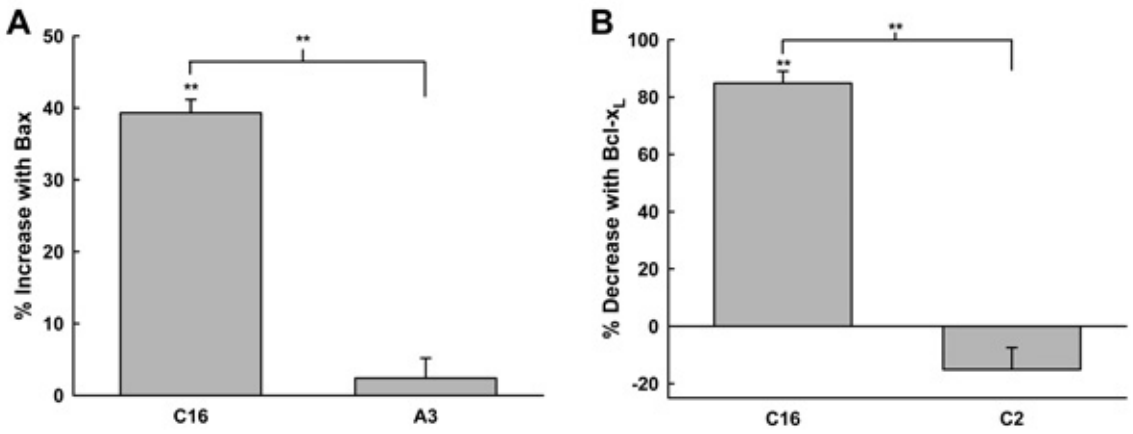

Figure 5.8 The effect of Bax and Bcl-xL on the ability to regulate channels made of ceramide or ceramide analogs at 37°C. These experiments were conducted in an identical fashion as described in the Methods section except the experiments were conducted at a constant temperature of 37°C. **A.** Bax (3.5nM) enhances ceramide channels but not those formed of **A3** (2.5µg of C_{16}-cer and 10µg of **A3** were added in a volume of 10µL). **B.** Bcl-xL (0.4µM) can inhibit channels formed of C_{16}-cer but not C_2-cer (2.5µg of C_{16}-cer and 10µg of C_2-cer were added in a volume of 10µL). Results from both **A** and **B** are consistent with results obtained at room temperature (Fig. 5.3A and 5.4B respectively)

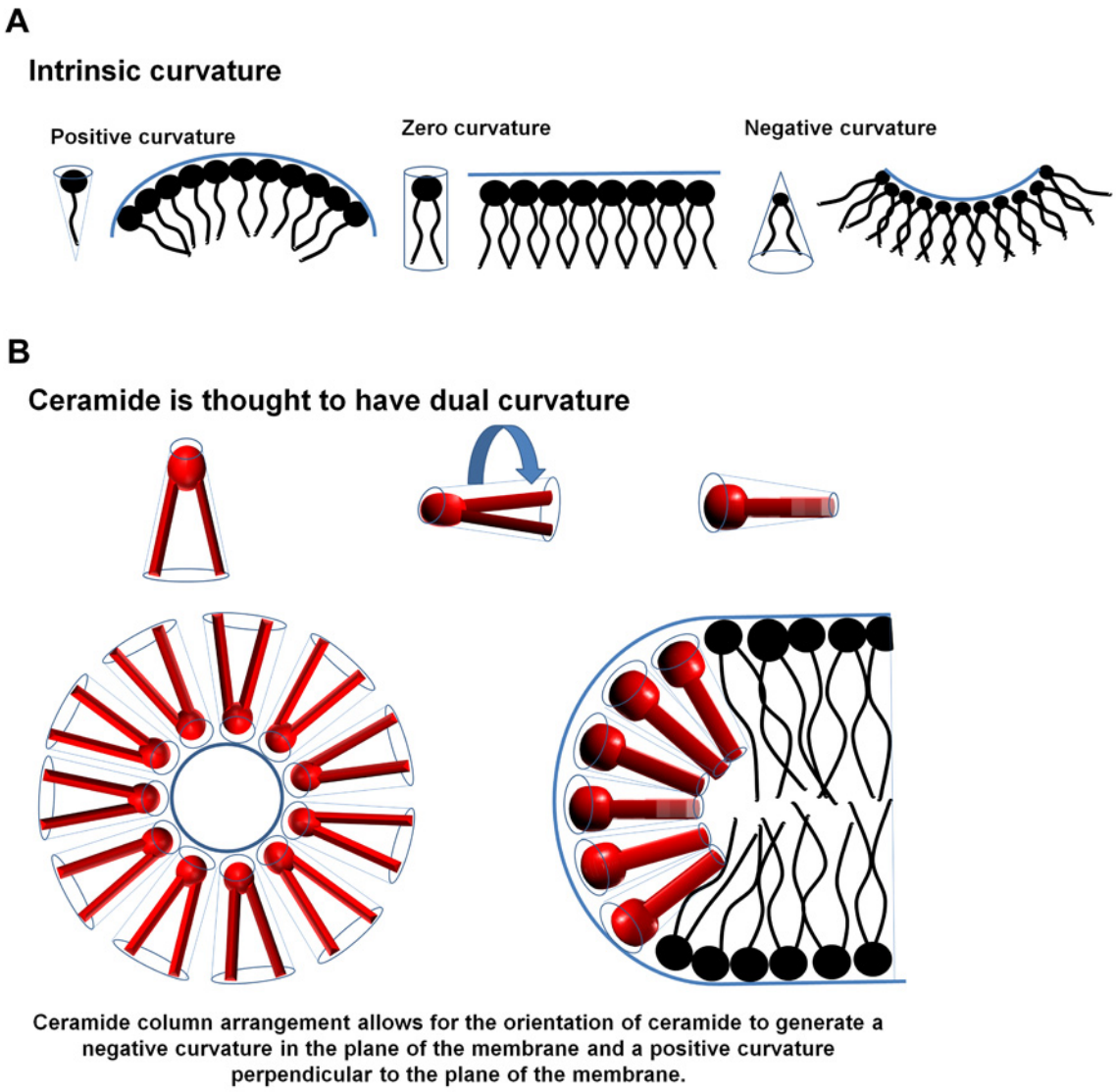

Figure 5.9 Membrane curvature depends upon the intrinsic curvature of its lipid components. Membrane phospholipids are shown in black and ceramide is shown in red. **A.** Intrinsic curvature is measure of size of the hydrophilic portion of a lipid relative to the hydrophobic region. Cylindrical lipids where the head group and tail region are of similar relative size display zero curvature as shown in the plane of the membrane. Positive intrinsic curvature results when the head group of the lipid is larger than the tail region leading to the formation of positive curvature of the membrane. The opposite is seen for lipids with negative intrinsic curvature. **B.** Ceramide is thought to have dual curvature; ceramide is known to have negative intrinsic curvature (left, top), however, rotating the molecule reveals a positive curvature (left, bottom). This dual curvature allows for the formation of stable ceramide channels in

membranes as reveled by molecular modeling studies conducted by (Anishkin et al., 2006). Negative curvature of ceramide allows for the formation of a cylindrical pore in the plane of the membrane (middle) while the positive curvature of ceramide allows for the formation of positive curvature perpendicular to the plane of the membrane (right). Together, these features allow for the formation of stable transmembrane ceramide channels in the mitochondrial outer membrane. This figure and the subsequent supplemental figures were made using Microsoft Powerpoint and Adobe Photoshop software.

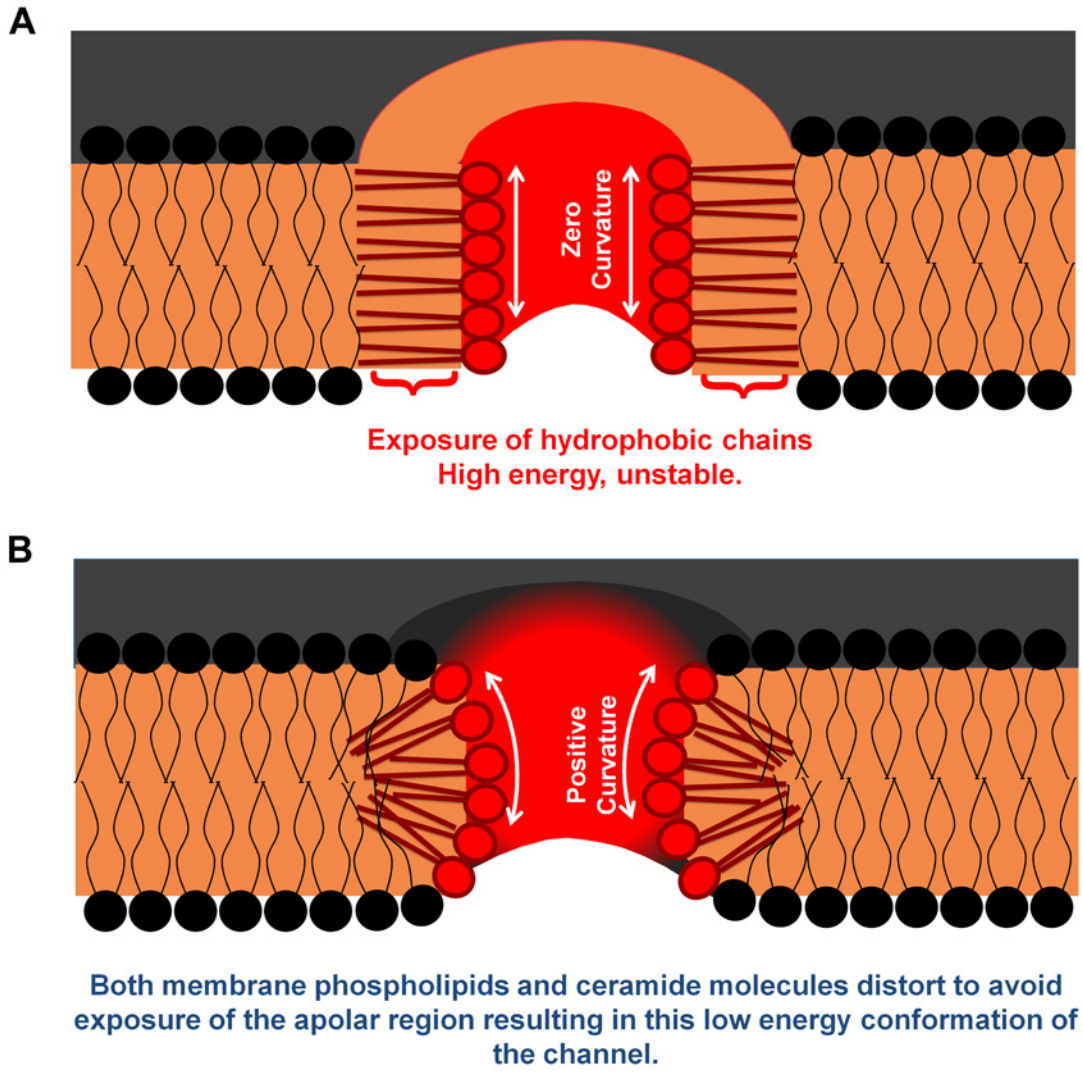

Figure 5.10 Cross section of a ceramide channel in the membrane. Membrane phospholipids are shown in black as is the surface of the membrane and ceramide is shown in red. The hydrophobic region is shown in tan. **A.** A ceramide channel is shown here in red as a cylindrical

channel formed by columns of ceramide. The columns are held together by a network of hydrogen bonds. If the channel were to have a zero curvature (as shown), or a negative curvature, perpendicular to the plane of the membrane, this would lead to the exposure of the apolar region of ceramide. This is structure is energetically unfavorable and highly unstable in an aqueous environment. **B.** Molecular modeling studies reveal that ceramide channels could form a positive curvature perpendicular to the plane of the membrane. This stable structure is formed by a distortion of both the membrane phospholipids and the ceramide molecules at the channel-membrane interface. This low-energy compromise effectively protects the hydrophobic region. Any factor that influence the channel between the two states illustrated in **A** and **B** can affect the stability of the channel and shift the dynamic equilibrium of ceramide to ceramide in the channel form or ceramide in the membrane.

curvature in the ceramide columns forming the channel that is positive in the direction normal to the plane of the membrane (Anishkin et al., 2006). This curvature reduces the distortion of the phospholipids in close proximity to the ceramide channel. Thus interfacing the ceramide molecules that would tend to have their long axis parallel with the membrane plane with the phospholipids whose long axis is normal to that plane requires a compromise distortion of both to minimize the overall energy level. This low-energy compromise might be interfered with by the interaction with Bcl-xL. Bcl-xL could bind at this interface, displacing the local phospholipids and allowing the ceramide column to relax by reducing the positive curvature. Evidence from the present study indicates that the hydrophobic groove of Bcl-xL is interacting with the hydrophobic chains of the ceramide molecules in a channel, chains that are buried within the membrane apolar environment. This is consistent with previous results by Siskind et al. 2008, who demonstrated that a Bcl-xL deletion mutant missing the transmembrane domain is unable to disassemble ceramide channels suggesting that the membrane active

form of Bcl-xL is required for ceramide channel regulation. Thus the binding of Bcl-xL to the end of one column and resulting relaxation of that column (Fig 5.11) would result in a mismatch with the curvature of adjacent ceramide columns and thus the generation of mechanical stress. The highly hydrogen-bonded structure of the channel would result in the propagation of the mechanical stress to the rest of the channel (Fig. 5.12). This high energy structure would then lead to the destabilization of the channel, shifting the dynamic equilibrium toward channel disassembly. This mechanism is consistent with previous results (Siskind et al., 2008) that indicate the formation of a 1:1 complex between Bcl-xL and the channel, requiring that the effects of this binding propagate through the channel structure in an allosteric manner.

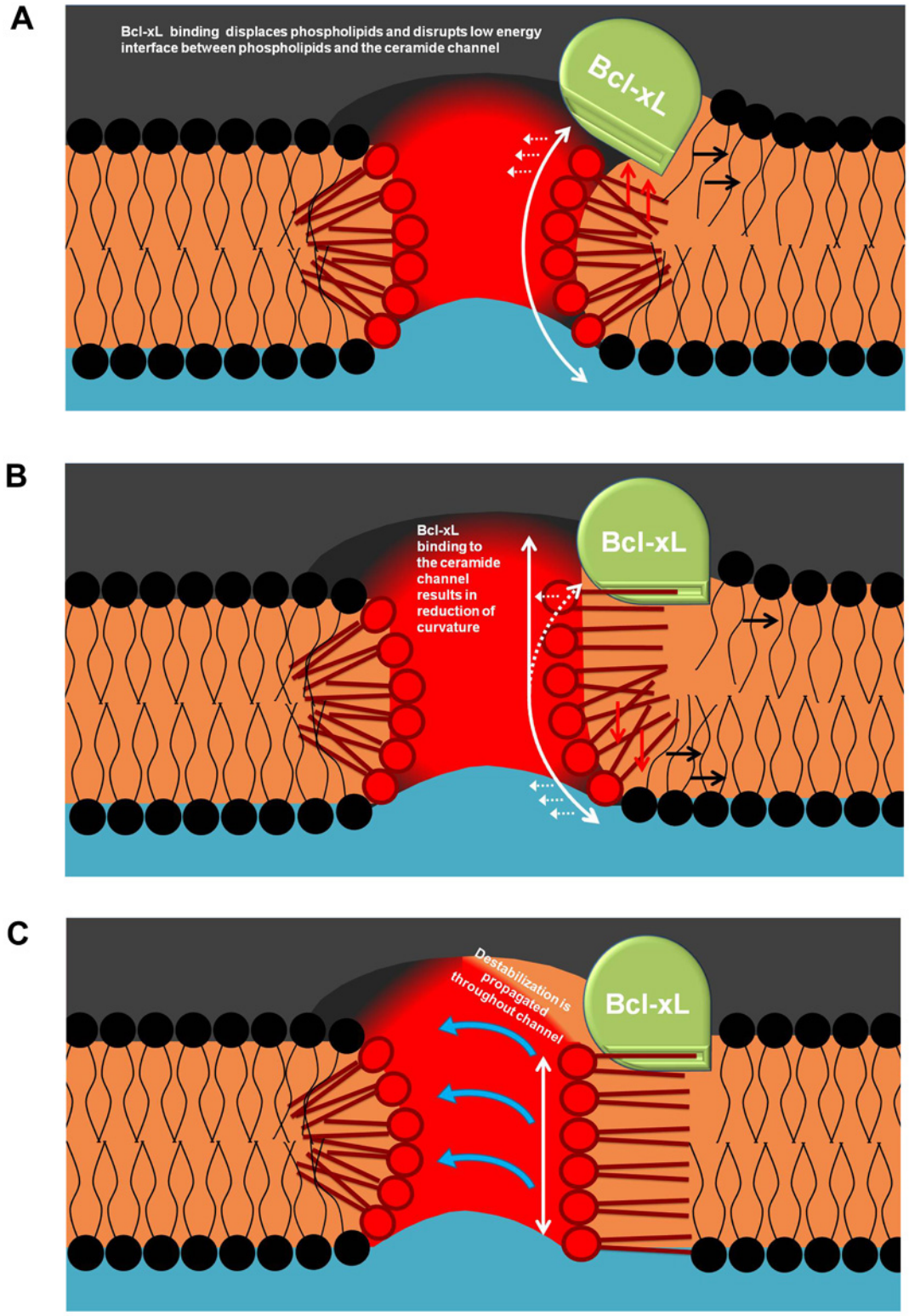

Figure 5.11 Model of Bcl-xL regulation of a ceramide channel. The membrane phospholipids and the surface of the membrane are shown here in black, ceramide molecules and the ceramide

channel is shown here in red. The hydrophobic region is shown in tan. **A.** Bcl-xL binding to the membrane displaces the phospholipids that form a continuous surface with the ceramide channel and contribute to forming the curvature that stabilizes the ceramide channel. The data from the present study indicate that Bcl-xL interacts with the apolar region of the ceramide channel, which is embedded within the membrane, and this interaction involves the hydrophobic groove of Bcl-xL. **B.** Bcl-xL may bind the apolar region of ceramide and influence positive curvature of the channel, possibly reducing this curvature to a zero or to a negative curvature as seen in **C**. Reduction of this positive curvature at the site of Bcl-xL binding would result in mechanical stress on adjacent columns, leading to the local exposure of the hydrophobic region (as seen in tan). Ceramide channels are composed of ceramide columns held together by a vast network of hydrogen bonds. As Bcl-xL induces a local destabilizing conformational change, this mechanical stress is propagated throughout the channel via the hydrogen bonded network (blue arrows), shifting the dynamic equilibrium of ceramide away from channel formation.

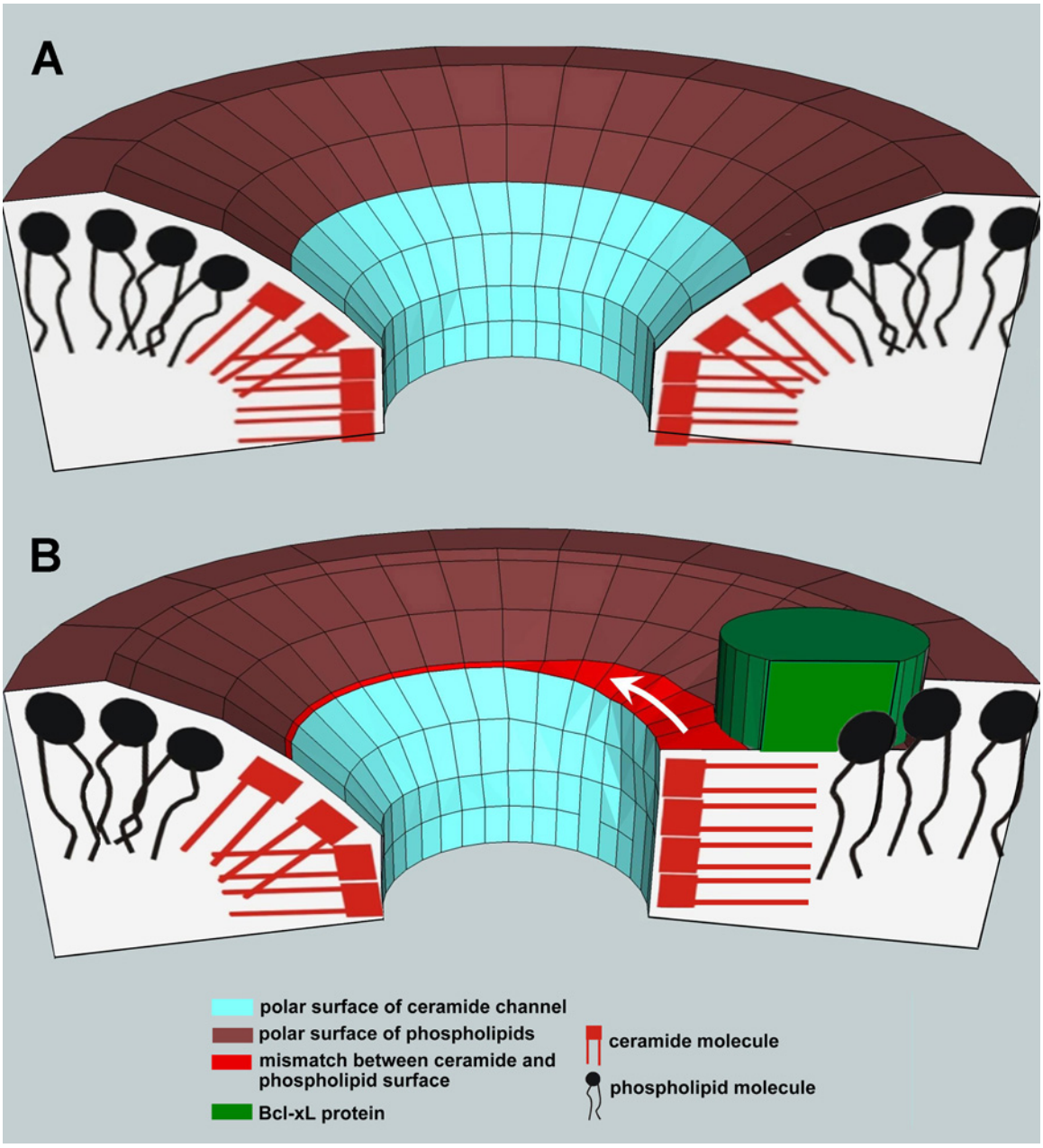

Figure 5.12 Model of the proposed influence of Bcl-xL binding on the stability of the ceramide channel. The model described in Fig. 5.11 is illustrated differently here using a TrueSpace (Caligari Corp.) model. **A.** The hydrogen bonded network of ceramide molecules that compose the polar surface of the ceramide channel are shown in blue. (Also seen in Fig 5.10B) **B**. The binding of Bcl-xL (green) to the aliphatic chain(s) of the ceramide at the end of a ceramide column in the channel should displace the phospholipids allowing the column to relax into a conformation with reduced positive curvature. However, interaction with adjacent columns results in a structural mismatch illustrated as a red fracture area between the ceramide channel

and the surrounding phospholipids. This should destabilize the adjacent columns leading to channel disassembly.

As for Bax, the results indicate that the chirality of the molecule's polar region and specifically the accessibility of the amide N-H group are key for Bax binding. This indicates that Bax may also be acting at the interface of the channel and the phospholipid membrane where there is access to the carboxamide group. However, unlike Bcl-xL, ceramide binding might favor the positive curvature of the ceramide columns, stabilizing the channel at the channel-membrane interface. This stabilization can result in the enlargement of ceramide channels to an optimal size (Fig. 5.13). Again these results are consistent with previous findings (Ganesan et al., 2010) as the binding of Bax influences the ceramide channel to enlarge to a size that fits optimally with the binding site of Bax. Previous results also indicated that multiple Bax structures bind to a single ceramide channel, presumably all acting to stabilize the ceramide channel in a particular state.

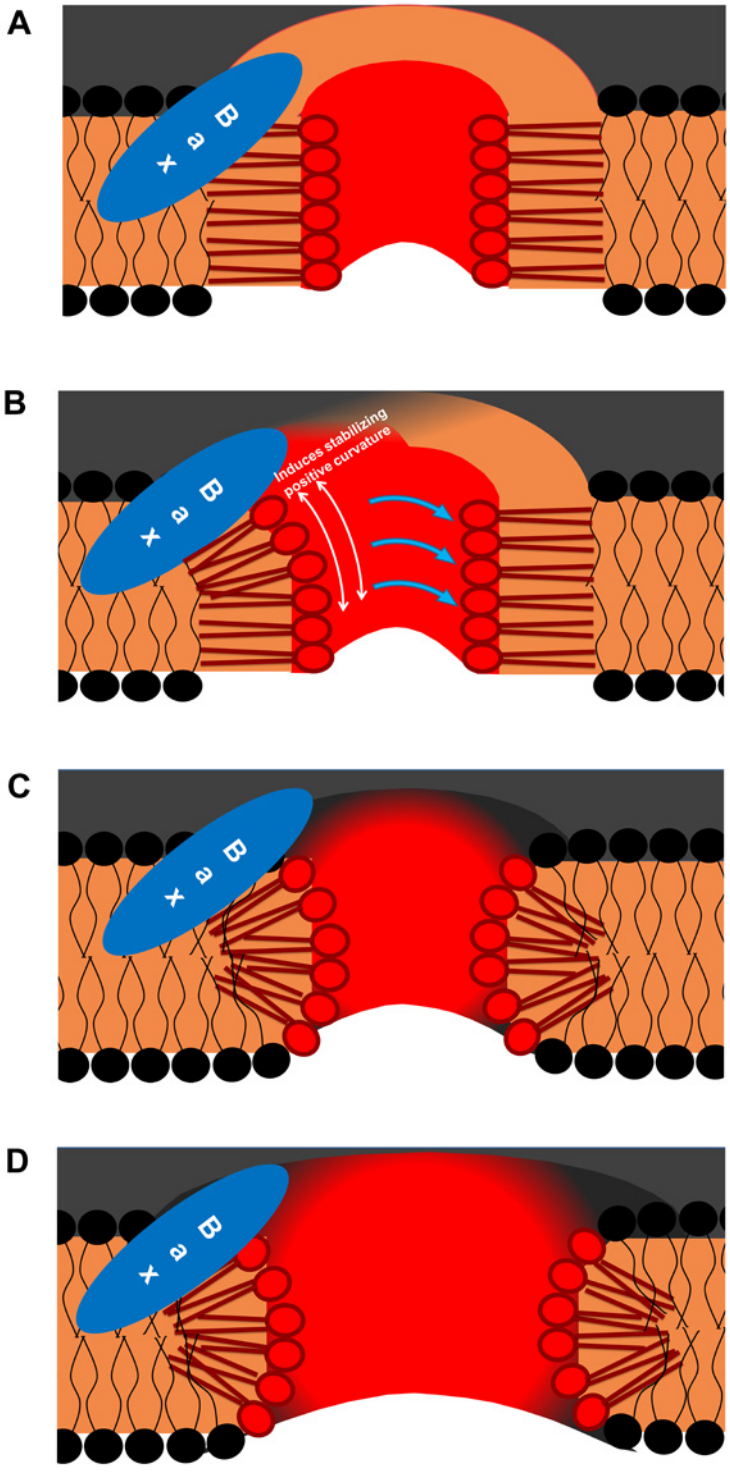

Figure 5.13 Model of activated-Bax regulation of a ceramide channel. The membrane phospholipids and the surface of the membrane is shown here in black, ceramide molecules and the ceramide channel is shown here in red. The hydrophobic region is shown in tan. **A.** Evidence

from this study indicates that Bax appears to be interacting with the top of the ceramide channel, where there is access to the amide N-H group, at the interface of the channel and the membrane. Bax may promote the stable conformation of the channel at this interface, as shown in **B**, allowing the channel and the membrane to interface correctly. The stabilizing effect of Bax is propagated throughout the channel (blue arrows) via the hydrogen bonded network of ceramide columns resulting in **C**. Bax has also been shown to enhance ceramide channel formation and the stabilizing effect of Bax may also allow for the enlargement of ceramide channels to an optimal size as indicated in studies published by (Ganesan et al., 2010).

5.4.6 Concluding remarks

Beyond the details, it is worth noting that highly-organized lipid assemblies, ceramide channels in this case, take a form dictated by the properties of their monomeric subunits and the environment in which they exist. However, the forms of these superstructures can be modified by interactions with regulating molecules, in this case Bcl-2 family proteins. Thus cells can control these superstructures at various levels: by controlling the supply of specific monomers at the membrane or cell compartment of interest, by changing the lipid environment of the membrane, and by producing proteins (or other regulating factors) that alter the form or stability of the final structure. Perhaps, in thinking about lipids one must go beyond thinking about lipid phases, fluidity, and phase transitions. Lipids can form superstructures with unique properties and the ability to be regulated much like the structures formed by proteins.

NOTE:

Shang H. Lin aided in repeating a portion of mitochondrial experiments. Dr. Yuri K. Peterson designed and ran molecular docking simulations and analyzed output data. Dr. Alicja Bielawska, Dr. Zdzlaw M. Szulc, and Dr. Robert Bittman provided ceramide analogs. I designed the study, purified the proteins used, performed all mitochondrial experiments, and analyzed the data.

CHAPTER 6

DISCUSSION AND FUTURE DIRECTIONS

DISCUSSION

In this dissertation, I presented my research on the multifaceted means of regulation of ceramide channels. Researching ceramide channels challenges one to look beyond the known scientific dogmas in the field of apoptosis and to look at the world of lipids in a new light. The ability of lipid monomers to self assemble into large stable channels is a novel idea but the precise molecular means of regulation would suggest this is no accident. In the field of apoptosis, the general consensus in the cell biology community is that Bax and/or Bak channels are the likely means of MOMP during apoptosis however, the role of ceramide in apoptosis has long been appreciated by those who study lipids. Thus, a key deficit in the understanding of the big picture of the apoptotic scheme is due to the lack of cross talk between these fields and the integration of existing knowledge. The work presented in this dissertation seeks to bridge this gap. It is clear that the properties of ceramide channels are in accordance with the known properties of the pore formed in mitochondria to initiate apoptosis and while Bax and/or Bak can form channels as well, the properties of Bax channels can vary widely (see section 1.3.1, 1.5.2). One of the biggest challenges facing the study of ceramide channels is the lack of pharmacological tools to detect ceramide channel formation *in vivo* and distinguish them from Bax or Bak channels. What is evident however is that there is a highly specific interaction between ceramide channels and the Bcl-2 family and the onset of apoptosis is not simply regulated by the action of proteins, but an intricate manipulation of lipid species as well. Understanding this relationship is key to piecing together the big picture of the apoptotic program as well as for its potential impact on

drug design and chemotherapeutics. In this chapter, I present feasible directions to explore in the study of ceramide channels.

Visualization of ceramide channels in MOM vesicles.

In 2008, while presenting a poster on ceramide channels at a national conference, one passer-by, without even stopping to examine the work, posed this question to me, "have ceramide channels ever been visualized?" At the time, as the man walked away, my only retort was to ask, "how many channels, of any kind, have?" Needless to say, visual evidence is invaluable and thankfully, a couple of years later, my colleagues Soumya Samanta and Johnny Stiban were able to visualize ceramide channels formed in negative stained liposomes using TEM (Samanta et al., 2011). Using the techniques they developed for that study, I would suggest to try to visualize ceramide channels in MOM vesicles as they more closely represent the physiological mitochondrial membrane environment. My colleagues also found that ceramide channels formed a continuum of sizes with an average of 10nm. To this regard it would be quite interesting to examine the effect of Bax and Bcl-xL on ceramide channel formation and size. For Bax, would the average ceramide channel size detected increase and would the opposite happen for Bcl-xL? Evidence from my work on Bax and Dr. Siskind's work on Bcl-xL would suggest that pretreating the vesicles with Bax or Bcl-xL before ceramide would yield the same results as treating them after ceramide channel formation. These suggested studies would provide greater insights into the balance of channel size vs. number of channels.

Understanding membrane specificity of ceramide channels.

Numerous studies indicate that ceramide can be generated in a number of subcellular compartments; however, channel formation is restricted to mitochondrial outer membranes. Ceramide channel formation can easily be demonstrated in simpler membrane models such as liposomes and planar phospholipid bilayer membranes. The problem of interest is how the lipid composition of the mitochondrial outer membrane contributes to ceramide channel formation and what lipid compositions are unfavorable to ceramide channels. These questions can be explored by employing the use of liposomes with various lipid compositions where ceramide channel formation can easily be detected spectrophotometrically by assaying for the release of fluorescently labeled molecules (Stiban et al., 2006).

The effect of Mcl-1 on ceramide channels

As described in chapter one, Bax and Bcl-xL are just two of a plethora of Bcl-2 family proteins that play a role in regulating the permeability of the mitochondrial outer membrane. Mcl-1, like Bcl-xL, is an anti-apoptotic Bcl-2 protein but there is a key difference between the two: their hydrophobic groove. Studies have shown that the hydrophobic groove of Bcl-xL is larger and more flexible than that of Mcl-1 and compounds that can bind well to the hydrophobic groove of Bcl-xL and Bcl-2, cannot bind well to the hydrophobic groove of Mcl-1 (Lee et al., 2009; Dutta et al., 2010; Liu et al., 2010; Acoca et al., 2011). Many studies have indicated that both Mcl-1 and Bcl-xL must be inhibited to induce apoptosis, thus the search for a pan-anti-apoptotic Bcl-2 family protein inhibitor has garnered much interest for its value to cancer therapy

(Nijhawan et al., 2003; Nguyen et al., 2007; Dutta et al., 2010; Acoca et al., 2011). The effect of purified Mcl-1 protein can be tested on ceramide channels on isolated mitochondria. Whether Mcl-1 can or cannot interact with ceramide channels may very well be related to the hydrophobic groove of the protein. If Mcl-1 does bind ceramide channels, Obatoclax, an inhibitor that specifically binds the Mcl-1 hydrophobic groove, could be tested for competition with ceramide. Regardless of the results, molecular docking studies could be used to estimate the binding energy of ceramide to Mcl-1 and compare that to the binding energy of ceramide to Bcl-xL.

REFERENCES

ACOCA, S., CUI, Q., SHORE, G. C. & PURISIMA, E. O. (2011). Molecular dynamics study of small molecule inhibitors of the Bcl-2 family. — Proteins 79, 2624-36.

AHN, E. H. & SCHROEDER, J. J. (2010). Induction of Apoptosis by Sphingosine, Sphinganine, and C-2-Ceramide in Human Colon Cancer Cells, but not by C-2-Dihydroceramide. — Anticancer Research 30.

ANDERSEN, J. L. & KORNBLUTH, S. (2012). Mcl-1 rescues a glitch in the matrix. — Nature Cell Biology 14.

ANISHKIN, A., SUKHAREV, S. & COLOMBINI, M. (2006). Searching for the molecular arrangement of transmembrane ceramide channels. — Biophys J 90, 2414-26.

ANNIS, M. G., SOUCIE, E. L., DLUGOSZ, P. J., CRUZ-AGUADO, J. A., PENN, L. Z., LEBER, B. & ANDREWS, D. W. (2005). Bax forms multispanning monomers that oligomerize to permeabilize membranes during apoptosis. — EMBO J 24, 2096-103.

ANTONSSON, B. (2004). Mitochondria and the Bcl-2 family proteins in apoptosis signaling pathways. — Molecular and Cellular Biochemistry 256, 141-155.

ANTONSSON, B., CONTI, F., CIAVATTA, A., MONTESSUIT, S., LEWIS, S., MARTINOU, I., BERNASCONI, L., BERNARD, A., MERMOD, J. J., MAZZEI, G., MAUNDRELL, K., GAMBALE, F., SADOUL, R. & MARTINOU, J. C. (1997). Inhibition of Bax channel-forming activity by Bcl-2. — Science 277, 370-372.

ANTONSSON, B., MONTESSUIT, S., LAUPER, S., ESKES, R. & MARTINOU, J. C. (2000). Bax oligomerization is required for channel-forming activity in liposomes and to trigger cytochrome c release from mitochondria. — Biochem J 345 Pt 2, 271-8.

ANTONSSON, B., MONTESSUIT, S., SANCHEZ, B. & MARTINOU, J. C. (2001). Bax is present as a high molecular weight oligomer/complex in the mitochondrial membrane of apoptotic cells. — J Biol Chem 276, 11615-23.

ARDAIL, D., MAALOUF, M., BOIVIN, A., CHAPET, O., BODENNEC, J., ROUSSON, R. & RODRIGUEZ-LAFRASSE, C. (2009). Diversity and complexity of ceramide generation after exposure of jerkat leukemia cells to irradiation. — International Journal of Radiation Oncology Biology Physics 73, 1211-1218.

BABIYCHUK, E. B., ATANASSOFF, A. P., MONASTYRSKAYA, K., BRANDENBERGER, C., STUDER, D., ALLEMANN, C. & DRAEGER, A. (2011). The Targeting of Plasmalemmal Ceramide to Mitochondria during Apoptosis. — Plos One 6.

BASANEZ, G., SHARPE, J. C., GALANIS, J., BRANDT, T. B., HARDWICK, J. M. & ZIMMERBERG, J. (2002). Bax-type apoptotic proteins porate pure lipid bilayers through a mechanism sensitive to intrinsic monolayer curvature. — Journal of Biological Chemistry 277, 49360-49365.

BASAÑEZ, G., ZHANG, J., CHAU, B. N., MAKSAEV, G. I., FROLOV, V. A., BRANDT, T. A., BURCH, J., HARDWICK, J. M. & ZIMMERBERG, J. (2001). Pro-apoptotic cleavage products of Bcl-xL form cytochrome c-conducting pores in pure lipid membranes. — J Biol Chem 276, 31083-91.

BECHINGER, B. (1997). Structure and functions of channel-forming peptides: magainins, cecropins, melittin and alamethicin. — J Membr Biol 156, 197-211.

BIEBERICH, E., HU, B., SILVA, J., MACKINNON, S., YU, R. K., FILLMORE, H., BROADDUS, W. C. & OTTENBRITE, R. M. (2002). Synthesis and characterization of novel ceramide analogs for induction of apoptosis in human cancer cells. — Cancer Lett 181, 55-64.

BIELAWSKA, A., CRANE, H. M., LIOTTA, D., OBEID, L. M. & HANNUN, Y. A. (1993). SELECTIVITY OF CERAMIDE-MEDIATED BIOLOGY - LACK OF ACTIVITY OF ERYTHRO-DIHYDROCERAMIDE. — Journal of Biological Chemistry 268, 26226-26232.

BIELAWSKI, J., PIERCE, J. S., SNIDER, J., REMBIESA, B., SZULC, Z. M. & BIELAWSKA, A. (2009). Comprehensive Quantitative Analysis of Bioactive Sphingolipids by High-Performance Liquid Chromatography-Tandem Mass Spectrometry. — In: Lipidomics: Vol 1: Methods and Protocols (D. Armstrong, ed), p. 443-467.

BIELAWSKI, J., SZULC, Z. M., HANNUN, Y. A. & BIELAWSKA, A. (2006). Simultaneous quantitative analysis of bioactive sphingolipids by high-performance liquid chromatography-tandem mass spectrometry. — Methods 39, 82-91.

BILLEN, L. P., SHAMAS-DIN, A. & ANDREWS, D. W. (2008). Bid: a Bax-like BH3 protein. — Oncogene 27.

BIONDA, C., PORTOUKALIAN, J., SCHMITT, D., RODRIGUEZ-LAFRASSE, C. & ARDAIL, D. (2004). Subcellular compartmentalization of ceramide metabolism: MAM (mitochondria-associated membrane) and/or mitochondria? — Biochem J 382, 527-33.

BIRBES, H., EL BAWAB, S., HANNUN, Y. A. & OBEID, L. M. (2001). Selective hydrolysis of a mitochondrial pool of sphingomyelin induces apoptosis. — FASEB J 15, 2669-79.

BIRBES, H., LUBERTO, C., HSU, Y. T., EL BAWAB, S., HANNUN, Y. A. & OBEID, L. M. (2005). A mitochondrial pool of sphingomyelin is involved in TNFalpha-induced Bax translocation to mitochondria. — Biochem J 386, 445-51.

BITTMAN, R. (2009). Synthetic lipids as bioactive molecules: Roles in regulation of cell function. — In: Wiley Encyclopedia of Chemical Biology (T. P. Begley, ed). Wiley & Sons Inc., New Jersey, p. 480-504.

BLICHER, A., WODZINSKA, K., FIDORRA, M., WINTERHALTER, M. & HEIMBURG, T. (2009). The Temperature Dependence of Lipid Membrane Permeability, its Quantized Nature, and the Influence of Anesthetics. — Biophysical Journal 96, 4581-4591.

BOISE, L. H., GONZALEZGARCIA, M., POSTEMA, C. E., DING, L. Y., LINDSTEN, T., TURKA, L. A., MAO, X. H., NUNEZ, G. & THOMPSON, C. B. (1993). BCL-X, A BCL-2-RELATED GENE THAT FUNCTIONS AS A DOMINANT REGULATOR OF APOPTOTIC CELL-DEATH. — Cell 74, 597-608.

BROCKMAN, H. L., MOMSEN, M. M., BROWN, R. E., HE, L., CHUN, J., BYUN, H. S. & BITTMAN, R. (2004). The 4,5-double bond of ceramide regulates its dipole potential, elastic properties, and packing behavior. — Biophys J 87, 1722-31.

BRUSTOVETSKY, T., LI, T., YANG, Y., ZHANG, J.-T., ANTONSSON, B. & BRUSTOVETSKY, N. (2010). BAX insertion, oligomerization, and outer membrane permeabilization in brain mitochondria: Role of permeability transition and SH-redox regulation. — Biochimica Et Biophysica Acta-Bioenergetics 1797, 1795-1806.

CARPINTEIRO, A., DUMITRU, C., SCHENCK, M. & GULBINS, E. (2008). Ceramide-induced cell death in malignant cells. — Cancer Letters 264.

CHALFANT, C. E., SZULC, Z., RODDY, P., BIELAWSKA, A. & HANNUN, Y. A. (2004). The structural requirements for ceramide activation of serine-threonine protein phosphatases. — Journal of Lipid Research 45, 496-506.

CHAPMAN, J. V., GOUAZÉ-ANDERSSON, V., MESSNER, M. C., FLOWERS, M., KARIMI, R., KESTER, M., BARTH, B. M., LIU, X., LIU, Y. Y., GIULIANO, A. E. & CABOT, M. C. (2010). Metabolism of short-chain ceramide by human cancer cells--implications for therapeutic approaches. — Biochem Pharmacol 80, 308-15.

CHARLES, A. G., HAN, T. Y., LIU, Y. Y., HANSEN, N., GIULIANO, A. E. & CABOT, M. C. (2001). Taxol-induced ceramide generation and apoptosis in human breast cancer cells. — Cancer Chemother Pharmacol 47, 444-50.

CHENG, E. H. Y., SHEIKO, T. V., FISHER, J. K., CRAIGEN, W. J. & KORSMEYER, S. J. (2003). VDAC2 inhibits BAK activation and mitochondrial apoptosis. — Science 301, 513-517.

CHIARA, F., CASTELLARO, D., MARIN, O., PETRONILLI, V., BRUSILOW, W. S., JUHASZOVA, M., SOLLOTT, S. J., FORTE, M., BERNARDI, P. & RASOLA, A. (2008). Hexokinase II detachment from mitochondria triggers apoptosis through the permeability transition pore independent of voltage-dependent anion channels. — PLoS One 3, e1852.

CHUN, J., BYUN, H. S., ARTHUR, G. & BITTMAN, R. (2003). Synthesis and growth inhibitory activity of chiral 5-hydroxy-2-N-acyl-(3E)-sphingenines: Ceramides with an unusual sphingoid backbone. — Journal of Organic Chemistry 68, 355-359.

CHUN, J., LI, G. Q., BYUN, H. S. & BITTMAN, R. (2002). Synthesis of new trans double-bond sphingolipid analogues: Delta(4,6),6 and Delta(6) ceramides. — Journal of Organic Chemistry 67, 2600-2605.

CIFONE, M. G., DEMARIA, R., RONCAIOLI, P., RIPPO, M. R., AZUMA, M., LANIER, L. L., SANTONI, A. & TESTI, R. (1994). APOPTOTIC SIGNALING THROUGH CD95 (FAS/APO-1) ACTIVATES AN ACIDIC SPHINGOMYELINASE. — Journal of Experimental Medicine 180.

CLARKE, S. (1976). Major polypeptide component of rat-liver mitochondria - carbamyl-phosphate synthetase. — Journal of Biological Chemistry 251, 950-961.

COLOMBINI, M. (1987a). Characterization of channels isolated from plant mitochondria. — Methods in Enzymology 148, 465-475.

—. (1987b). Characterization of channels isolated from plant-mitochondria. — Methods in Enzymology 148, 465-475.

COTE, J. & RUIZCARRILLO, A. (1993). PRIMERS FOR MITOCHONDRIAL-DNA REPLICATION GENERATED BY ENDONUCLEASE-G. — Science 261.

D'HERDE, K., DE PREST, B., MUSSCHE, S., SCHOTTE, P., BEYAERT, R., VAN COSTER, R. & ROELS, F. (2000). Ultrastructural localization of cytochrome c in apoptosis demonstrates mitochondrial heterogeneity. — Cell Death and Differentiation 7, 331-337.

DAI, Q., LIU, J., CHEN, J., DURRANT, D., MCINTYRE, T. M. & LEE, R. M. (2004). Mitochondrial ceramide increases in UV-irradiated HeLa cells and is mainly derived from hydrolysis of sphingomyelin. — Oncogene 23, 3650-8.

DAUM, G., BÖHNI, P. C. & SCHATZ, G. (1982). Import of proteins into mitochondria. Cytochrome b2 and cytochrome c peroxidase are located in the intermembrane space of yeast mitochondria. — J Biol Chem 257, 13028-33.

DEJEAN, L. M., MARTINEZ-CABALLERO, S., GUO, L., HUGHES, C., TEIJIDO, O., DUCRET, T., ICHAS, F., KORSMEYER, S. J., ANTONSSON, B., JONAS, E. A. & KINNALLY, K. W. (2005). Oligomeric Bax is a component of the putative cytochrome c release channel MAC, mitochondrial apoptosis-induced channel. — Mol Biol Cell 16, 2424-32.

DI PAOLA, M., ZACCAGNINO, P., MONTEDORO, G., COCCO, T. & LORUSSO, M. (2004). Ceramide induces release of pro-apoptotic proteins from mitochondria by either a

Ca2+-dependent or a Ca2+-independent mechanism. — Journal of Bioenergetics and Biomembranes 36, 165-170.

DOUCE, R., BOURGUIGNON, J., BROUQUISSE, R. & NEUBURGER, M. (1987). Isolation of plant mitochondria: general principles and criteria of integrity. — Methods Enzymol 148, 403-415.

DUMITRU, C. A., WELLER, M. & GULBINS, E. (2009). Ceramide metabolism determines glioma cell resistance to chemotherapy. — J Cell Physiol 221, 688-95.

DUTTA, S., GULLÁ, S., CHEN, T. S., FIRE, E., GRANT, R. A. & KEATING, A. E. (2010). Determinants of BH3 binding specificity for Mcl-1 versus Bcl-xL. — J Mol Biol 398, 747-62.

EL BAWAB, S., USTA, J., RODDY, P., SZULC, Z. M., BIELAWSKA, A. & HANNUN, Y. A. (2002). Substrate specificity of rat brain ceramidase. — Journal of Lipid Research 43, 141-148.

ELRICK, M. J., FLUSS, S. & COLOMBINI, M. (2006). Sphingosine, a product of ceramide hydrolysis, influences the formation of ceramide channels. — Biophys J 91, 1749-56.

ER, E., OLIVER, L., CARTRON, P.-F., JUIN, P., MANON, S. & VALLETTE, F. M. (2006). Mitochondria as the target of the pro-apoptotic protein Bax. — Biochimica Et Biophysica Acta-Bioenergetics 1757.

ESTABROOK, R. & HOLOWINS.A. (1961). Studies on content and organization of respiratory enzymes of mitochondria. — Journal of Biophysical and Biochemical Cytology 9, 19-28.

FLOWERS, M., FABRIAS, G., DELGADO, A., CASAS, J., LUIS ABAD, J. & CABOT, M. C. (2012). C6-Ceramide and targeted inhibition of acid ceramidase induce synergistic decreases in breast cancer cell growth. — Breast Cancer Research and Treatment 133.

GANESAN, V., PERERA, M. N., COLOMBINI, D., DATSKOVSKIY, D., CHADHA, K. & COLOMBINI, M. (2010). Ceramide and activated Bax act synergistically to permeabilize the mitochondrial outer membrane. — Apoptosis 15, 553-62.

GARCIA-SAEZ, A. J., CORAIOLA, M., SERRA, M. D., MINGARRO, I., MENESTRINA, G. & SALGADO, J. (2005). Peptides derived from apoptotic bax and bid reproduce the poration activity of the parent full-length proteins. — Biophysical Journal 88.

GARCIA-SAEZ, A. J., CORAIOLA, M., SERRA, M. D., MINGARRO, I., MULLER, P. & SALGADO, J. (2006). Peptides corresponding to helices 5 and 6 of Bax can independently form large lipid pores. — Febs Journal 273.

García-Ruiz, C., Colell, A., Marí, M., Morales, A. & Fernández-Checa, J. C. (1997). Direct effect of ceramide on the mitochondrial electron transport chain leads to generation of reactive oxygen species. Role of mitochondrial glutathione. — J Biol Chem 272, 11369-77.

Gavathiotis, E., Reyna, D. E., Davis, M. L., Bird, G. H. & Walensky, L. D. (2010). BH3-Triggered Structural Reorganization Drives the Activation of Proapoptotic BAX. — Molecular Cell 40.

Ghafourifar, P., Klein, S. D., Schucht, O., Schenk, U., Pruschy, M., Rocha, S. & Richter, C. (1999). Ceramide induces cytochrome c release from isolated mitochondria - Importance of mitochondrial redox state. — Journal of Biological Chemistry 274.

Goldstein, J. C., Munoz-Pinedo, C., Ricci, J. E., Adams, S. R., Kelekar, A., Schuler, M., Tsien, R. Y. & Green, D. R. (2005). Cytochrome c is released in a single step during apoptosis. — Cell Death and Differentiation 12.

Goping, I. S., Gross, A., Lavoie, J. N., Nguyen, M., Jemmerson, R., Roth, K., Korsmeyer, S. J. & Shore, G. C. (1998). Regulated targeting of BAX to mitochondria. — Journal of Cell Biology 143.

Grösch, S., Schiffmann, S. & Geisslinger, G. (2011). Chain length-specific properties of ceramides. — Prog Lipid Res.

Guihard, G., Bellot, G., Moreau, C., Pradal, G., Ferry, N., Thomy, R., Fichet, P., Meflah, K. & Vallette, F. M. (2004). The mitochondrial apoptosis-induced channel (MAC) corresponds to a late apoptotic event. — Journal of Biological Chemistry 279, 46542-46550.

Hanada, K., Kumagai, K., Yasuda, S., Miura, Y., Kawano, M., Fukasawa, M. & Nishijima, M. (2003). Molecular machinery for non-vesicular trafficking of ceramide. — Nature 426, 803-809.

Hannun, Y. A. & Obeid, L. M. (2008). Principles of bioactive lipid signalling: lessons from sphingolipids. — Nat Rev Mol Cell Biol 9, 139-50.

He, L., Byun, H. S. & Bittman, R. (2000a). A stereocontrolled, efficient synthetic route to bioactive sphingolipids: synthesis of phytosphingosine and phytoceramides from unsaturated ester precursors via cyclic sulfate intermediates. — J Org Chem 65, 7618-26.

He, L. L., Byun, H. S. & Bittman, R. (2000b). Stereoselective preparation of ceramide and its skeleton backbone modified analogues via cyclic thionocarbonate intermediates derived by catalytic asymmetric dihydroxylation of alpha,beta-unsaturated ester precursors. — Journal of Organic Chemistry 65, 7627-7633.

HEFFERNAN-STROUD, L. A. & OBEID, L. M. (2011). p53 and regulation of bioactive sphingolipids. — Adv Enzyme Regul 51, 219-28.

HEIMLICH, G., MCKINNON, A. D., BERNARDO, K., BRDICZKA, D., REED, J. C., KAIN, R., KRONKE, M. & JURGENSMEIER, J. M. (2004). Bax-induced cytochrome c release from mitochondria depends on alpha-helices-5 and -6. — Biochemical Journal 378.

HEISKANEN, K. M., BHAT, M. B., WANG, H. W., MA, J. J. & NIEMINEN, A. L. (1999). Mitochondrial depolarization accompanies cytochrome c release during apoptosis in PC6 cells. — Journal of Biological Chemistry 274.

HEMANN, M. T. & LOWE, S. W. (2006). The p53-Bcl-2 connection. — Cell Death and Differentiation 13.

HSU, Y. T. & YOULE, R. J. (1997). Nonionic detergents induce dimerization among members of the Bcl-2 family. — Journal of Biological Chemistry 272, 13829-13834.

ITOH, M., KITANO, T., WATANABE, M., KONDO, T., YABU, T., TAGUCHI, Y., IWAI, K., TASHIMA, M., UCHIYAMA, T. & OKAZAKI, T. (2003). Possible role of ceramide as an indicator of chemoresistance: decrease of the ceramide content via activation of glucosylceramide synthase and sphingomyelin synthase in chemoresistant leukemia. — Clin Cancer Res 9, 415-23.

IVASHYNA, O., GARCIA-SAEZ, A. J., RIES, J., CHRISTENSON, E. T., SCHWILLE, P. & SCHLESINGER, P. H. (2009). Detergent-activated BAX Protein Is a Monomer. — Journal of Biological Chemistry 284, 23935-23946.

JARVIS, W. D., KOLESNICK, R. N., FORNARI, F. A., TRAYLOR, R. S., GEWIRTZ, D. A. & GRANT, S. (1994). INDUCTION OF APOPTOTIC DNA-DAMAGE AND CELL-DEATH BY ACTIVATION OF THE SPHINGOMYELIN PATHWAY. — Proceedings of the National Academy of Sciences of the United States of America 91.

JURGENSMEIER, J. M., XIE, Z. H., DEVERAUX, Q., ELLERBY, L., BREDESEN, D. & REED, J. C. (1998). Bax directly induces release of cytochrome c from isolated mitochondria. — Proceedings of the National Academy of Sciences of the United States of America 95, 4997-5002.

KARASAVVAS, N., ERUKULLA, R. K., BITTMAN, R., LOCKSHIN, R. & ZAKERI, Z. (1996). Stereospecific induction of apoptosis in U937 cells by N-octanoyl-sphingosine stereoisomers and N-octyl-sphingosine - The ceramide amide group is not required for apoptosis. — European Journal of Biochemistry 236, 729-737.

KASHKAR, H., WIEGMANN, K., YAZDANPANAH, B., HAUBERT, D. & KRONKE, M. (2005). Acid sphingomyelinase is indispensable for UV light-induced bax conformational

change at the mitochondrial membrane. — Journal of Biological Chemistry 280, 20804-20813.

KERR, J. F. R., WYLLIE, A. H. & CURRIE, A. R. (1972). APOPTOSIS - BASIC BIOLOGICAL PHENOMENON WITH WIDE-RANGING IMPLICATIONS IN TISSUE KINETICS. — British Journal of Cancer 26, 239-&.

KHODJAKOV, A., RIEDER, C., MANNELLA, C. A. & KINNALLY, K. W. (2004). Laser micro-irradiation of mitochondria: is there an amplified mitochondrial death signal in neural cells? — Mitochondrion 3, 217-227.

KLUCK, R. M., ESPOSTI, M. D., PERKINS, G., RENKEN, C., KUWANA, T., BOSSY-WETZEL, E., GOLDBERG, M., ALLEN, T., BARBER, M. J., GREEN, D. R. & NEWMEYER, D. D. (1999). The pro-apoptotic proteins, Bid and Bax, cause a limited permeabilization of the mitochondrial outer membrane that is enhanced by cytosol. — Journal of Cell Biology 147, 809-822.

KOHLER, C., GAHM, A., NOMA, T., NAKAZAWA, A., ORRENIUS, S. & ZHIVOTOVSKY, B. (1999). Release of adenylate kinase 2 from the mitochondrial intermembrane space during apoptosis. — Febs Letters 447, 10-12.

KOHYAMA-KOGANEYA, A., SASAMURA, T., OSHIMA, E., SUZUKI, E., NISHIHARA, S., UEDA, R. & HIRABAYASHI, Y. (2004). Drosophila glucosylceramide synthase: a negative regulator of cell death mediated by proapoptotic factors. — J Biol Chem 279, 35995-6002.

KOMORI, H., ICHIKAWA, S., HIRABAYASHI, Y. & ITO, M. (1999). Regulation of intracellular ceramide content in B16 melanoma cells. Biological implications of ceramide glycosylation. — J Biol Chem 274, 8981-7.

KRAMMER, P. H., ARNOLD, R. & LAVRIK, I. N. (2007). Life and death in peripheral T cells. — Nature Reviews Immunology 7, 532-542.

KROEMER, G., GALLUZZI, L. & BRENNER, C. (2007). Mitochondrial membrane permeabilization in cell death. — Physiological Reviews 87.

KROESEN, B. J., JACOBS, S., PETTUS, B. J., SIETSMA, H., KOK, J. W., HANNUN, Y. A. & DE LEIJ, L. F. (2003). BcR-induced apoptosis involves differential regulation of C16 and C24-ceramide formation and sphingolipid-dependent activation of the proteasome. — J Biol Chem 278, 14723-31.

KROESEN, B. J., PETTUS, B., LUBERTO, C., BUSMAN, M., SIETSMA, H., DE LEIJ, L. & HANNUN, Y. A. (2001). Induction of apoptosis through B-cell receptor cross-linking occurs via de novo generated C16-ceramide and involves mitochondria. — Journal of Biological Chemistry 276, 13606-13614.

KRYSKO, D. V., ROELS, F., LEYBAERT, L. & D'HERDE, K. (2001). Mitochondrial transmembrane potential changes support the concept of mitochondrial

heterogeneity during apoptosis. — Journal of Histochemistry & Cytochemistry 49, 1277-1284.

KUWANA, T., MACKEY, M. R., PERKINS, G., ELLISMAN, M. H., LATTERICH, M., SCHNEITER, R., GREEN, D. R. & NEWMEYER, D. D. (2002). Bid, Bax, and lipids cooperate to form supramolecular openings in the outer mitochondrial membrane. — Cell 111, 331-342.

LAHIRI, S. & FUTERMAN, A. H. (2005). LASS5 is a bona fide dihydroceramide synthase that selectively utilizes palmitoyl-CoA as acyl donor. — Journal of Biological Chemistry 280.

LAVIAD, E. L., ALBEE, L., PANKOVA-KHOLMYANSKY, I., EPSTEIN, S., PARK, H., MERRILL, A. H. & FUTERMAN, A. H. (2008). Characterization of ceramide synthase 2: tissue distribution, substrate specificity, and inhibition by sphingosine 1-phosphate. — J Biol Chem 283, 5677-84.

LAVIE, Y., CAO, H., VOLNER, A., LUCCI, A., HAN, T. Y., GEFFEN, V., GIULIANO, A. E. & CABOT, M. C. (1997). Agents that reverse multidrug resistance, tamoxifen, verapamil, and cyclosporin A, block glycosphingolipid metabolism by inhibiting ceramide glycosylation in human cancer cells. — J Biol Chem 272, 1682-7.

LAVRIK, I. N. & KRAMMER, P. H. (2009). Life and Death Decisions in the CD95 System: Main Pro-and Anti-Apoptotic Modulators. — Acta naturae 1.

LAZAROU, M., STOJANOVSKI, D., FRAZIER, A. E., KOTEVSKI, A., DEWSON, G., CRAIGEN, W. J., KLUCK, R. M., VAUX, D. L. & RYAN, M. T. (2010). Inhibition of Bak Activation by VDAC2 Is Dependent on the Bak Transmembrane Anchor. — Journal of Biological Chemistry 285.

LEBER, B., LIN, J. & ANDREWS, D. W. (2010). Still embedded together binding to membranes regulates Bcl-2 protein interactions. — Oncogene 29.

LEE, A. C., XU, X., BLACHLY-DYSON, E., FORTE, M. & COLOMBINI, M. (1998). The role of yeast VDAC genes on the permeability of the mitochondrial outer membrane. — Journal of Membrane Biology 161, 173-181.

LEE, E. F., CZABOTAR, P. E., YANG, H., SLEEBS, B. E., LESSENE, G., COLMAN, P. M., SMITH, B. J. & FAIRLIE, W. D. (2009). Conformational changes in Bcl-2 pro-survival proteins determine their capacity to bind ligands. — J Biol Chem 284, 30508-17.

LEIST, M., SINGLE, B., CASTOLDI, A. F., KUHNLE, S. & NICOTERA, P. (1997). Intracellular adenosine triphosphate (ATP) concentration: A switch in the decision between apoptosis and necrosis. — Journal of Experimental Medicine 185, 1481-1486.

LI, F., SRINIVASAN, A., WANG, Y., ARMSTRONG, R. C., TOMASELLI, K. J. & FRITZ, L. C. (1997a). Cell-specific induction of apoptosis by microinjection of cytochrome c -

Bcl-x(L) has activity independent of cytochrome c release. — Journal of Biological Chemistry 272, 30299-30305.

LI, P., NIJHAWAN, D., BUDIHARDJO, I., SRINIVASULA, S. M., AHMAD, M., ALNEMRI, E. S. & WANG, X. D. (1997b). Cytochrome c and dATP-dependent formation of Apaf-1/caspase-9 complex initiates an apoptotic protease cascade. — Cell 91.

LIN, S. H., PERERA, M. N., TOAN, N., DATSKOVSKIY, D., MILES, M. & COLOMBINI, M. (2011). Bax Forms Two Types of Channels, One of Which Is Voltage-Gated. — Biophysical Journal 101.

LIU, Q., MOLDOVEANU, T., SPRULES, T., MATTA-CAMACHO, E., MANSUR-AZZAM, N. & GEHRING, K. (2010). Apoptotic Regulation by MCL-1 through Heterodimerization. — Journal of Biological Chemistry 285.

LIU, X. S., KIM, C. N., YANG, J., JEMMERSON, R. & WANG, X. D. (1996). Induction of apoptotic program in cell-free extracts: Requirement for dATP and cytochrome c. — Cell 86.

LIU, Y. Y., HAN, T. Y., GIULIANO, A. E. & CABOT, M. C. (2001). Ceramide glycosylation potentiates cellular multidrug resistance. — FASEB J 15, 719-30.

LIU, Y. Y., HAN, T. Y., GIULIANO, A. E., ICHIKAWA, S., HIRABAYASHI, Y. & CABOT, M. C. (1999). Glycosylation of ceramide potentiates cellular resistance to tumor necrosis factor-alpha-induced apoptosis. — Exp Cell Res 252, 464-70.

LIU, Y. Y., HAN, T. Y., YU, J. Y., BITTERMAN, A., LE, A., GIULIANO, A. E. & CABOT, M. C. (2004). Oligonucleotides blocking glucosylceramide synthase expression selectively reverse drug resistance in cancer cells. — J Lipid Res 45, 933-40.

LIU, Y. Y., PATWARDHAN, G. A., BHINGE, K., GUPTA, V., GU, X. & JAZWINSKI, S. M. (2011). Suppression of Glucosylceramide Synthase Restores p53-Dependent Apoptosis in Mutant p53 Cancer Cells. — Cancer Research 71, 2276-2285.

LOVELL, J. F., BILLEN, L. P., BINDNER, S., SHAMAS-DIN, A., FRADIN, C., LEBER, B. & ANDREWS, D. W. (2008). Membrane binding by tBid initiates an ordered series of events culminating in membrane permeabilization by Bax. — Cell 135, 1074-84.

LUCCI, A., HAN, T. Y., LIU, Y. Y., GIULIANO, A. E. & CABOT, M. C. (1999a). Modification of ceramide metabolism increases cancer cell sensitivity to cytotoxics. — Int J Oncol 15, 541-6.

—. (1999b). Multidrug resistance modulators and doxorubicin synergize to elevate ceramide levels and elicit apoptosis in drug-resistant cancer cells. — Cancer 86, 300-11.

LUCKEN-ARDJOMANDE, S., MONTESSUIT, S. & MARTINOU, J. C. (2008). Bax activation and stress-induced apoptosis delayed by the accumulation of cholesterol in mitochondrial membranes. — Cell Death and Differentiation 15, 484-493.

MAJNO, G. & JORIS, I. (1995). APOPTOSIS, ONCOSIS, AND NECROSIS - AN OVERVIEW OF CELL-DEATH. — American Journal of Pathology 146, 3-15.

MANION, M. K., O'NEILL, J. W., GIEDT, C. D., KIM, K. M., ZHANG, K. Y. & HOCKENBERY, D. M. (2004). Bcl-XL mutations suppress cellular sensitivity to antimycin A. — J Biol Chem 279, 2159-65.

MARGOLIASH, E. & FROHWIRT, N. (1959). Spectrum of horse-heart cytochrome-c. — Biochemical Journal 71, 570-578.

MARTINEZ-CABALLERO, S., DEJEAN, L. M., KINNALLY, M. S., OH, K. J., MANNELLA, C. A. & KINNALLY, K. W. (2009). Assembly of the Mitochondrial Apoptosis-induced Channel, MAC. — Journal of Biological Chemistry 284.

MARTINOU, J. C., DESAGHER, S. & ANTONSSON, B. (2000). Cytochrome c release from mitochondria: all or nothing. — Nature Cell Biology 2.

MATSKO, C. M., HUNTER, O. C., RABINOWICH, H., LOTZE, M. T. & AMOSCATO, A. A. (2001). Mitochondrial lipid alterations during Fas- and radiation-induced apoptosis. — Biochem Biophys Res Commun 287, 1112-20.

MEGHA, SAWATZKI, P., KOLTER, T., BITTMAN, R. & LONDON, E. (2007). Effect of ceramide N-acyl chain and polar headgroup structure on the properties of ordered lipid domains (lipid rafts). — Biochim Biophys Acta 1768, 2205-12.

MENUZ, V., HOWELL, K. S., GENTINA, S., EPSTEIN, S., RIEZMAN, I., FORNALLAZ-MULHAUSER, M., HENGARTNER, M. O., GOMEZ, M., RIEZMAN, H. & MARTINOU, J. C. (2009). Protection of C. elegans from anoxia by HYL-2 ceramide synthase. — Science 324, 381-4.

MIKHAILOV, V., MIKHAILOVA, M., PULKRABEK, D. J., DONG, Z., VENKATACHALAM, M. A. & SAIKUMAR, P. (2001). Bcl-2 prevents Bax oligomerization in the mitochondrial outer membrane. — J Biol Chem 276, 18361-74.

MINN, A. J., VELEZ, P., SCHENDEL, S. L., LIANG, H., MUCHMORE, S. W., FESIK, S. W., FILL, M. & THOMPSON, C. B. (1997). Bcl-x(L) forms an ion channel in synthetic lipid membranes. — Nature 385.

MIZUTANI, Y., KIHARA, A. & IGARASHI, Y. (2005). Mammalian Lass6 and its related family members regulate synthesis of specific ceramides. — Biochem J 390, 263-71.

MONTAL, M. & MUELLER, P. (1972). Formation of bimolecular membranes from lipid monolayers and a study of their electrical properties. — Proc Natl Acad Sci U S A 69, 3561-6.

MONTESSUIT, S., SOMASEKHARAN, S. P., TERRONES, O., LUCKEN-ARDJOMANDE, S., HERZIG, S., SCHWARZENBACHER, R., MANSTEIN, D. J., BOSSY-WETZEL, E., BASAÑEZ, G., MEDA, P. & MARTINOU, J. C. (2010). Membrane remodeling induced by the dynamin-related protein Drp1 stimulates Bax oligomerization. — Cell 142, 889-901.

MUCHMORE, S. W., SATTLER, M., LIANG, H., MEADOWS, R. P., HARLAN, J. E., YOON, H. S., NETTESHEIM, D., CHANG, B. S., THOMPSON, C. B., WONG, S. L., NG, S. C. & FESIK, S. W. (1996). X-ray and NMR structure of human Bcl-x(L), an inhibitor of programmed cell death. — Nature 381.

MULLEN, T. D. & OBEID, L. M. (2011). Ceramide and Apoptosis: Exploring the Enigmatic Connections Between Sphingolipid Metabolism and Programmed Cell Death. — Anticancer Agents Med Chem, *In Press*.

—. (2012). Ceramide and Apoptosis: Exploring the Enigmatic Connections between Sphingolipid Metabolism and Programmed Cell Death. — Anti-Cancer Agents in Medicinal Chemistry 12.

MUNOZ-PINEDO, C., GUIO-CARRION, A., GOLDSTEIN, J. C., FITZGERALD, P., NEWMEYER, D. D. & GREEN, D. R. (2006). Different mitochondrial-intermembrane space proteins are released during apoptosis in a manner that is coordinately initiated but can vary in duration. — Proceedings of the National Academy of Sciences of the United States of America 103, 11573-11578.

NECHUSHTAN, A., SMITH, C. L., HSU, Y. T. & YOULE, R. J. (1999). Conformation of the Bax C-terminus regulates subcellular location and cell death. — Embo Journal 18.

NEISE, D., GRAUPNER, V., GILLISSEN, B. F., DANIEL, P. T., SCHULZE-OSTHOFF, K., JAENICKE, R. U. & ESSMANN, F. (2008). Activation of the mitochondrial death pathway is commonly mediated by a preferential engagement of Bak. — Oncogene 27, 1387-1396.

NGUYEN, M., MARCELLUS, R. C., ROULSTON, A., WATSON, M., SERFASS, L., MURTHY MADIRAJU, S. R., GOULET, D., VIALLET, J., BÉLEC, L., BILLOT, X., ACOCA, S., PURISIMA, E., WIEGMANS, A., CLUSE, L., JOHNSTONE, R. W., BEAUPARLANT, P. & SHORE, G. C. (2007). Small molecule obatoclax (GX15-070) antagonizes MCL-1 and overcomes MCL-1-mediated resistance to apoptosis. — Proc Natl Acad Sci U S A 104, 19512-7.

NIJHAWAN, D., FANG, M., TRAER, E., ZHONG, Q., GAO, W., DU, F. & WANG, X. (2003). Elimination of Mcl-1 is required for the initiation of apoptosis following ultraviolet irradiation. — Genes Dev 17, 1475-86.

NOVGORODOV, S. A., GUDZ, T. I. & OBEID, L. M. (2008a). Long-chain ceramide is a potent inhibitor of the mitochondrial permeability transition pore. — Journal of Biological Chemistry 283.

—. (2008b). Long-chain ceramide is a potent inhibitor of the mitochondrial permeability transition pore. — J Biol Chem 283, 24707-17.

OBEID, L. M., LINARDIC, C. M., KAROLAK, L. A. & HANNUN, Y. A. (1993). PROGRAMMED CELL-DEATH INDUCED BY CERAMIDE. — Science 259.

OTERA, H., OHSAKAYA, S., NAGAURA, Z. I., ISHIHARA, N. & MIHARA, K. (2005). Export of mitochondrial AIF in response to proapoptotic stimuli depends on processing at the intermembrane space. — Embo Journal 24.

PARSONS, D. F., WILLIAMS, G. R. & CHANCE, B. (1966). Characteristics of isolated and purified preparations of the outer and inner membranes of mitochondria. — Ann N Y Acad Sci 137, 643-66.

PATWARDHAN, G. A., ZHANG, Q. J., YIN, D. M., GUPTA, V., BAO, J. X., SENKAL, C. E., OGRETMEN, B., CABOT, M. C., SHAH, G. V., SYLVESTER, P. W., JAZWINSKI, S. M. & LIU, Y. Y. (2009). A New Mixed-Backbone Oligonucleotide against Glucosylceramide Synthase Sensitizes Multidrug-Resistant Tumors to Apoptosis. — Plos One 4.

PERERA, M. N., GANESAN, V., SISKIND, L. J., SZULC, Z. M., BIELAWSKI, J., BIELAWSKA, A., BITTMAN, R. & COLOMBINI, M. (2012). Ceramide channels: Influence of molecular structure on channel formation in membranes. — Biochimica et Biophysica Acta (BBA) - Biomembranes 1818, 1291-1301.

PETTUS, B. J., CHALFANT, C. E. & HANNUN, Y. A. (2002). Ceramide in apoptosis: an overview and current perspectives. — Biochim Biophys Acta 1585, 114-25.

PEWZNER-JUNG, Y., BEN-DOR, S. & FUTERMAN, A. H. (2006). When do Lasses (longevity assurance genes) become CerS (ceramide synthases)?: Insights into the regulation of ceramide synthesis. — J Biol Chem 281, 25001-5.

PHILLIPS, S. C., TRIOLA, G., FABRIAS, G., GONI, F. M., DUPRE, D. B. & YAPPERT, M. C. (2009). cis- versus trans-Ceramides: Effects of the Double Bond on Conformation and H-Bonding Interactions. — Journal of Physical Chemistry B 113, 15249-15255.

PRUETT, S. T., BUSHNEV, A., HAGEDORN, K., ADIGA, M., HAYNES, C. A., SULLARDS, M. C., LIOTTA, D. C. & MERRILL, A. H. (2008). Biodiversity of sphingoid bases ("sphingosines") and related amino alcohols. — J Lipid Res 49, 1621-39.

QIAN, S., WANG, W., YANG, L. & HUANG, H. W. (2008). Structure of transmembrane pore induced by Bax-derived peptide: evidence for lipidic pores. — Proc Natl Acad Sci U S A 105, 17379-83.

QUINTANS, J., KILKUS, J., MCSHAN, C. L., GOTTSCHALK, A. R. & DAWSON, G. (1994). CERAMIDE MEDIATES THE APOPTOTIC RESPONSE OF WEHI-231 CELLS TO ANTIIMMUNOGLOBULIN, CORTICOSTEROIDS AND IRRADIATION. — Biochemical and Biophysical Research Communications 202.

RENAULT, T. T. & MANON, S. (2011). Bax: Addressed to kill. — Biochimie 93, 1379-1391.

REYNOLDS, C. P., MAURER, B. J. & KOLESNICK, R. N. (2004). Ceramide synthesis and metabolism as a target for cancer therapy. — Cancer Lett 206, 169-80.

RIEBELING, C., ALLEGOOD, J. C., WANG, E., MERRILL, A. H. & FUTERMAN, A. H. (2003). Two mammalian longevity assurance gene (LAG1) family members, trh1 and trh4, regulate dihydroceramide synthesis using different fatty acyl-CoA donors. — J Biol Chem 278, 43452-9.

RODRIGUEZ-LAFRASSE, C., ALPHONSE, G., ALOY, M. T., ARDAIL, D., GÉRARD, J. P., LOUISOT, P. & ROUSSON, R. (2002). Increasing endogenous ceramide using inhibitors of sphingolipid metabolism maximizes ionizing radiation-induced mitochondrial injury and apoptotic cell killing. — Int J Cancer 101, 589-98.

RODRIGUEZ-LAFRASSE, C., ALPHONSE, G., BROQUET, P., ALOY, M. T., LOUISOT, P. & ROUSSON, R. (2001). Temporal relationships between ceramide production, caspase activation and mitochondrial dysfunction in cell lines with varying sensitivity to anti-Fas-induced apoptosis. — Biochemical Journal 357, 407-416.

ROUCOU, X., ROSTOVTSEVA, T., MONTESSUIT, S., MARTINOU, J. C. & ANTONSSON, B. (2002). Bid induces cytochrome c-impermeable Bax channels in liposomes. — Biochemical Journal 363, 547-552.

SAMANTA, S., STIBAN, J., MAUGEL, T. K. & COLOMBINI, M. (2011). Visualization of ceramide channels by transmission electron microscopy. — Biochim Biophys Acta 1808, 1196-201.

SANSOM, M. S. P. (1998). Peptides and lipid bilayers: dynamic interactions. — Current Opinion in Colloid & Interface Science 3, 518-524.

SARASTE, A. (1999). Morphologic criteria and detection of apoptosis. — Herz 24.

SAWADA, M., NAKASHIMA, S., BANNO, Y., YAMAKURA, H., TAKENAKA, K., SHINODA, J., NISHIMURA, Y., SAKAI, N. & NOZAWA, Y. (2006). Influence of Bax or Bcl-2 overexpression on the ceramide-dependent apoptosis pathway in glioma cells. — Oncogene 25, 7440-7440.

SCHAFER, B., QUISPE, J., CHOUDHARY, V., CHIPUK, J. E., AJERO, T. G., DU, H., SCHNEITER, R. & KUWANA, T. (2009). Mitochondrial Outer Membrane Proteins

Assist Bid in Bax-mediated Lipidic Pore Formation. — Molecular Biology of the Cell 20, 2276-2285.

SCHLESINGER, P. H., GROSS, A., YIN, X. M., YAMAMOTO, K., SAITO, M., WAKSMAN, G. & KORSMEYER, S. J. (1997). Comparison of the ion channel characteristics of proapoptotic BAX and antiapoptotic BCL-2. — Proceedings of the National Academy of Sciences of the United States of America 94, 11357-11362.

SEARLE, J., KERR, J. F. R. & BISHOP, C. J. (1982). NECROSIS AND APOPTOSIS - DISTINCT MODES OF CELL-DEATH WITH FUNDAMENTALLY DIFFERENT SIGNIFICANCE. — Pathology Annual 17, 229-259.

SHIMENO, H., SOEDA, S., SAKAMOTO, M., KOUCHI, T., KOWAKAME, T. & KIHARA, T. (1998). Partial purification and characterization of sphingosine N-acyltransferase (ceramide synthase) from bovine liver mitochondrion-rich fraction. — Lipids 33, 601-5.

SILVA, M. T. (2010). Secondary necrosis: The natural outcome of the complete apoptotic program. — Febs Letters 584, 4491-4499.

SILVA, M. T., DO VALE, A. & DOS SANTOS, N. M. N. (2008). Secondary necrosis in multicellular animals: an outcome of apoptosis with pathogenic implications. — Apoptosis 13, 463-482.

SISKIND, L. J. (2005). Mitochondrial ceramide and the induction of apoptosis. — J Bioenerg Biomembr 37, 143-53.

SISKIND, L. J. & COLOMBINI, M. (2000). The lipids C2- and C16-ceramide form large stable channels. Implications for apoptosis. — J Biol Chem 275, 38640-4.

SISKIND, L. J., DAVOODY, A., LEWIN, N., MARSHALL, S. & COLOMBINI, M. (2003). Enlargement and contracture of C2-ceramide channels. — Biophys J 85, 1560-75.

SISKIND, L. J., FEINSTEIN, L., YU, T., DAVIS, J. S., JONES, D., CHOI, J., ZUCKERMAN, J. E., TAN, W., HILL, R. B., HARDWICK, J. M. & COLOMBINI, M. (2008). Anti-apoptotic Bcl-2 Family Proteins Disassemble Ceramide Channels. — J Biol Chem 283, 6622-30.

SISKIND, L. J., FLUSS, S., BUI, M. & COLOMBINI, M. (2005). Sphingosine forms channels in membranes that differ greatly from those formed by ceramide. — J Bioenerg Biomembr 37, 227-36.

SISKIND, L. J., KOLESNICK, R. N. & COLOMBINI, M. (2002). Ceramide channels increase the permeability of the mitochondrial outer membrane to small proteins. — J Biol Chem 277, 26796-803.

—. (2006). Ceramide forms channels in mitochondrial outer membranes at physiologically relevant concentrations. — Mitochondrion 6, 118-25.

SISKIND, L. J., MULLEN, T. D., ROMERO ROSALES, K., CLARKE, C. J., HERNANDEZ-CORBACHO, M. J., EDINGER, A. L. & OBEID, L. M. (2010). The BCL-2 protein BAK is required for long-chain ceramide generation during apoptosis. — J Biol Chem 285, 11818-26.

SOTTOCASA, G. L., KUYLENSTIERNA, B., ERNSTER, L. & BERGSTRAND, A. (1967). [72c] Separation and some enzymatic properties of the inner and outer membranes of rat liver mitochondria. — In: Methods in Enzymology (M. E. P. Ronald W. Estabrook, ed). Academic Press, p. 448-463.

STIBAN, J., CAPUTO, L. & COLOMBINI, M. (2008). Ceramide synthesis in the endoplasmic reticulum can permeabilize mitochondria to proapoptotic proteins. — J Lipid Res 49, 625-34.

STIBAN, J., FISTERE, D. & COLOMBINI, M. (2006). Dihydroceramide hinders ceramide channel formation: Implications on apoptosis. — Apoptosis 11, 773-80.

SUZUKI, M., YOULE, R. J. & TJANDRA, N. (2000). Structure of Bax: coregulation of dimer formation and intracellular localization. — Cell 103, 645-54.

TAN, C. B., DLUGOSZ, P. J., PENG, J., ZHANG, Z., LAPOLLA, S. M., PLAFKER, S. M., ANDREWS, D. W. & LIN, J. L. (2006). Auto-activation of the apoptosis protein Bax increases mitochondrial membrane permeability and is inhibited by Bcl-2. — Journal of Biological Chemistry 281.

TERRONES, O., ANTONSSON, B., YAMAGUCHI, H., WANG, H. G., LIU, J., LEE, R. M., HERRMANN, A. & BASAÑEZ, G. (2004). Lipidic pore formation by the concerted action of proapoptotic BAX and tBID. — J Biol Chem 279, 30081-91.

THOMAS, R. L., MATSKO, C. M., LOTZE, M. T. & AMOSCATO, A. A. (1999). Mass spectrometric identification of increased C16 ceramide levels during apoptosis. — Journal of Biological Chemistry 274, 30580-30588.

TSE, C., SHOEMAKER, A. R., ADICKES, J., ANDERSON, M. G., CHEN, J., JIN, S., JOHNSON, E. F., MARSH, K. C., MITTEN, M. J., NIMMER, P., ROBERTS, L., TAHIR, S. K., XIAO, Y., YANG, X., ZHANG, H., FESIK, S., ROSENBERG, S. H. & ELMORE, S. W. (2008). ABT-263: a potent and orally bioavailable Bcl-2 family inhibitor. — Cancer Res 68, 3421-8.

USTA, J., EL BAWAB, S., RODDY, P., SZULC, Z. M., HANNUN, Y. A. & BIELAWSKA, A. (2001). Structural requirements of ceramide and sphingosine based inhibitors of mitochondrial ceramidase. — Biochemistry 40, 9657-9668.

VANCE, J. E. (1990). Phospholipid synthesis in a membrane fraction associated with mitochondria. — Journal of Biological Chemistry 265, 7248-7256.

VANDER HEIDEN, M. G., CHANDEL, N. S., SCHUMACKER, P. T. & THOMPSON, C. B. (1999). Bcl-x(L) prevents cell death following growth factor withdrawal by facilitating mitochondrial ATP/ADP exchange. — Molecular Cell 3.

VENKATARAMAN, K., RIEBELING, C., BODENNEC, J., RIEZMAN, H., ALLEGOOD, J. C., SULLARDS, M. C., MERRILL, A. H. & FUTERMAN, A. H. (2002). Upstream of growth and differentiation factor 1 (uog1), a mammalian homolog of the yeast longevity assurance gene 1 (LAG1), regulates N-stearoyl-sphinganine (C18-(dihydro)ceramide) synthesis in a fumonisin B1-independent manner in mammalian cells. — J Biol Chem 277, 35642-9.

VON AHSEN, O., RENKEN, C., PERKINS, G., KLUCK, R. M., BOSSY-WETZEL, E. & NEWMEYER, D. D. (2000). Preservation of mitochondrial structure and function after Bid- or Bax-mediated cytochrome c release. — Journal of Cell Biology 150, 1027-1036.

VON HAEFEN, C., WIEDER, T., GILLISSEN, B., STARCK, L., GRAUPNER, V., DORKEN, B. & DANIEL, P. T. (2002). Ceramide induces mitochondrial activation and apoptosis via a Bax-dependent pathway in human carcinoma cells. — Oncogene 21, 4009-4019.

WEI, M. C., ZONG, W. X., CHENG, E. H. Y., LINDSTEN, T., PANOUTSAKOPOULOU, V., ROSS, A. J., ROTH, K. A., MACCREGOR, G. R., THOMPSON, C. B. & KORSMEYER, S. J. (2001). Proapoptotic BAX and BAK: A requisite gateway to mitochondrial dysfunction and death. — Science 292.

WENDT, M. D., SHEN, W., KUNZER, A., MCCLELLAN, W. J., BRUNCKO, M., OOST, T. K., DING, H., JOSEPH, M. K., ZHANG, H., NIMMER, P. M., NG, S. C., SHOEMAKER, A. R., PETROS, A. M., OLEKSIJEW, A., MARSH, K., BAUCH, J., OLTERSDORF, T., BELLI, B. A., MARTINEAU, D., FESIK, S. W., ROSENBERG, S. H. & ELMORE, S. W. (2006). Discovery and structure-activity relationship of antagonists of B-cell lymphoma 2 family proteins with chemopotentiation activity in vitro and in vivo. — J Med Chem 49, 1165-81.

WIECKOWSKI, M. R., VYSSOKIKH, M., DYMKOWSKA, D., ANTONSSON, B., BRDICZKA, D. & WOJTCZAK, L. (2001). Oligomeric C-terminal truncated Bax preferentially releases cytochrome c but not adenylate kinase from mitochondria, outer membrane vesicles and proteoliposomes. — Febs Letters 505, 453-459.

WIJESINGHE, D. S., MASSIELLO, A., SUBRAMANIAN, P., SZULC, Z., BIELAWSKA, A. & CHALFANT, C. E. (2005). Substrate specificity of human ceramide kinase. — J Lipid Res 46, 2706-16.

WOJTCZAK, L., ZALUSKA, H., WRONISZEWSKA, A. & WOJTCZAK, A. B. (1972). Assay for the intactness of the outer membrane in isolated mitochondria. — Acta Biochim Pol 19, 227-34.

WU, B. X., RAJAGOPALAN, V., RODDY, P. L., CLARKE, C. J. & HANNUN, Y. A. (2010). Identification and characterization of murine mitochondria-associated neutral sphingomyelinase (MA-nSMase), the mammalian sphingomyelin phosphodiesterase 5. — J Biol Chem 285, 17993-8002.

YANG, Z., KHOURY, C., JEAN-BAPTISTE, G. & GREENWOOD, M. T. (2006). Identification of mouse sphingomyelin synthase 1 as a suppressor of Bax-mediated cell death in yeast. — Fems Yeast Research 6, 751-762.

YAO, Y., BOBKOV, A. A., PLESNIAK, L. A. & MARASSI, F. M. (2009). Mapping the Interaction of Pro-Apoptotic tBID with Pro-Survival BCL-XL. — Biochemistry 48.

ZHANG, Z., ZHU, W., LAPOLLA, S. M., MIAO, Y., SHAO, Y., FALCONE, M., BOREHAM, D., MCFARLANE, N., DING, J., JOHNSON, A. E., ZHANG, X. C., ANDREWS, D. W. & LIN, J. (2010). Bax Forms an Oligomer via Separate, Yet Interdependent, Surfaces. — Journal of Biological Chemistry 285.

ZHIVOTOVSKY, B., ORRENIUS, S., BRUSTUGUN, O. T. & DOSKELAND, S. O. (1998). Injected cytochrome c induces apoptosis. — Nature 391, 449-450.

ZHOU, H., HOU, Q. & HSU, Y. T. (2006). The BH3 domain of Bax is essential for regulating its solubility and mitochondrial targeting. — Faseb Journal 20.

ZHOU, L. & CHANG, D. C. (2008). Dynamics and structure of the Bax-Bak complex responsible for releasing mitochondrial proteins during apoptosis. — Journal of Cell Science 121, 2186-2196.

ZONG, W. X., LINDSTEN, T., ROSS, A. J., MACGREGOR, G. R. & THOMPSON, C. B. (2001). BH3-only proteins that bind pro-survival Bcl-2 family members fail to induce apoptosis in the absence of Bax and Bak. — Genes Dev 15, 1481-6.